SNOWMELT MODELLING AND ENERGY EXCHANGE BETWEEN THE ATMOSPHERE AND A MELTING SNOW COVER

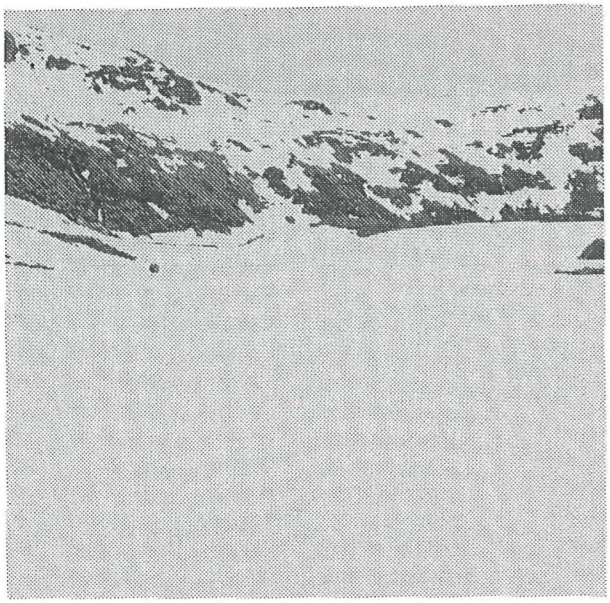

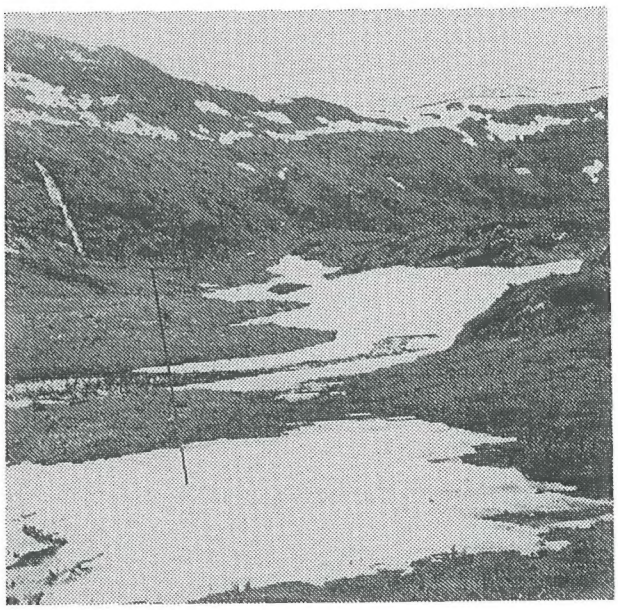

Knut Harstveit

Geophysical Institute, Meteorological Division
University of Bergen
Scientific Report no 4, 1984

CONTENTS

Snowmelt Modelling and Energy Exchange between the Atmosphere and a Melting Snow Cover

by

Knut Harstveit

Geophysical Institute, Meteorological Division
University of Bergen, 1984

Abstract.

Snowmelt modelling in different climatic regions and various types of terrain is of major importance in snow hydrology.

During 1979-82 a field research programme was carried out at Dyrdalen (60°21'N, 5°31'E), an area of rough terrain in the maritime climatic region near the coast of western Norway.

Runoff from 9 m^2 plots of snow cover was recorded by lysimetry at four locations, two of which were situated above the timberline, at 437 and 632 m a.s.l., respectively. The other two stations (both at 285 m a.s.l.) were located in an area partly timbered by deciduous trees. Wind speed, air temperature, air humidity, radiation, and precipitation data were also recorded.

When the melting rate (= snowpack runoff-rainfall) and the net radiation were measured, the turbulent heat exchange between the snowpack and the atmosphere was computed as a residual from the energy balance equation of the snowpack. These computed values were used to find "optimal" empirical constants in aerodynamical equations expressing the turbulent fluxes as functions of the wind speed and the temperature/vapour pressure differences between the measurements 2 m above the ground (0.6 - 1.8 m above the snow surface) and the values at the surface. These empirical constants agree reasonably well with those found by other investigators. The obtained constants proved to be near optimal for the area above as well as below the timberline.

This energy balance model yielded higher model efficiency than a degree-day model for locations above the timberline, while the degree-day model was the better in the wooded area. The degree-day model, however, has to be tuned to the actual type of vegetation.

The efficiency of the models proved to be high also when data for wind speed, air temperature, and air humidity were extrapolated from records at stations up to a distance of some 10-20 km. High quality estimates of net radiation are needed to get reliable results during fine weather, while rather rough estimates are sufficient during cloudy weather.

List of the most frequently used symbols.

α	= albedo	(%, fraction of unity)
C	= cloud cover	(%, fraction of unity, octants)
C_D	= bulk transfer coefficient	
C_p	= spesific heat of dry air	($J\ kg^{-1}K^{-1}$)
γ	= $\frac{C \cdot P_a}{0.622\ L_i}$	($mb\ K^{-1}$)
e	= vapour pressure	(mb)
e_o	= vapour saturation pressure at the surface	(mb)
ε	= emissitivity of snow	(fraction of unity)
g	= acceleration of gravity	(ms^{-2})
k	= degree-day factor	($mm\ day^{-1}{}^{\circ}C^{-1}$)
k_p	= ratio between ground level records of precipitation and records some height (1.6, 2 m) above the surface)	
κ	= von Karman's constant	(0.41)
L_i	= latent heat of sublimation	($J\ kg^{-1}$)
n	= number of observations	
P_a	= air pressure	(mb)
P	= true precipitation	(mm)
P_B	= observed precipitation by Belfort instrument	(mm)
P_L	= observed rain amount by lysimeter	(mm)
P_m	= observed precipitation	(mm)
P_O	= observed rain amount by OTA ground level instrument	(mm)

Q_E	= latent heat flux	(Wm^{-2})
Q_{ex}	= extraterrestrial global radiation	(Wm^{-2})
Q_H	= sensible heat flux	(Wm^{-2})
$Q_{L\downarrow}$	= incoming longwave radiation	(Wm^{-2})
Q_M	= computed energy consumption for snowmelt	(Wm^{-2})
Q_M'	= observed " " "	(Wm^{-2})
Q_N	= net radiation	(Wm^{-2})
Q_S	= global radiation	(Wm^{-2})
R_{i_B}	= bulk Richardson number	(dimensionless)
R_{i_c}	= critical Richardson number	"
R2	= model efficiency	"
ρ_a	= density of air	($kg\ m^{-3}$)
ρ_w	= density of water	($kg\ m^{-3}$)
SD	= standard deviation	
S_m	= predicted daily snowmelt by the degree-day model	($mm\ day^{-1}$)
σ	= Stephan Bolzmann constant	($Wm^{-2}K^{-4}$)
σ_r	= residual error	
T	= air temperature	(°C, K)
t	= time of exposure to open air of the snow at the surface	(days)
T_*	= threshold temperature	(°C)
u	= wind speed	(ms^{-1})
Z_0	= surface roughness	(cm)
Z	= recording level	(m)

Subscripts a : air level 0 : surface

1. Introduction.

Snow and ice, which are common features of the Norwegian environment, play a significant role in the hydrological cycle. The accumulation and melting of snow strongly affect runoff from high altitude and/or high latitude catchments. An adequate understanding of the physics of snowmelt is therefore of vital importance to water resources management in such areas. High precipitation amounts, with significant snow accumulation and frequent snowmelt caused by extremely diverse weather conditions, make the western part of southern Norway well-suited for studies of certain relationships between snowmelt and weather. Knowledge of the snow distribution, snowmelt and water movements in snow are essential in planning hydroelectric power production and for predicting snowmelt floods.

During winter, snow is the most frequent type of precipitation in extensive parts of the country, and in the mountains the snow accumulation season usually lasts from October to May. The snowmelt usually takes place in March and April in the lowlands, and in May and June in the mountains. The times are somewhat later at high latitudes. Near the western coast the snow cover is highly unstable due to the maritime location. Snow accumulation events and snowmelt periods are both common throughout the winter. At low altitudes (<300 m a.s.l.) near the sea, winter precipitation is generally rain or sleet; at medium altitudes (300-600 m a.s.l.) there is usually a main snowmelt period in spring, and several periods with heavy rain or snowmelt during the snow accumulation season.

The snow is distributed in variable patterns depending mainly on terrain parameters and surface wind. Large variations in snow depth are found on horizontal scales of 10-1000 m. Newly fallen snow has low density, i.e. 50-300 $kg \cdot m^{-3}$, the highest values being found for wet or wind-packed snow. The density increases with time to 300-600 $kg\ m^{-3}$, as the snow crystals grow. The time scale of the density increase depends mainly on the level and

variations of the air temperature. Heavy rain episodes may accelerate the process. A wet snow pack (0°C) holds a certain amount of liquid water against the gravitational force. This amount, expressed as a percentage of the total snow weight, is called the free water of the snow pack. The maximum free water content is called the liquid water capacity. U.S.A.C.E. (1956) report it to be 2-5% by weight. Colbeck (1974) and Nyberg and Hårsmar (1971) give the value 4%. The actual value obviously varies considerably. In addition, during rain and snowmelt episodes the snow pack contains liquid water percolating downward.

A dense and grainy snow pack with free water at liquid capacity is said to be ripe. Any rain or melt water entering the snow surface now leaves the bottom as discharge. The percolating time varies with depth and nature of the snow pack, but it is usually on the order of a few hours or less (Colbeck, 1972).

The melting process requires energy which is supplied as net radiation, and sensible and latent heat from the atmosphere. The ground heat flux and heat from rain also make minor contributions. The air temperature may be a useful index of snowmelt since it is often correlated with net radiation, and with the turbulent fluxes of sensible and latent heat.

Accordingly, meteorology plays a major role in snow hydrology. The subject is also closely related to glaciology. U.S.A.C.E. in their work Snow hydrology (1956) discuss the subject in its entirety. Extensive studies of water movements in snow have been made in the U.S.A. and Canada during the last 20 years (Colbeck, 1972, Wankiewicz, 1978). The problem of snow distribution in Norway has been discussed by Tveit (1979), Andersen and Ødegaard, (1980) and others. Operative models for water field discharge, including snowmelt, have been developed in several countries. In Scandinavia, Bergstrøm (1976) developed a model for snowmelt using a temperature index method. This model is the most frequently used in Scandinavia today.

Sverdrup (1936) was the first to carry out extensive studies of the energy exchange between a snow surface and the atmosphere. Wallén (1948) examined the energy balance of a Swedish glacier surface during five summer seasons and found the relative contributions of net radiation, sensible heat and latent heat to be 55%, 29%, and 16%, respectively. Paterson (1969) presented a table covering many glacier examinations which showed highly variable contributions. U.S.A.C.E. (1955, 1956) carried out lysimeter studies of snowmelt in order to develop a model based on the energy balance of the snow cover. Liljequist (1956-57) made extensive studies of radiation and turbulent fluxes at an Antarctic field. Studies of this problem were also carried out in the U.S.S.R., published by Kuzmin (1961, in English 1972). Krauss (1966) examined glacier ablation and produced curves of ablation for different values of air pressure, wind speed, air temperature, air humidity, global radiation, albedo, and surface roughness. Holmgren (1971) studied the energy balance of an Arctic glacier during three summer seasons; he found the most favourable conditions for snowmelt here to be strong wind and advection of warm and humid air. Anderson (1964, 1967, 1968, 1973, 1976) carried out further studies to solve the problem of complete energy balance. He also took into account stability corrections for the turbulent heat fluxes, and modelled the energy transfer within the snowpack. In Norway snowpack discharge has been recorded by lysimeter (Tveit, 1977), and changes of snow weight by snow pillow (Furmyr, 1975), but the data have not been used for energy balance studies. Snowpack discharge may also be calculated from regular observations of snow depth and density. For areal estimates, field discharge may also be directly recorded.

The question of whether an energy balance model can be an improvement on existing snowmelt models is of considerable interest. Therefore, a field research programme supported by the Norwegian National Committee for Hydrology and University of Bergen was carried out near the coast of western Norway. In this paper the

energy balance model and a temperature index model are tested against lysimeter data at a woodless index point during periods where the snow pack could be considered ripe and isothermal, except for daily variations. It is also attempted to assay how snowmelt is modified in areas partly timbered by birch and other deciduous trees. The data requirement and tuning of the models are also discussed. Preliminary results on some of these topics are given by Harstveit (1981).

2. Site Description and Climate.

2.1. Site Description

During 1978-1979 two stations, Dyrdalsvatn (437 m a.s.l.) and Austlihylla (632 m a.s.l.), were established in the Dyrdalen area (Fig. 2.2) for recording snowmelt.

Dyrdalen (60°21'N, 5°31'E) is situated above the timberline, about 11 km ESE of Bergen. The precipitation catchment area (3.34 km^2, 435-806 m a.s.l.) is a rough mountainous area (Fig. 2.3), but on a smaller scale (~100 m) the terrain is smoother. The main direction of the valley is SSW-NNE, and it is situated above the timberline.

The soil and morain masses extend to a depth of 0-2 m. Boggy ground and low vegetation of grass, heather, and moss are predominant. A more detailed description of the field in general, the geology, and the vegetation is given by Gjessing et al. (1980).

During the winter 1980-81 the station network was extended with two stations at Frotveit (285 m a.s.l., Fig. 2.2). These stations are situated about 5 km SW of Dyrdalen, and the distance between them is 70 m. Though the terrain in this area is less rough, there are considerable variations on a smaller scale (Fig. 2.5). The direction of the valley is SW-NE, and it is partly timbered by birch and other deciduous trees, and some small area with densely planted spruce. The terrain and vegetation around the stations are illustrated in Fig. 2.5. One station is located at an open place, and the other one in a grove consisting mainly of birch and some older and rowan.

Data from weather stations (1-3, Fig. 2.1) operated by the Norwegian Meteorological Institute are also used in this investigation, together with radiation data from Bergen - Florida, published by Geophysical Institute, University of Bergen (Radiation Yearbook 1-18).

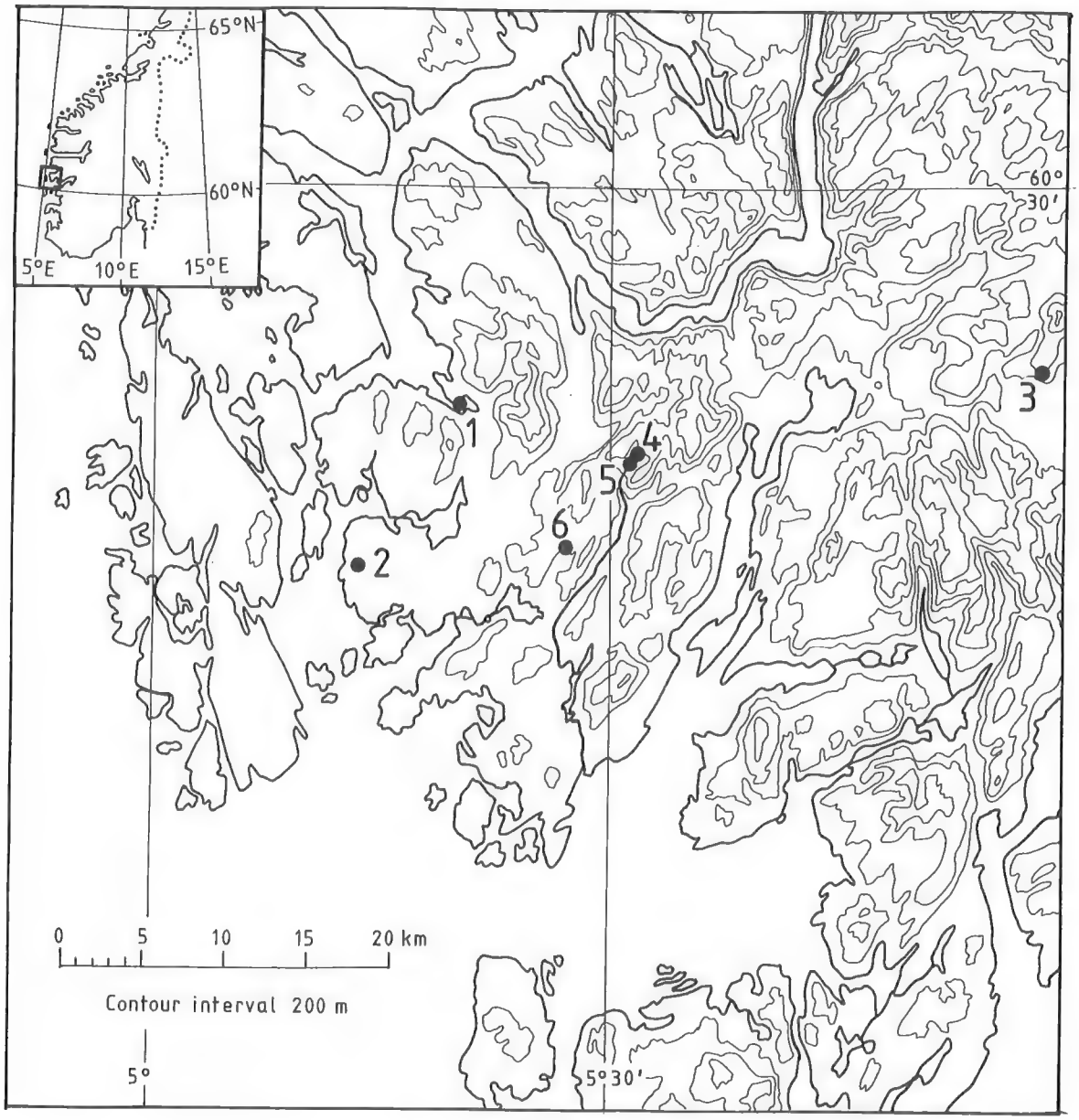

Fig. 2.1. Map of the area.
1 Bergen, 2 Flesland, 3 Kvamskogen, 4 Austlihylla,
5 Dyrdalsvatn, 6 Frotveit.

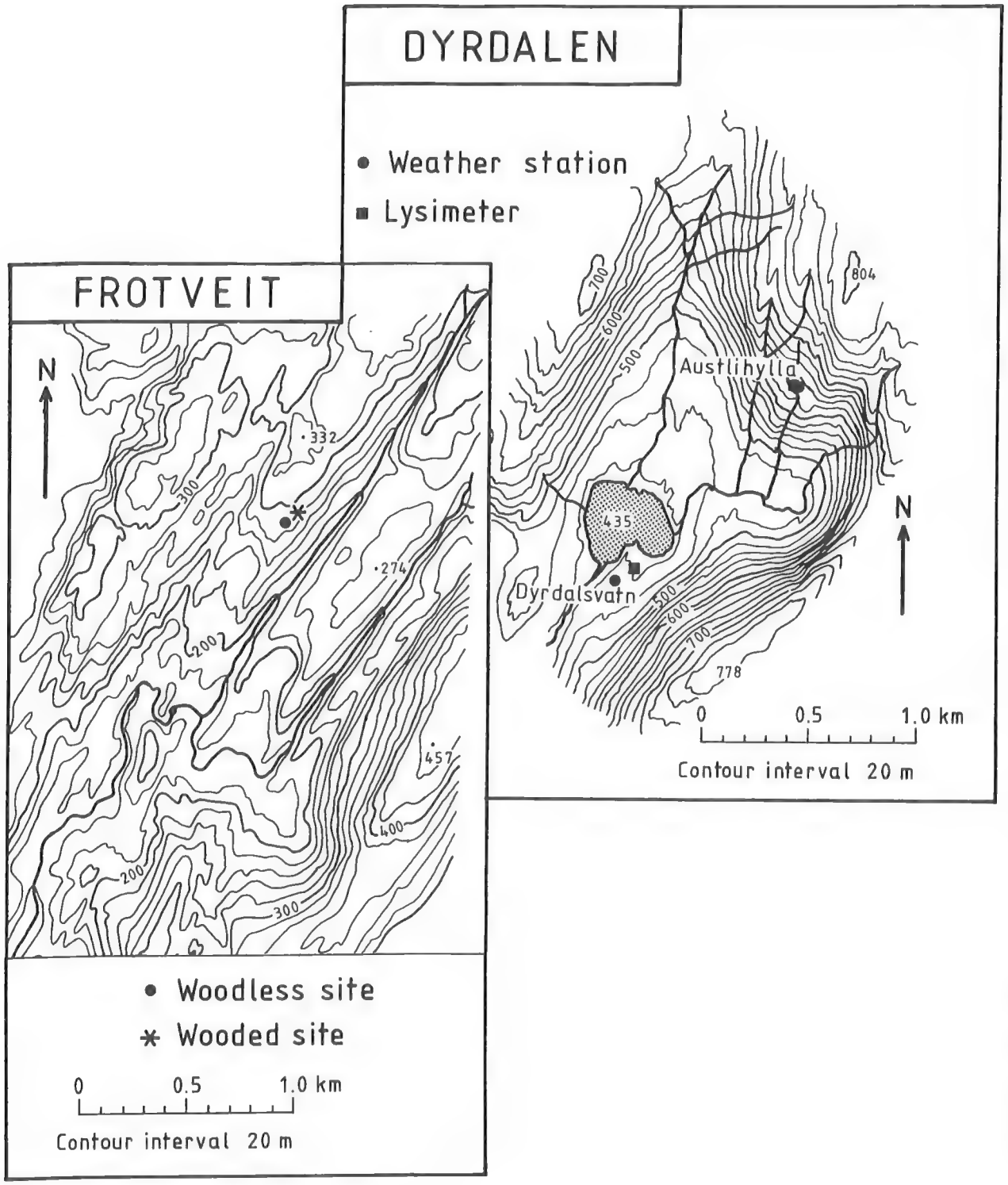

Fig. 2.2. Map of the Dyrdalen and Frotveit areas.

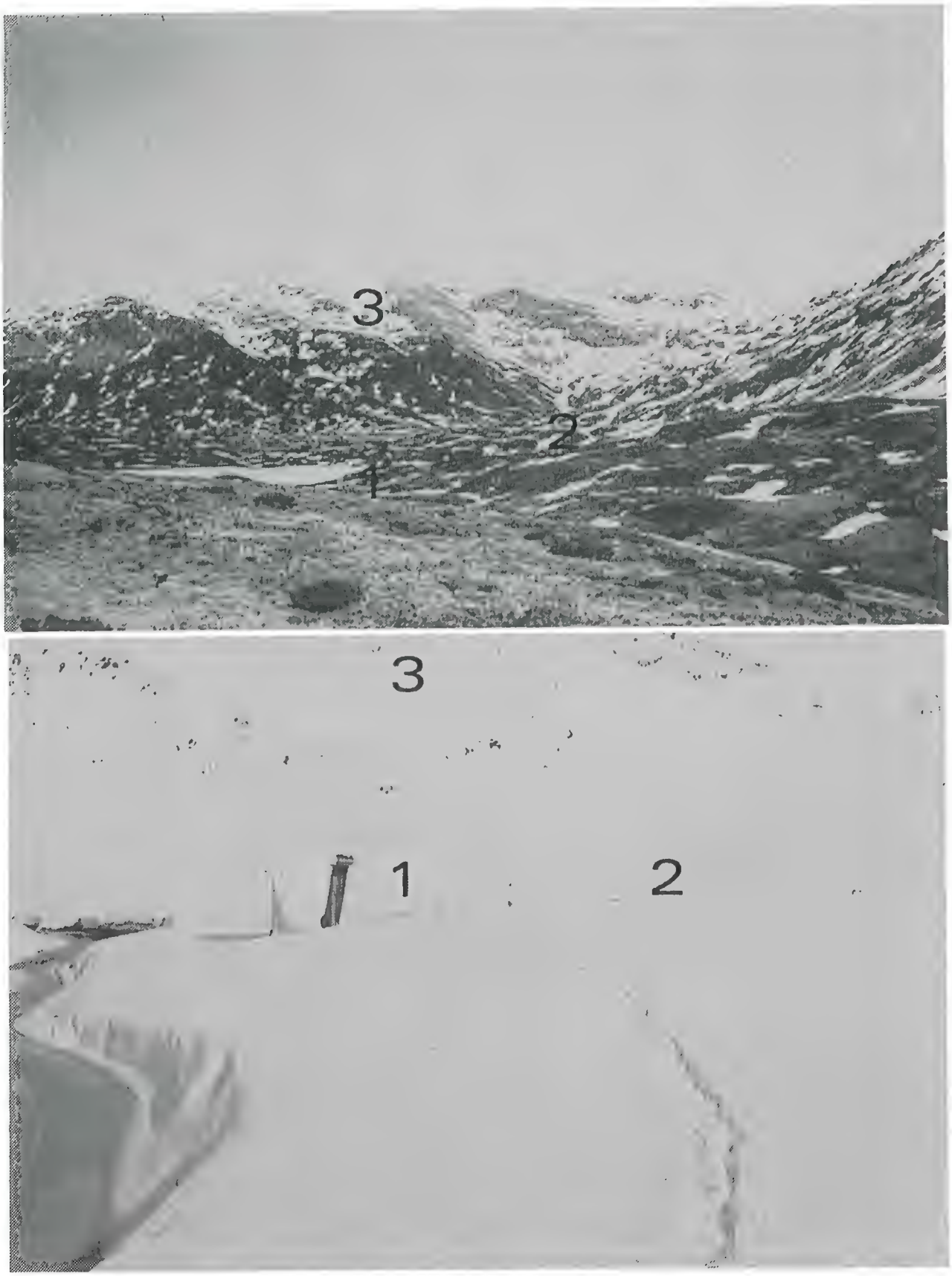

Fig. 2.3. View of Dyrdalen. The snow amounts in March 1979 (below).
1. Dyrdalsvatn (Weather station)
2. Dyrdalsvatn (Lysimeter)
3. Austlihylla

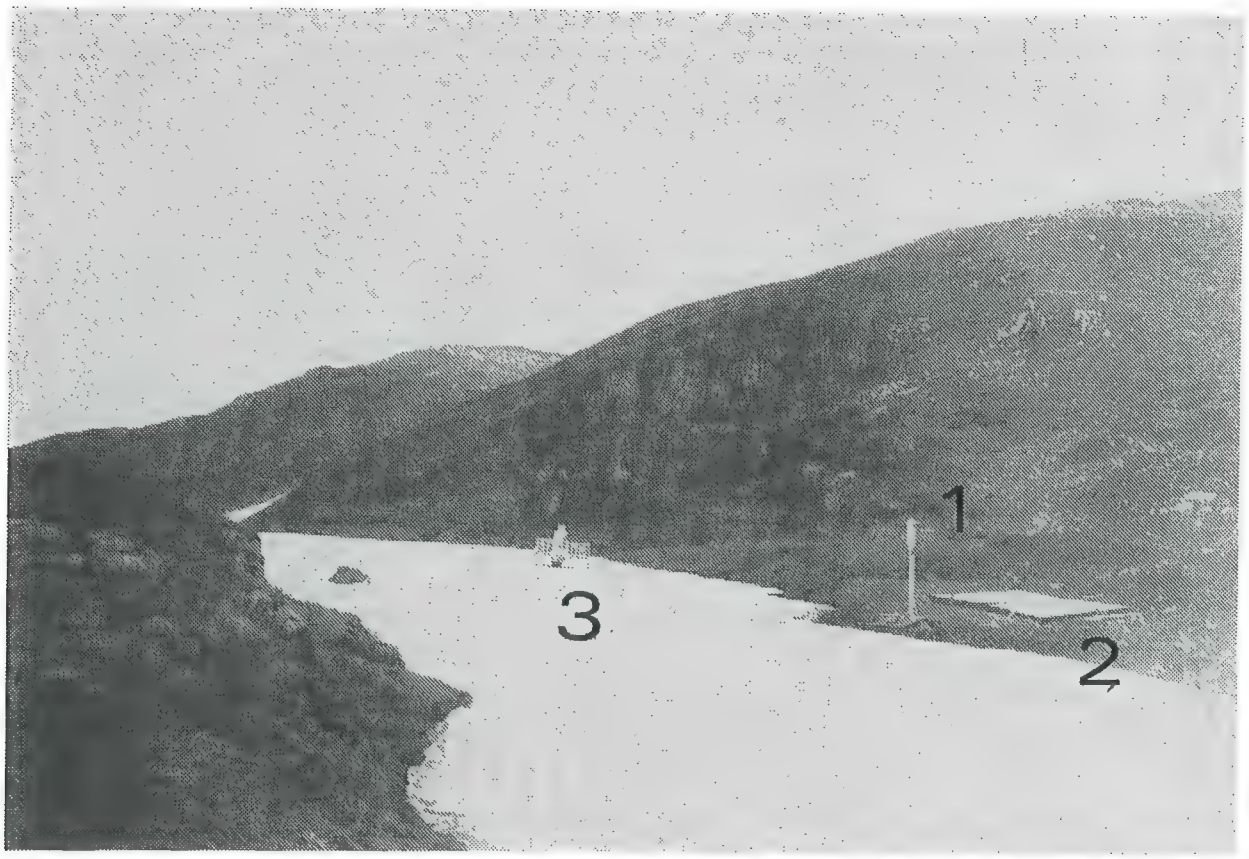

Fig. 2.4. Austlihylla snowmelt station on June 13, 1979.
The snow-drift is illustrated. (The Belfort precipitation gauge which had been damaged by snow weight during this winter was moved to the right of the lysimeter in July.)
1. Weather station
2. Lysimeter
3. Belfort rain gauge

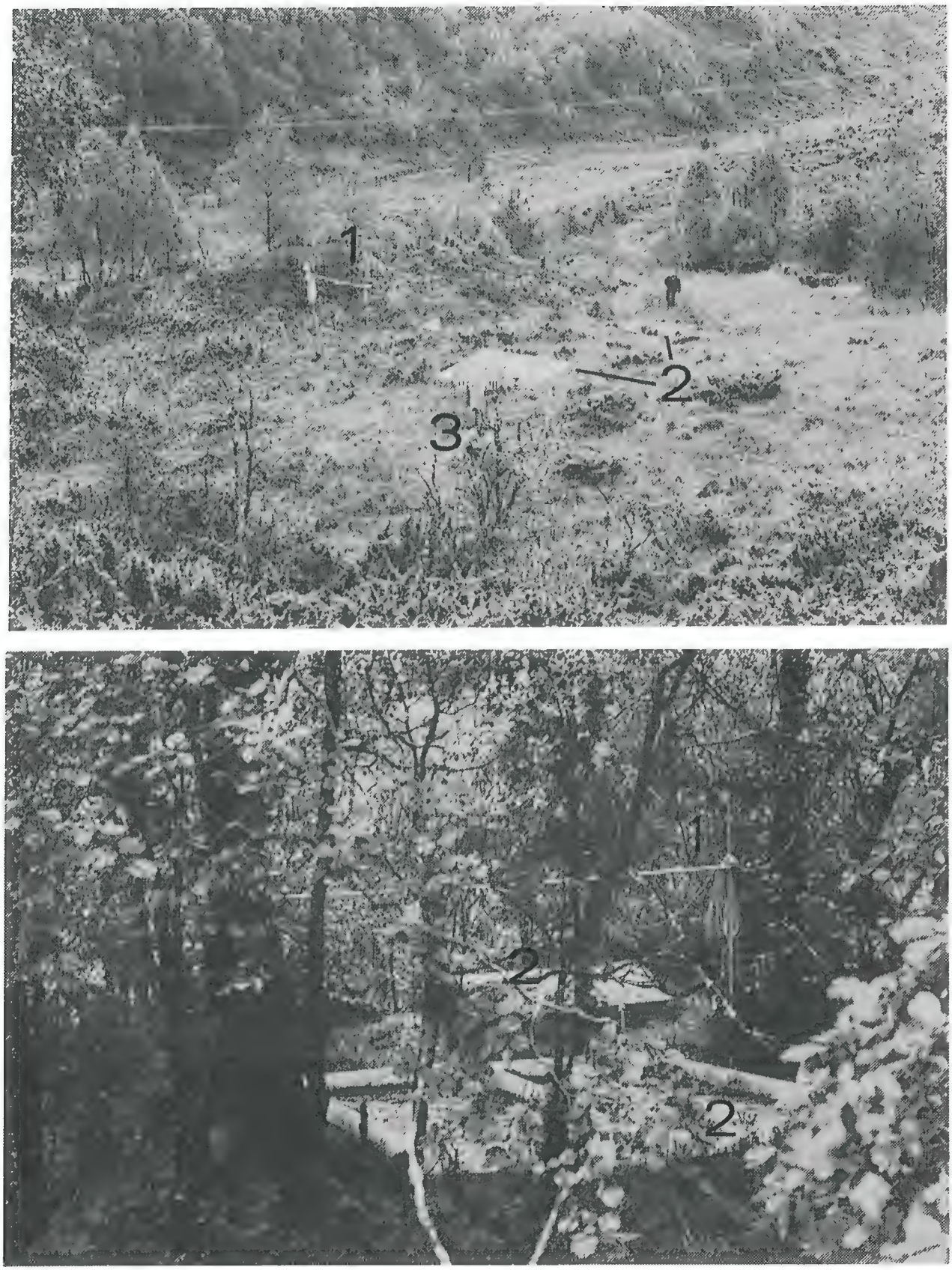

Fig. 2.5. The woodless (above) and wooded (below) site at Frotveit.

1. Stand for Radiation records
   Anemometer
   Hygrometer
   Thermometer
2. Snow lysimeter
3. Rain gauge

2.2. Climatic Review.

Western Norway is exposed to prevailing westerly and south-westerly winds which bring mild and moist air from the North Atlantic Ocean over the country all year. The standard normal of the annual air temperature is about 7 to 8°C in the lower districts, while the monthly values are about 0°C in January and 15°C in July. In March the standard normal is about 2 to 3°C, 5 to 6°C in April, and 10°C in May. The standard deviation of the monthly mean temperature is 2 to 3°C in winter, and 1 to 1.5°C during the rest of the year; it is highest for locations exposed to cold drainage, and lowest near the sea. The annual and monthly values for Bergen and Kvamskogen are illustrated in Fig. 2.6. The temperatures at Dyrdalen should be close to those of Kvamskogen.

The precipitation is high throughout the year (Fig. 2.7). 34% of the annual amount falls in September-November, and 17% in March-May. There is a maximum zone of precipitation in the mountains 30-60 km inland (Førland, 1980 a). The local variations, however, are large due to the rough terrain. The standard normal of the annual precipitation, which is 1958 mm in Bergen and 2755 mm at Kvamskogen, is estimated to 3300 mm at Dyrdalen (Abildsnes, 1980). The highest precipitation amounts recorded at Kvamskogen are: 151 mm in 24 hours (07 p.m. - 07 p.m.), 864 mm over one calendar month, and 4506 mm over one calendar year.

It is difficult to give an adequate description of the wind conditions in the area due to the rough terrain. Fig. 2.8 shows wind roses from Flesland, which is a relatively exposed wind station, near the coast. The monsoon effects are significant with predominating northwesterly to northerly winds in summer and easterly to southeasterly winds in winter. The frequent southeasterly to southerly winds throughout the whole year reflect the cyclones coming from southwest. The surface wind speed at Dyrdalsvatn should be of the same strength in such situations.

For winds from east to southeast, Dyrdalsvatn is sheltered by high mountains. Austlihylla is exposed to these directions, and also to northwesterly winds. Frotveit is far more sheltered than the two higher stations, being most exposed to southwest and northeast.

The cloud cover in Bergen was in average (1901-60) 5.6 octants. The annual distribution (Fig. 2.9) shows a minimum in May. The relative sunshine duration shows a maximum i April-May and a minimum in December. The average duration during 1965-79 was 31% of the possible value.

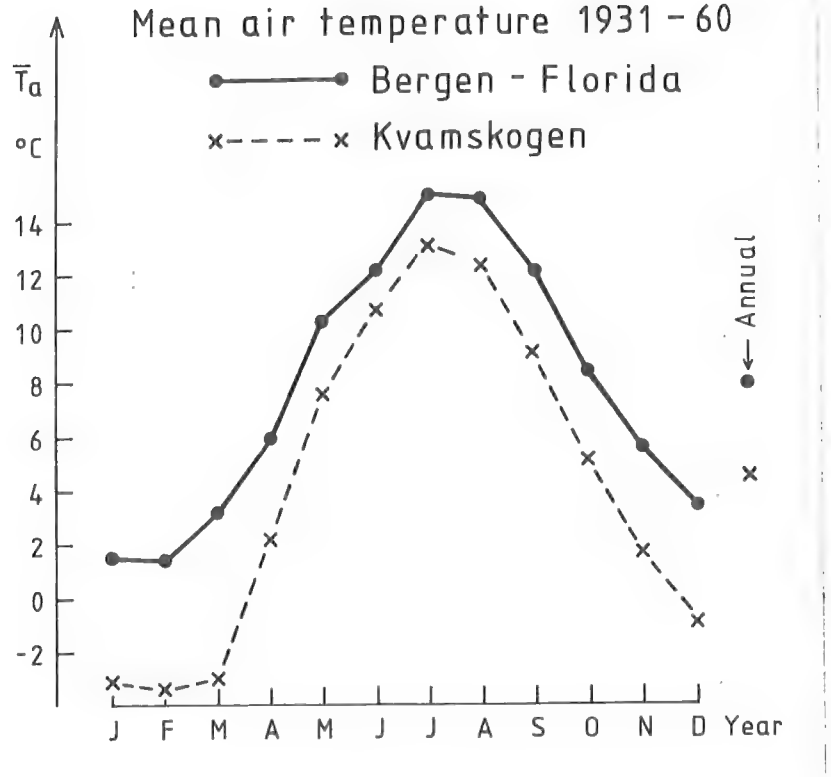

Fig. 2.6. Monthly and annual means of air temperature at Bergen - Florida and Kvamskogen during the period 1931-60.

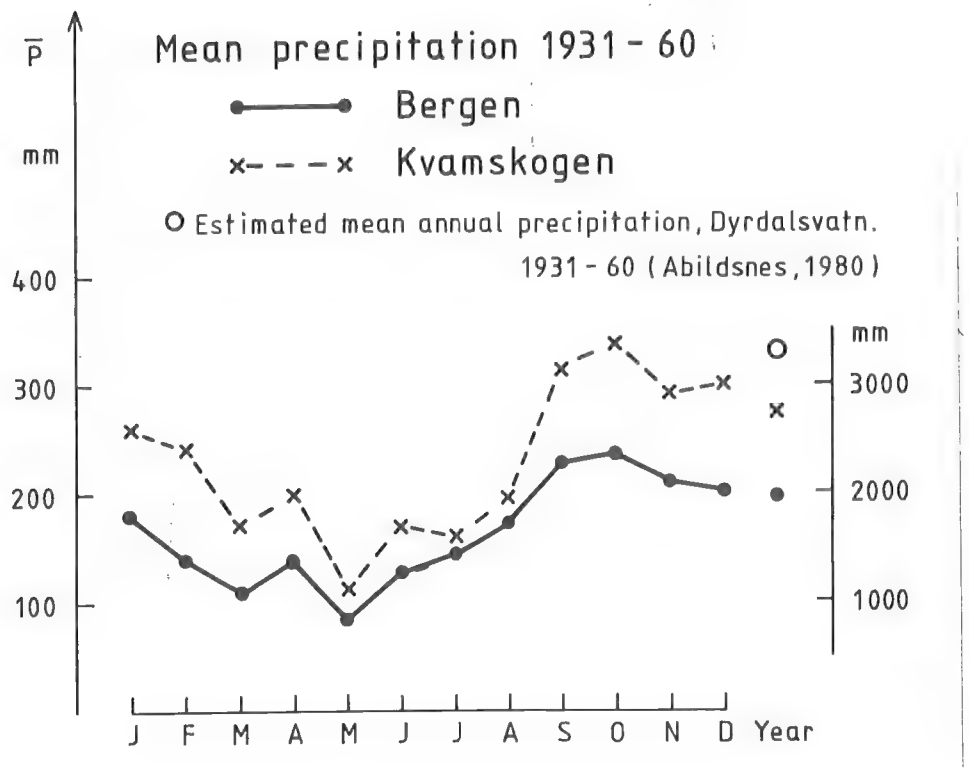

Fig. 2.7. Monthly and annual means of precipitation at Bergen-Fredriksberg and Kvamskogen during the period 1931-60.

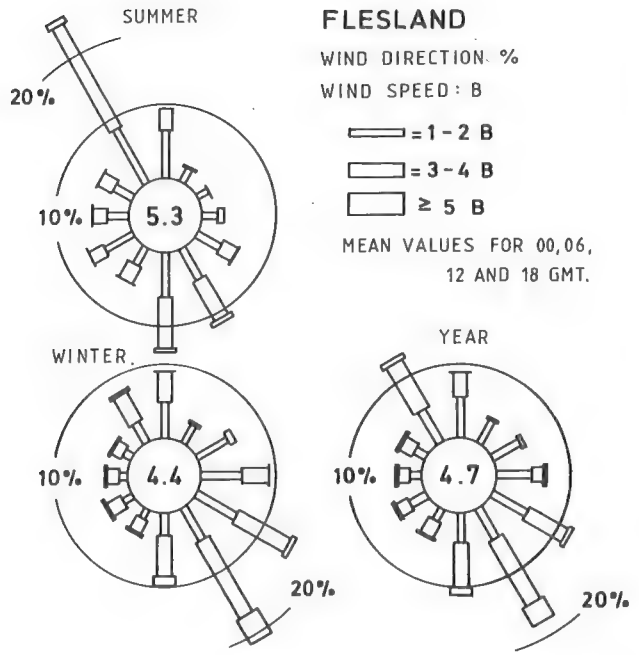

Fig. 2.8. Mean seasonal and annual wind roses for Flesland, 1956-65. % of observations in each of 12 direction sectors; relative fraction of observations in each of 3 speed (Beaufort, B) intervals; % calm at center. Summer: June-August. Winter: December-February.

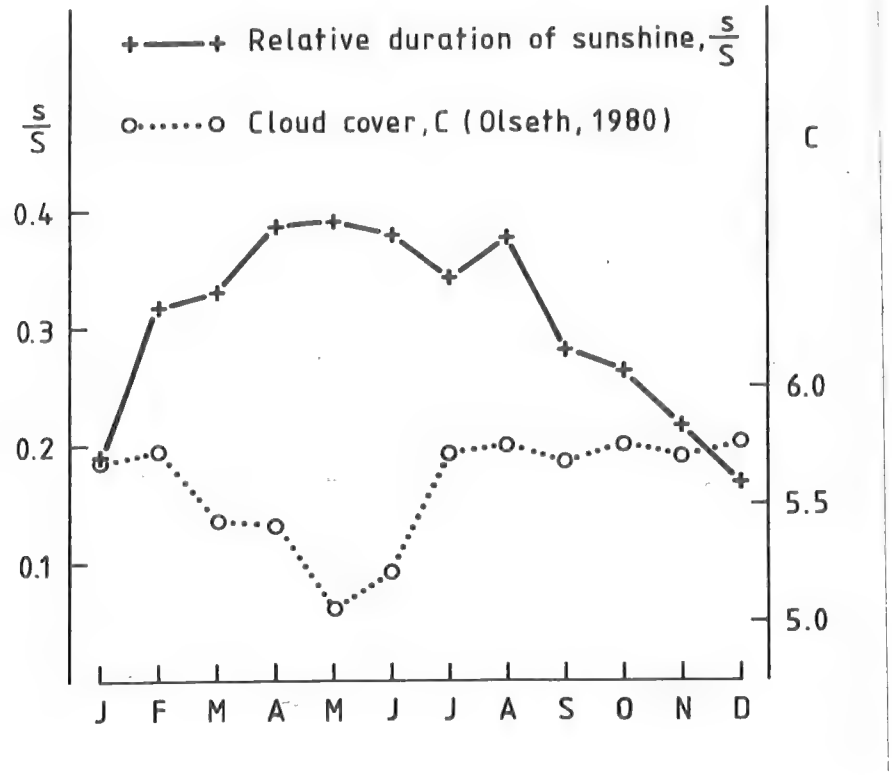

Fig. 2.9. Monthly values of the cloud cover (1901-60) in octants, and the relative duration of sunshine (1965-79).

3. Instrumentation and Methods.

3.1. Instruments, Data and Data Quality.

In the Dyrdalen-Frotveit area records were made at four stations (Table 3.1). All sensors were placed 2 m above snow-free ground, except for the precipitation gauges (1.6 m), and the snow lysimeters (ground level). The micrometeorological instruments had a mean height of roughly 1.3 m above the snow surface during snowmelt.

The data were recorded on magnetic tape every 30 minute by dataloggers manufactured by Aanderaa Instruments, Bergen.

Table 3.1.
Instrumentation and recording periods during snowmelt.

Instrument	Austlihylla	Frotveit I	Frotveit II	Dyrdalsvatn
Snow lysimeter	1980-82	1981-82	1981-82	1979-82
Precipitation gauge	1980-82	1981-82		1979-82
Thermometer	1979-82	1981-82	1981-82	1979-82
Hair hygrometer	1980-82	1981-82	1981	1979-82
Anemometer	1980-82	1981-82	1981-82	1979-82
Net radiometer (Total radiation)		1981	1981	
Net radiometer*				1980-82
Pyranometer (Upfacing)		1981	1981	1979-82
Pyranometer (Downfacing)		1981		1979-82

* Adaptor covering lower hemisphere
I : woodless site
II : wooded site

The snow lysimeter

Snowpack discharge was recorded by a snow lysimeter, described by Tveit (1977) and illustrated in Fig. 3.1. Two polyester vats with walls 0.15 m high were placed side by side at ground level covering a total area of 9 m^2. The vats were allowed to snow down,

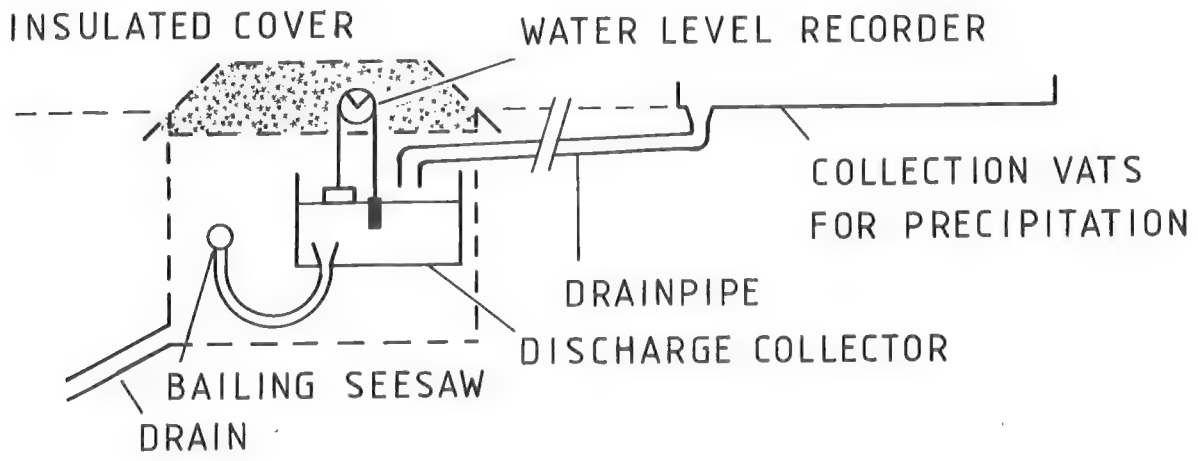

Fig. 3.1. Principle of the snow lysimeter used at Dyrdalen and Frotveit 1979-1982.

and during snowmelt the discharge was recorded by measuring the water level of a tank of capacity 112.5 l (12.5 mm discharge). This collector tank is automatically emptied by a bailing seasaw when the water level reaches the top. It is placed well beneath ground level and insulated against frost. To avoid boundary effects, the data series were truncated either when the snow coverage in the lysimeter fell to less than 90% of the bottom area, or when the corresponding water equivalent fell to less than 50 mm.

The snow cover near to the Dyrdalsvatn snow lysimeter was almost complete during all the snowmelt periods recorded.

Due to percolation resistance in the snow there is a time lag between actual and recorded snowmelt. For daily totals during rain-free snowmelt episodes, however, the well-defined diurnal wave makes time lag corrections unessential, except at Austlihylla where a deep snow cover prevailed. During rain-on-snow events some correction of the timing of the discahrge was necessary, mainly at Austlihylla, and was carried out by comparing lysimeter discharge and rain gauge records.

U.S.A.C.E. (1955) report that there may be a net flow of liquid water over the walls of a lysimeter. When that flow was eliminated (using a technique of adapting the lysimeter edges to the snow depth), their data were very accurate.

Some checks of lysimeter data at Dyrdalsvatn are summed up in Table 3.2. The water equivalent, w.e., determined by measuring snow depth and density on the lysimeter vats, is added to recorded precipitation, P_m , and estimated condensation, CD , accumulated until the lysimeter is completely empty. When comparing this sum to the accumulated lysimeter discharge for the same period, only small deviations are found, indicating that flow across the lysimeter edges at Dyrdalsvatn is a rather small source of error.

By a rough guess the standard error of daily snowmelt is estimated to be within 5%. The mean free water content of the snowpack is supposed to be 4% (Capt. 1). In some cases the snow cover is strongly layered, and the free water content may deviate considerably from this mean value (Colbeck, 1972). The error will then be larger.

At Austlihylla the terrain is sloping (Fig. 2.2), and the snow cover is deep due to the local snow-drifting, conditions which make a significant flow across the lysimeter more likely. However, due to breaks in the lysimeter data series, there is no avaiable snowmelt period for checking at this station.

Table 3.2. Results from checks of lysimeter data of Dyrdalsvatn (see text). Numbers in brackets are rough estimates of the standard errors.

Parameter	Date of measuring, w.e. May 10, 1979	April 16, 1980	April 19, 1982
Number of days till the lysimeter was dry	13	18	6
Water equivalent (w.e.), mm	440 (18)	273 (14)	98 (4)
Precipitation (P_m), mm	210 (20)	56 (6)	28 (3)
Estimated condensation (CD), mm	10 (4)	-6 (2)	0 (1)
w.e. + P_m + CD	660 (27)	323 (13)	126 (5)
Discharge (Q), mm	650 (13)	295 (6)	129 (3)

Table 3.3. Comparison of the daily discharge records from separated lysimeter vats (a,b) at Frotveit during snowmelt 1982. In brackets standard deviation of daily values.

	Woodless site	Wooded site
Number of days	9	11
Daily discharge, Q_a (mm)	14.8 (12.1)	16.3 (13.8)
Daily discharge, Q_b (mm)	15.3 (11.7)	15.4 (12.9)
Correlation coefficient	r_{ab} = 0.998	r_{ab} = 0.999

In 1982 the lysimeter vats at both stations at Frotveit were equipped with separate recorders. Results from the available data are shown in Table 3.3. The correlation coefficients between records for adjacent vats are very high. The systematic deviations are small, especially for the open site. For the wooded site this deviation is probably caused by differential shading by surrounding trees. The analysis indicates that the quality of the discharge data from the lysimeters at Frotveit is high. The standard error should be as low as for Dyrdalsvatn, suggested to be within 5%.

Rain records.

Records of liquid precipitation generally include several sources of error. A comprehensive discussion is given by Dahlström (1970), and Killingtveit (1976). The aerodynamical effect usually represents the largest error. Local effects (vegetation, wind conditions) at the station may make the records unrepresentative of the surrounding area. Other error sources are splash out or into the collector, wetting of the collector, evaporation loss and general interpretation errors introduced when deciphering the data.

Precipitation records were made by weighing pluviographs, type Belfort equipped with Alter type wind shields, 1.6 m above snow-free ground at Dyrdalsvatn, Austlihylla and Frotveit (open site). At Dyrdalsvatn precipitation was also recorded by a tipping bucket pluviograph (OTA) at ground level during parts of the summer seasons. The lysimeters also functioned as ground level rain recorders during parts of the snow-free seasons.

The ground level records are assumed to be free of aerodynamical effects. The integrated error of the OTA record should therefore be very small, and clearly within 0.5-1 mm for daily totals (Förland, 1980). The errors in the lysimeter rain data are within $\pm$ 2% except for splash effects (Killingtveit, 1976). For the Belfort records the error due to aerodynamical effects usually is considerably larger than the integrated error due to other effects ($\pm$ 1 mm for daily totals) (Førland, 1980). At Austlihylla only a few

records are available due to mechanical problems, so no analysis was carried out using those data. The few data indicate, however, that the aerodynamical effect is larger and more variable than at Dyrdalsvatn.

Fig. 3.2 shows some results from an analysis of data recorded during the snow-free seasons of 1979 and 1980. Daily precipitation records, $P_m \geq 10$ mm are grouped according to the amount, 3 in each group. The group mean values of P_o, P_B, and P_L (defined in Fig.3.2) are calculated, and the ratios between corresponding group mean values are plotted against daily precipitation. Lines of linear regression are drawn, though neither of the regression coefficients are statistically significant. However, splash loss from the lysimeter during heavy rain can explain the negative slope of the lines 2 and 3. The figure indicates that the splash loss increases some 1-2% for each 10 mm increase in daily precipitation for totals between 10 and 60 mm. For small daily totals the splash loss is assumed to be zero due to the edges of the lysimeter which catch splash from light precipitation. Accordingly, for daily totals below 10 mm no splash loss from the lysimeter is assumed, and equations 2 and 3 are not valid. For a daily total of 10 mm the OTA and Dyrdalsvatn lysimeter records only deviate with 0.4%. The splash loss is assumed to be zero during rain on snow events, and the equation

$$P \approx P_{LD} \approx P_o = K_p P_B \quad , \qquad (3.1.1)$$

where P is true precipitation, and K_p is the ratio between ground level and 1.6 m level precipitation records, should then be valid.

From Fig. 3.2 $\frac{\bar{P}_o}{\bar{P}_B} = 1.09$ and 1.06 (for $\bar{P}_o = 10$ mm) for the two data sets, comparing data recorded at Dyrdalsvatn by the OTA gauge ($\bar{P}_o$) and the Belfort gauge ($\bar{P}_B$). The difference may be due to different wind conditions during the days involved. Furthermore, $\bar{P}_{LD}/\bar{P}_B = 1.10$ for the set of highest $\frac{\bar{P}_o}{\bar{P}_B}$ value. The average value

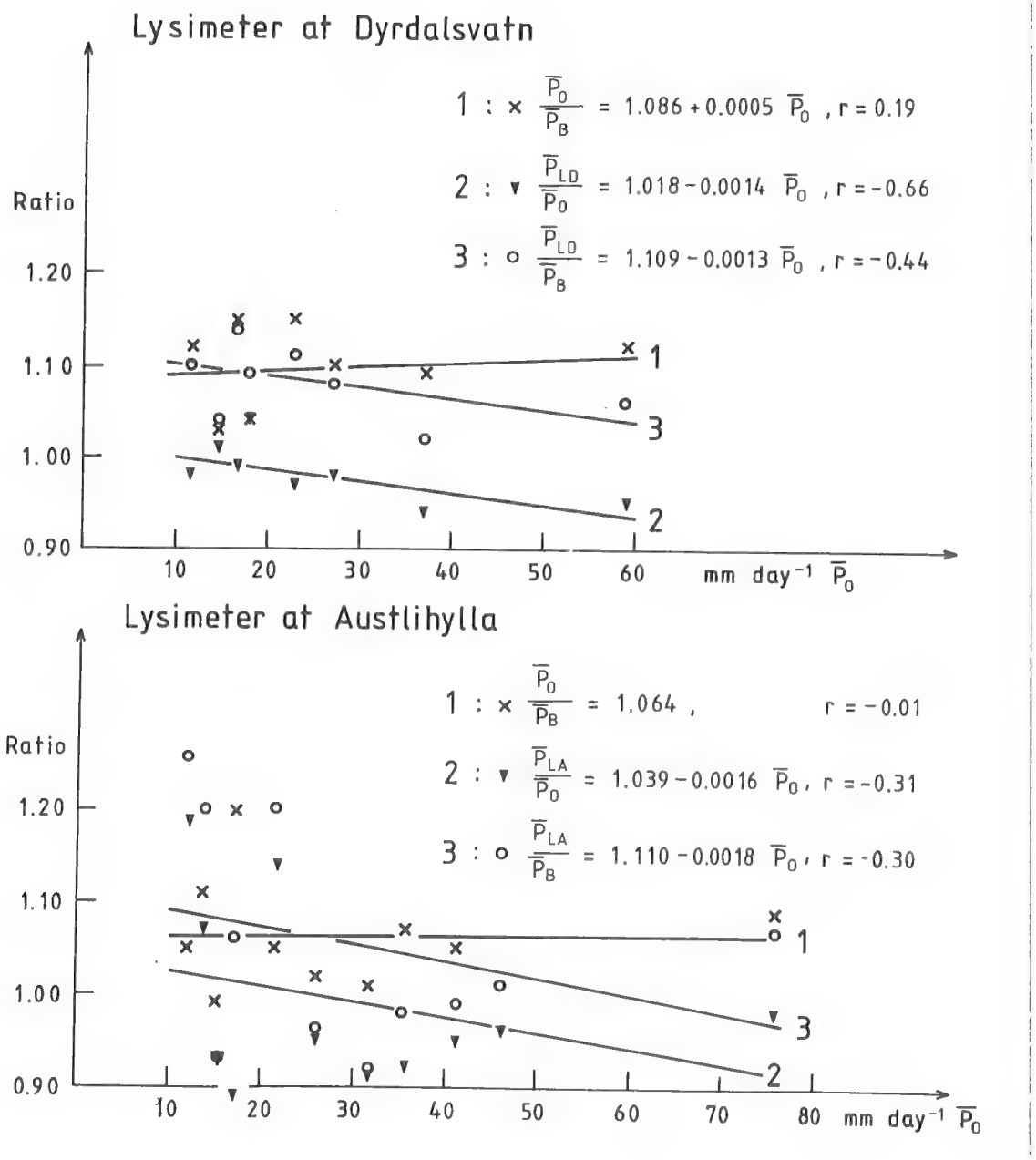

Fig. 3.2. Relation between ratio of recorded rain amount between different recorders and daily totals of precipitation. Each data point represents a group mean value of 3 observations.

P_O : Total of precipitation recorded by OTA pluviograph, Dyrdalsvatn.
P_B : " " by Belfort pluviograph, Dyrdalsvatn.
P_{LA}: " " by lysimeter, Austlihylla.
P_{LD}: " " by lysimeter, Dyrdalsvatn.

of K_p therefore is taken to be 1.08. Abildsnes (1980) found the value 1.08 between ground level and wind-shielded 2 m level precipitation records at Dyrdalsvatn. Furmyr (1975) found 1.09 at Fillefjell.

For Austlihylla $\frac{\bar{P}_{LA}}{\bar{p}_o}$ = 1.02 (for $\bar{p}_o$ = 10 mm), suggesting a 2% increase in precipitation amounts from Dyrdalsvatn to Austlihylla. Therefore, K'_p is put to 1.10, where K'_p is analogous to K_p with the effects of the intersite distance included. When the data published by Abildsnes (1980, pp. 27) are used the precipitation amounts at Dyrdalsvatn and Austlihylla are found to be very equal on the average. There were, however, significant differences between individual episodes depending mainly on the wind direction. From Fig. 3.2. it appears that the dispersion of the $\frac{P_L}{P_B}$ values are larger for the lysimeter at Austlihylla than for Dyrdalsvatn, which should be expected since P_B is recorded at Dyrdalsvatn. The standard deviations of $\frac{P_L}{P_B}$ for daily totals were respectively 17% (n=24) and 6% (n=30) of average ratios at Austlihylla and Dyrdalsvatn.

During the snow-free and leafless season at Frotveit, daily precipitation above 10 mm was recorded for 10 days. The average daily total was only 16 mm and the standard deviation 4 mm for those days. Splash effects should be rather small due to the lack of heavy precipitation records. Therefore the average value of $\frac{P_L}{P_B}$, where P_L is the lysimeter total and P_B is the total recorded by the wind-shielded Belfort rain gauge situated at the woodless site, can be used directly as an estimate for the correction factor of P_B. The values 1.04 and 0.98 are found for the open and wooded sites, respectively, with standard deviation of 5% and, 11%. The low factor at the open site should be due to the lower wind speeds in the area compared to Dyrdalen. For the wooded site the even lower factor 0.98 reflects the fact that some of the precipitation is intercepted on the trees. The standard deviation of 11% reflects that the interception is variable.

To sum up, the daily totals recorded by the wind-shielded Belfort rain gauge at Dyrdalsvatn should be multiplied by 1.08 to estimate true precipitation at this site, and by 1.10 to give estimates

for Austlihylla. At Frotveit the totals recorded by the Belfort gauge should be multiplied by 1.04 to estimate the true precipitation at the woodless site, and by 0.98 to give estimates for the wooded site. These factors are averaged values. The actual values vary with the wind conditions, and for the wooded site, the interception conditions. In percents the standard deviations for the factor K_p (6%, 17%, 5%, and 11%) should be reasonable estimates for the error due to the aerodynamical effect when a first order correction is made. The standard error, ΔP (mm) of "true" precipitation is then given by,

$$\Delta P = P\left(\left(\frac{\Delta K_p}{K_p}\right)^2 + \left(\frac{\Delta P_{BR}}{P_B}\right)^2\right)^{\frac{1}{2}} \text{(mm)} , \qquad (3.1.2)$$

where ΔP_{BR} ($\pm$ 1 mm) is the integrated error due to other effects of the precipitation totals recorded at the Belfort gauge, P_B. For heavy precipitation the second term under the radical is small and the standard error is given by, $\frac{\Delta K_P}{K_P} \cdot P$ (mm) or $\frac{\Delta K_P}{K_P} 100$ (%).

Precipitation during snowmelt.

The precipitation form is related to the air temperature. In Fig. 3.3 is shown the probability for liquid precipitation as a function of the air temperature, T, based on a study in the U.S.A. (U.S.A.C.E., 1956). At $T = 1.5°C$ the probability is 50%. Furmyr (1975) and Killingtveit (1976) both report 1.1°C as the temperature where the precipitation changes from snow to rain.

Accordingly, the precipitation in the Dyrdalen-Frotveit area is assumed to be liquid when the air temperature exceeds 1.1°C. Additional information such as direct observation or obviously snow-covered pyranometers may in some cases improve this classification. Periods with large fluctuations in the precipitation form are excluded from the analysis due to the errors introduced by estimating the rainfall contribution.

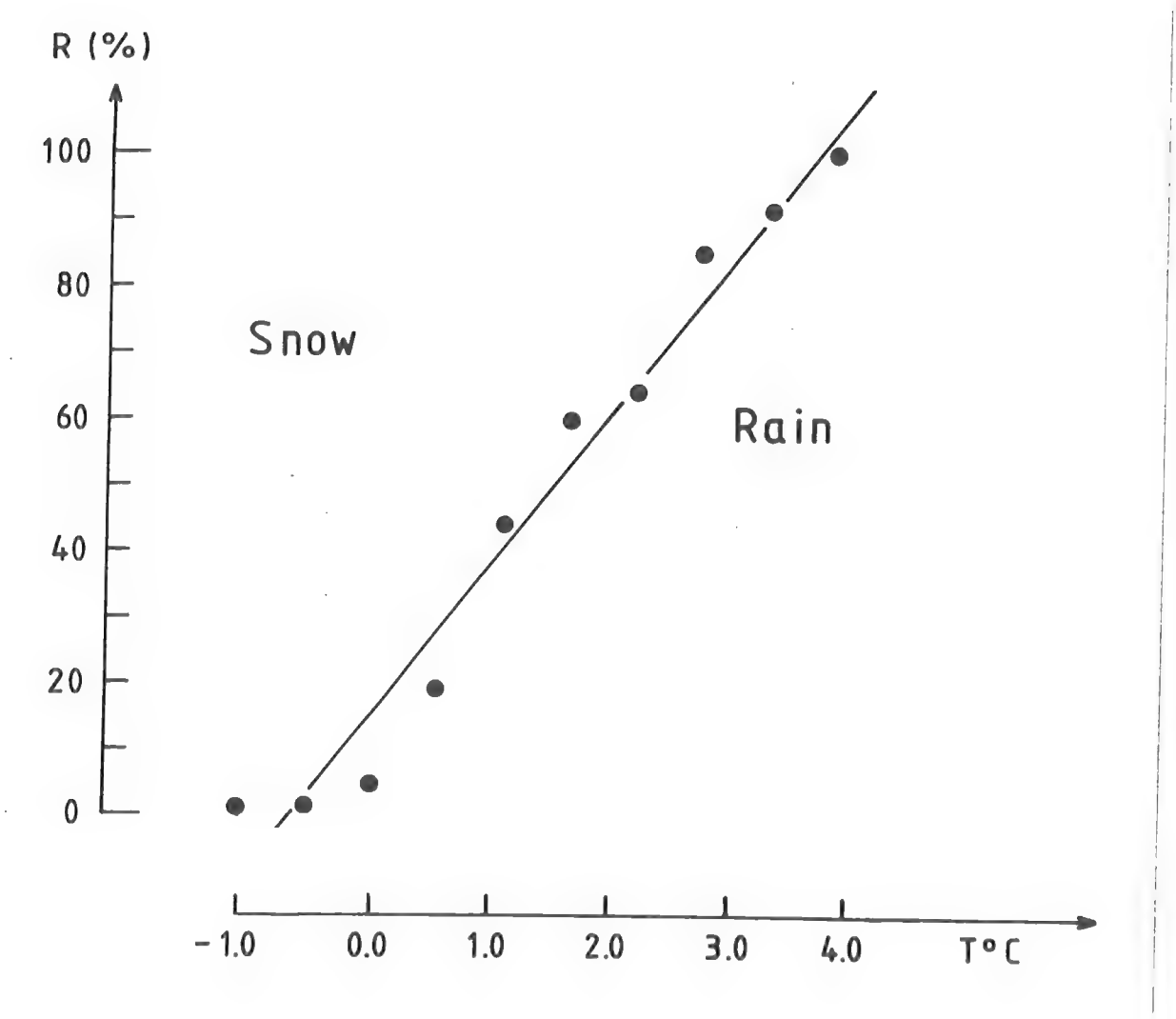

Fig. 3.3. Precipitation form in per cent as group mean values of precipitation within groupes of 0.56°C between -1.4 and -4.1°C (Data from Table 3 - 02.03, U.S.A.C.E., 1956).

During precipitation the snowmelt rate is given by subtracting the rain amounts from the discharge. Standard errors of precipitation records then increase the standard errors of the snowmelt rate. The following example illustrates this effect (for Dyrdalsvatn):

The standard error of the discharge is assumed to be $\pm$ 5%. For a daily snowmelt total of 40 mm this error makes the error of the snowmelt records to $\pm$ 2 mm. If 40 mm rain falls in addition to the snowmelt assumed, the discharge error is $\pm$ 4 mm, and eq. (3.1.2)

gives $\Delta P = 2.6$ mm . The error of the snowmelt total then is increased to $((2.6)^2+4^2)^{\frac{1}{2}}$mm $\approx$ 5 mm or 12%.

For precipitation at air temperatures between 0°C and 3°C, the inaccuracies are further increased due to the mentioned inaccuracies in the classification of the precipitation form.

Air temperature

Platinum resistance thermometers with a resolution of 0.1°C were mounted in radiation screens and the air temperatures were recorded every 30 minutes. The 0°C level was tested by ice calibration twice a year, and the deviation seldom exceeded 0.1°C. Simonsen (1976) found fairly good protection against longwave loss as well as shortwave gain by using radiation screens of the type used in this investigation. Skartveit (1976) estimated the deviation between air temperature observed with an aspirated psyhcrometer and recorded by platinum thermometers in radiation screens of the same type during daytime in clear weather in snow-free conditions. He found a systematic deviation of 0.2°C and a standard deviation of 0.7°C. The low systematic deviation indicates fairly good performance of the radiation screens. Different sampling frequencies and the turbulent character of the air temperature are probably the main reasons for the standard deviation of 0.7°C. During snow covered ground conditions some higher deviations may occur, due to the high reflected radiation flux from the snow cover.

The standard deviation of 0.7°C of the difference between the two types of temperature records referred to, indicates a standard error of 0.5°C for each of the record types. This estimate is adopted for the half-hourly records at the Dyrdalen-Frotveit area. For daily averages, this error obviously is reduced (to 0.1-0.2°C).

Air humidity

Relative humidity was recorded by Lambrecht Feuchtgeber 800 with an 11 cm long hair bundle placed in a radiation screen. The instruments were calibrated at the laboratory once a year, and routine checks against an Assman psychrometer in the field were

performed. The accuracy of the corrected values are within $\pm$ 2% R.H. (Skartveit, 1976). If the standard error of the half-hourly values of the air temperature, T , is $\pm$ 0.5°C, this will be approximately equivalent to a standard error in the vapour pressure, e , of $\pm$ 0.3 mb when T = 3°C . For daily means the error should be within $\pm$ 0.1 mb.

Wind speed

The wind speed was recorded by a 3 cup anemometer with a resolution of 115 m integrated wind travel (0.06 ms^{-1} for $\frac{1}{2}$ hourly means), and a threshold speed about 0.3 ms^{-1}. Skartveit (1976) tested the stability of the calibration factor and found it to be within $\pm$ 1%. The rotor is mounted between two horizontal solid plates, which may introduce spurious aerodynamical effects. During winter the rotor may seize due to snow and ice, but during snowmelt this should not be the case.

At Dyrdalsvatn a 80 cm high fence surrounded the micrometeorological station to protect against grazing sheep and cattle. This may influence the wind speed at the 2 m level. The lysimeter was placed at a distance of some 100 m outside the fence. Thus, the wind field may be different at the lysimeter and the site of recording, but the local variation is probably small, due to the openness of the area on this scale (Fig. 2.3). The wind speed at the wooded site, Frotveit II, was recorded 2 m above the lysimeter. The wind speed in the wood was low, so the relative error is high, due to the threshold speed of the anemometer.

According to the discussion above the errors of the wind speed values are difficult to quantify exactly. A rough guess is 0.2-0.5 m/s for hourly values and 0.1-0.3 m/s for daily values.

Radiation

Global radiation and reflected solar radiation were measured with a Gorczynski solarimeter with Sonntag thermopiles. According to

Sonntag (1964), this instrument has an accuracy of $\pm$ 3%. The thermopile can be considered independent of temperature, solar altitude, and azimuth (Radiation Yearbook, 1980).

The instruments were calibrated each year, and the stability of the calibration factors was within 3%. An albedo of 60-70% and an inaccuracy of $\pm$ 3% in each of the daily recorded incoming and reflected shortwave radiation terms produce a standard error of some 10% in absorbed shortwave radiation. The errors of the two fluxes are probably correlated, making this standard error even lower.

Net radiation, Q_N , is defined by,

$$Q_N = Q_S(1-\alpha) + Q_{L\downarrow} - Q_{L\uparrow} \quad , \qquad (3.1.3)$$

where Q_S is the global radiation, α the albedo of the surface, $Q_{L\downarrow}$ the incoming and $Q_{L\uparrow}$ the outgoing longwave radiation. Assuming the emissitivity of snow, $\varepsilon \tilde{\sim} 1$ (Anderson, 1976, used the value 0.99), then $Q_{L\uparrow} = \sigma T_o^4$, where σ is the Stefan Bolzmann constant ($5.669 \cdot 10^{-8} Wm^{-2}K^{-4}$) and T_o is the snow surface temperature.

Q_N was measured by Siemen Ersking net radiometers. Calibrations made at the Radiation Observatory in Bergen show that the factors given by the manufacturer should be lowered by some 10%. This result was also found by B. Holmgren, Uppsala (pers.comm.). At Dyrdalsvatn only the incoming total radiation was measured, by changing the lower lupolen hemisphere for an adaptor. The instrumental temperature, T_i , was also recorded, and we have from (3.1.3):

$$Q_{L\downarrow} = Q'_N + \sigma T_i^4 - Q_S \quad , \qquad (3.1.4)$$

where Q'_N is the net radiation at a black surface of temperature, T_i

It should be reasonable to accept a 10% error in the average records of Q'_N . For daily values this error will be lower. T_o is very precisely determined, and Q_S : $\pm$ 3% . For average values of

100 Wm^{-2} for Q'_N, 330 Wm^{-2} for σT_i^4, and 150 Wm^{-2} for Q_S, then $Q_{L\downarrow}$ = 280 Wm^{-2} with an error of $\pm$ 10 Wm^{-2} or less. The accuracy of $Q_{L\downarrow}$ when recording Q'_N by the more accurate Schulze net radiometer is $\pm$ 2% (Paulsen, pers. comm.), which is 6 Wm^{-2} in our case. It should then be reasonable to put the accuracy of $Q_{L\downarrow}$ (daily values), when using the Ersking instrument, to $\pm$ 8 Wm^{-2} ($\pm$ 3%).

The outgoing longwave radiation, σT_o^4, is constant when the snow surface temperature, T_o, is at the melting point. When the air temperature, T_a, < 273 K, a snow surface temperature parameterization given by

$$T_o = 2 \cdot T_a - 273 \quad (°K) \qquad (3.1.5)$$

may be used (Harstveit, 1981). Since the snow surface is at melting point during most of the field measurements used, the error of the term σT_o^4 is small. The errors influencing the accuracy of Q_N are then due to absorbed shortwave radiation (< 10%) and $Q_{L\downarrow}$. For average values of these quantities (some 50 Wm^{-2} and 280 Wm^{-2}) a simple error analysis produces a standard error of $\pm$ 10 Wm^{-2} for daily values of Q_N.

Dew formation on the hemispheres may some times enlarge the errors.

Extrapolated data of incoming longwave radiation, $Q_{L\downarrow}$, recorded in Bergen were used to fill gaps in the measurements at Dyrdalsvatn. Harstveit (1981) estimates an average decrease in $Q_{L\downarrow}$ of 24 Wm^{-2} from the Radiation Observatory in Bergen to Dyrdalen based on the height gradient suggested by Kuzmin (1961). During 1980-82 $Q_{L\downarrow}$ was recorded at Dyrdalsvatn. A comparison of the records from Bergen and Dyrdalsvatn during spring snowmelt (65 days) showed a mean difference of 17 Wm^{-2} with a standard deviation of 11 Wm^{-2}. Given the limited accuracy of longwave radiation measurements and the possibility of differing cloudiness between the two stations, the measured 17 Wm^{-2} mean difference is in reasonable agreement with the estimated 24 Wm^{-2} mean difference. The value 17 Wm^{-2} is used in this investigation.

3.2. The Energy Balance Model for Snowmelt.

The complete energy exchange for a snowpack can be written:

$$Q_M + Q_I = Q_N + Q_H + Q_E + Q_G + Q_R \quad , \qquad (3.2.1)$$

where

Q_M = energy used in melting the snow

Q_I = changes in internal energy of the snow pack

Q_N = net radiation of the snow cover

Q_H = sensible heat flux from the atmosphere

Q_E = latent heat flux from the atmosphere

Q_G = heat flux from the ground

Q_R = energy gained from rainwater.

In the case of snowmelt some of these terms are negligible. The snow pack may be composed of water in liquid and solid phase. For a snow pack which is not ripe or isothermal any energy supply will first be used to increase the internal energy of the snow pack, by raising the temperature or increasing the free water content. Analogously, energy loss will correspond to a decrease of the internal energy. During parts of the spring snowmelt season such variations occur througout the day. In this investigation only days where the snow pack can be considered ripe and isothermal, except for daily variations, are used. For daily totals Q_I is therefore a negligible term.

Heat is stored in the ground during the summer season. In winter this stored heat may be used in melting the snow. The heat flux, Q_G , may be expressed by

$$Q_G = K_G \frac{dT_G}{dz} \quad (Wm^{-2}) \quad , \qquad (3.2.2)$$

where K_G is thermal conductivity and $\frac{dT_G}{dz}$ temperature gradient in the surface layer of the soil. U.S.A.C.E. (1956) found this heat flux to be in the range of 0-4 Wm^{-2}, equivalent to 0-1 mm

daily snowmelt. Granger (1977) found about the same values in Canadian prairie environments. This flux is accordingly considered negligible in our case.

When rain of temperature $T_R < 0°C$ falls on a melting snow cover the rain water will be cooled to 0°C and the released heat used in melting the snow. For a ripe and isothermal snow pack

$$Q_R = T_R \cdot P_I C_w \rho_w \qquad (Wm^{-2}) \quad , \qquad (3.2.3)$$

where P_I is the rainfall rate (mm day^{-1}) and C_w and ρ_w are spesific heat and density of water, respectively. Thus, a daily total of 10 mm rain at a temperature of 5°C yields $Q_R = 2.4\ Wm^{-2}$, which would produce 0.6 mm melt water. Therefore, the term Q_R is in general negligible.

Accordingly, net radiation, Q_N, and the turbulent fluxes of sensible (Q_H) and latent (Q_E) heat from the atmosphere are the significant energy fluxes feeding the energy consumption, Q_M, in snowmelt, viz.

$$Q_M = Q_N + Q_H + Q_E \quad , \qquad (3.2.4)$$

which is the basic equation of our energy balance model.

3.3. Turbulent Fluxes of Heat.

Here we will first show how the turbulent fluxes can be estimated from measurements of air temperature, air humidity, and wind speed. Net radiation will be discussed in a subsequent chapter.

Sensible (Q_H), and latent (Q_E) heat is exchanged between the surface and the atmosphere due to vertical gradients in the air temperature and vapour pressure above the snow surface. Since almost 100% of this heat is transferred by turbulence, these are highly wind-dependent. During neutral stability the turbulent heat fluxes may be expressed by

$$Q_H = \rho_a c_p C_D u \, (T_a - T_o) \quad , \qquad (3.3.1)$$

$$Q_E = \frac{\rho_a c_p C_D}{\gamma} u \, (e_a - e_o) \quad , \qquad (3.3.2)$$

where Q_H and Q_E are defined positive downwards, ρ_a is the density and c_p the spesific heat of the air, T is the air temperature (°C), e is the vapour pressure (mb) and u is the wind speed at the level a (ms^{-1}). C_D is the bulk transfer coefficient, which from theoretical considerations assuming idealized experimental conditions, turns out to be

$$C_D = \kappa^2 / (\ln \frac{Z_a}{Z_o})^2 \quad , \qquad (3.3.3)$$

where κ is von Karman's constant (0.41), Z_a the instrumental height (m), and Z_o is the surface roughness (m). γ is defined by

$$\gamma = \frac{c_p \cdot P_a}{0.622 \, L_i} \quad (mb \cdot K^{-1}) \quad , \qquad (3.3.4)$$

where P_a is the atmospheric pressure (mb) and L_i is the latent heat of sublimation ($JK^{-1}kg^{-1}$).

The stratification above a melting snow cover is generally stable, and the equations (3.3.1) and (3.3.2) should be modified according to the Monin-Obukhov similarity theory, which is also based on idealized conditions. Following Anderson (1976),

$$Q_H = f(u)(T_a - T_o) \qquad (3.3.5)$$

$$Q_E = \frac{1}{\gamma}(u)(e_a - e_o) \quad , \qquad (3.3.6)$$

where $f(u)$ is the wind function defined by

$$f(u) = \rho_a c_p C_D (1 - Ri_c^{-1} Ri_B)^2 u \quad . \qquad (3.3.7)$$

Ri_c is the critical Richardson number, and Ri_B is the bulk Richardson number, defined by

$$Ri_B = \frac{2\ g\ Z_a (T_a - T_o)}{(T_a + T_o) u^2} \quad , \qquad (3.3.8)$$

where the temperatures are given in °K, and g is the acceleration of gravity. The Richardson number reflects the ratio of the consumption of energy by the buoyancy forces to the rate of production by wind shear. The critical Richardson number is the value of Ri_B beyond which turbulent conditions no longer exist. Businger (1973) found this value to be 0.15-0.25. Brutsaert (1972) found that increasing evaporation and radiation losses increase Ri_c. He concluded that there is no critical value, rather a range of values between 0.25 and 0.5, below which turbulence is very likely, and above which turbulence is improbable.

When Ri_c and C_D are known we may compute the heat fluxes Q_H and Q_E from data of the surface temperature, and the air temperature, humidity and wind speed at a level Z_a. To determine C_D the surface roughness, Z_o, must be known.

During snowmelt periods, T_o and e_o are assumed to be 0°C, and 6.11 mb, respectively, which should in general be valid except for some calm, cold nights. Usually Ri_B exceeds Ri_c during such nights, and the theory fails. Due to fluctuations in the average wind field, turbulence will occur as soon as Ri_B falls below Ri_c. This "bursting" process is described by Brutsaert (1972). The average turbulence during these nights, however, is small, and

Q_H+Q_E is negligible (Harstveit, 1981). For stations where low wind speeds prevail during the day the theory will not be suitable.

The required horizontal homogeneity of the parameters and input data is not fulfilled most places in Western Norway due to the rough terrain. At Dyrdalsvatn the small scale variations (100-300 m scale) are small when the snow covers most of the ground, which was the usual situation during the periods of recorded snowmelt discussed here. On a larger scale, however, the terrain is rather rough (Fig. 2.2), and this may make the method less accurate. At Austlihylla the scale of horizontal homogeneity is smaller (50-100m), which further increases the inaccuracy. A snow-drift 200 to 300 m long and 20 to 30 m wide usually builds up there, and this drift does not disappear until June or late May. At Frotveit the diverse vegetation makes the application of the theory rather doubtful.

Accordingly, the question arises whether a simpler wind function may be substituted for (3.3.7). The following functions are tested:

$$f_1(u) = a_1(1-Ri_B Ri_c^{-1})^2 u \quad , \qquad (3.3.9)$$

$$f_2(u) = a_2 u + b_2 \quad , \qquad (3.3.10)$$

and $$f_3(u) = a_3 u^{b_3} \quad . \qquad (3.3.11)$$

Now, we recall that if net radiation, Q_N , is measured, the melting rate, Q_M , may be predicted from eq. (3.2.4) provided the turbulent fluxes (Q_H , Q_E) are estimated from any of the wind functions (3.3.9)-(3.3.11) and the recorded air temperature, air humidity, and wind speed. The adjustable constants of these wind functions are then optimized by minimizing the residual error σ_r :

$$\sigma_r = (\Sigma(Q_M' - Q_M)^2 n^{-1})^{\frac{1}{2}} \quad , \qquad (3.3.12)$$

where Q_M' is the measured and Q_M the computed daily snowmelt, and n is the number of days. As a measure of the goodness of the models, we may also use the efficiency of the model, R2 , defined by

$$R2 = 1-\sigma_r^2 SD^{-2} \qquad (3.3.13)$$

where SD is the standard deviation of the recorded daily snowmelt, defined here by

$$SD = \{\frac{1}{n-1}\Sigma(Q_M' - \overline{Q_M'})^2\}^{\frac{1}{2}} \qquad (3.3.14)$$

with $\overline{Q_M'}$ as the mean of recorded daily snowmelt.

The wind function $f_1(u)$ implies an explicit account of varying stability. The optimal value of a_1 is related to the temporal average of surface roughness, z_o. Eq. (3.3.9) then corresponds to eq. (3.3.7), and, recalling eq. (3.3.3), it is seen that a_1 is given by

$$a_1 = \rho_a c_p C_D = \rho_a c_p \frac{\kappa^2}{(\ln \frac{z_a}{z_o})^2} \quad (Jm^{-3}K^{-1}) \quad , \quad (3.3.15)$$

and from this we get,

$$z_o = z_a e^{-(\rho_a c_p)^{\frac{1}{2}} \kappa a^{-\frac{1}{2}}} \qquad (m) \qquad (3.3.16)$$

In this way it is possible to calculate a temporal average of surface roughness from assumptions of Ri_c, and records of air temperature, air humidity, and wind speed at a level z_a, net radiation and snowmelt rate.

The simpler wind functions (3.3.10), and (3.3.11) may be interpreted as weighted averages of actual stability conditions. The linear wind function (3.3.10) should be suitable also for wind-sheltered sites in that b_2 may be interpreted as an average of the turbulent activity for zero wind speed records. b_2 should of course be positive if adequately determined.

3.4. Degree-Day Models for snowmelt.

The degree-day (or temperature index) model in its most simple form is a linear regression model, stating that the daily snowmelt, S_m, is related to the daily mean temperature, $\bar{T}$, by

$$S_m = \begin{cases} k(\bar{T} - T^*) , & \bar{T} \geq T^* \\ 0 , & \bar{T} \leq T^* \end{cases} \qquad (\text{mm day}^{-1}) \qquad (3.4.1)$$

where the degree-day constant, k (mm $day^{-1}°C^{-1}$) , and the threshold temperature, T* (°C), should be determined by regression analysis. The model says nothing about the physical processes causing snowmelt, and is therefore more or less a blackbox model. The advantage of the model is its simplicity, and its success is due to the fact that the air temperature is more or less correlated to air humidity and net radiation, and hence to the terms Q_N , Q_H , and Q_E in the energy balance model (3.2.4). This intercorrelation is different for different weather types, different seasons, and different terrains, however, and there is usually no correlation between wind speed and air temperature. The greatest disadvantage is that it has to be optimized for the specific area before it can be applied with any confidence. In areas exposed to wind and changing weather it fails. Østrem (1974) clearly demonstrates this point. He found fairly good correlation between runoff and air temperature (r = 0.74 for the ablation season 1971) at Austre Memurubre (61°33'N, 8°30'E), a valley glacier in the central part of Southern Norway sheltered against westerly weather. The Ålfotbreen glacier (61°45'N, 5°40'E), covering exposed mountains near the coast of Western Norway, however, did not seem to respond significantly to variations in air temperature (r=0.05). The investigation of Hendrie and Price (1978) clearly shows that different degree-day constants have to be applied for deciduous and coniferous forests.

Various improved forms of the degree-day method are in use today. The daily mean air temperature may be substituted by daily maximum or daily minimum temperature, and the model may be improved by taking physical principles into account. Otnes and Ræstad (1979) suggest the equation

$$S_m = [k_1(1 - \cos \frac{2\pi I}{365}) + k_2][\bar{T} - T^*] \quad , \qquad (3.4.2)$$

where I is the day number of the year. Such a seasonal dependence should appear due to variations in global radiation and albedo,

ripening of the snowpack, and small scale advective effects during periods with partly snow-covered ground. Kuusisto (1978) suggests improvements by adding a radiation term to the model.

Use of different degree-day constants during humid and dry weather may also improve the model. This is suggested by Anderson (1976) and Obled (1973). The snowmelt, Sm, may then be given by,

$$Sm = \begin{cases} k_1(T-T^*_1) \text{ , } T > T^*_1 \\ 0 \text{ , } T \leq T^*_1 \end{cases} \text{ , dry weather}$$

$$\begin{cases} k_2(T-T^*_2) \text{ , } T > T^*_2 \\ 0 \text{ , } T \leq T^*_2 \end{cases} \text{ , humid weather} \qquad (3.4.2)$$

where the cloud cover, or a precipitation indicator may be used in classifying the weather type. Roughly speaking, however, all the mentioned refinements of the simple degree-day model more or less implicitly draw in fragments of the energy balance model.

4. Results and Discussion.

4.1. Observed Data.

The deviation from the longterm average of the air temperature and the total of precipitation during the winter and the spring 1979-82 are shown in Table 4.1. The most distinct deviations are that the winters (1979-80) were colder than normal, April (1979-81) drier, May 1979 colder and wetter, and May 1981 warmer and drier.

Table 4.1. Deviation from the longterm average (1931-60) air temperature at Bergen-Florida and percent of the longterm average precipitation total at Bergen-Fredriksberg during winter and spring 1979-82.

	Winter season (Jan., Feb., March)		April		May	
1979	-1.9°C	112 %	+0.2°C	63 %	-2.5 %	196 %
1980	-0.8°C	63 %	+0.4°C	57 %	+0.4°C	74 %
1981	-0.4°C	146 %	-1.0°C	41 %	+2.0°C	44 %
1982	+0.6°C	120 %	-0.5°C	124 %	-0.6°C	127 %

In accordance with the low air temperature, very few snowmelt episodes occurred in Dyrdalen during the winters 1979 and 1980, and in 1979 the snow amounts were particularly large (Fig. 2.3).

The periods of recorded snowmelt during which the snowpack could be classified as approximately ripe and isothermal except for diurnal variations are shown in Table 4.2. The spring snowmelt season in 1979 should be commented on. During most of April the snow was melting. From April 29 through May 6 snowpack again accumulated. This newly fallen snow ripened very rapidly, but the snowpack was strongly layered in the first half of May. During the subsequent days the whole snowpack quickly melted off.

Diurnal averages of air temperature, humidity, wind speed, and totals of precipitation and snowmelt at Dyrdalsvatn in 1979-82 are shown in Fig. 4.1. Also shown are the radiation fluxes and albedo of the snow surface. The mean melting rate was 11.4 mm day^{-1} with a standard deviation of 15.3 mm day^{-1}. On May 21, 1979, there was recorded a melting of 110 mm (which requires an energy input of 430 Wm^{-2}).

At Frotveit measurements were carried out within a deciduous wood and at an open site nearby. Fig. 4.2 shows the weather conditions during recorded snowmelt 1981 and 1982. Air temperature and humidity are nearly identical at the two sites. On the average the air temperature is 0.1° lower and the relative humidity 2% higher within the wood than outside. This promotes a corresponding increase of 0.1 mb of the water vapour pressure. More significant deviations are found in the wind speed records, average values being 0.3 ms^{-1} and 0.6 ms^{-1}, respectively, and by correlating daily values observed at the two sites, a correlation coefficient of only 0.58 appeared. A check against maps shows that for southerly winds (up-valley), which are often accompanied by precipitation, the wind speed is considerably higher at the open site. For down-valley winds, which often prevail during clear weather in early spring, the wind speed may be slightly higher at the wooded site. The open site is then sheltered by the wood.

For 12 days during March-April 1982 the average wind speed at Dyrdalsvatn was 1.4 ms^{-1}, and only 0.4 ms^{-1} at the woodless Frotveit site. The low wind speed values at Frotveit are due to the topography and vegetation conditions.

At Austlihylla (Fig. 2.2, 2.4) air temperature, air humidity, and wind speed were recorded together with snowpack discharge (snow lysimeter). Precipitation data extrapolated from Dyrdalsvatn (pp. 27) were used.

Table 4.2. Periods of recorded snowmelt in the Dyrdalen and Frotveit areas during 1979-82.

Station	Period						Number of days
Dyrdalsvatn	April	1	to		30	1979	30
	May	1	to		21	1979	21
	Febr.	15	to		22	1980	8
	April	12	to	May	1	1980	20
	May	1	to		9	1981	9
	Febr.	3	to		14	1982	12
	March	25	to	April	7	1982	14
	April	15	to		22	1982	8
							122
Austlihylla	April	17,	and				
	April	23	to	May	1	1980	10
	April	1	to		20	1981	20
	May	1	to		10	1981	10
	March	28	to	April	7	1982	11
	April	15	to		27	1982	13
	May	7	to		24	1982	18
							82
Frotveit I (II)	April	3 (4)	to				
I : woodless site		14 (12)				1981	12 (9)
II: wooded site	Jan.	16	to		18	1982	3
	March	23	to	April	5	1982	14
							29 (26)

Table 4.3. Available (+) and missing (-) radiation records at the open (FI) and at the wooded (FII) sites at Frotveit, and at Dyrdalsvatn during the period of recorded snowmelt at Frotveit 1981. Q_S denotes the incoming shortwave radiation, α the albedo, and Q_N the net radiation.

Station	Rad. term	3/4	4/4	5/4	6/4	7/4	8/4	9/4	10/4	11/4	12/4	13/4	14/4
FI	Q_s	+	+	+	+	+	+	+	+	+	+	+	+
	αQ_s	+	+	+	+	+	+	+	+	+	+	+	+
	Q_N	+	+	+	+	+	+	-	-	-	-	-	-
FII	Q_s	-	-	-	-	-	+	+	+	+	+	+	+
	αQ_s	-	-	-	-	-	-	-	-	-	-	-	-
	Q_N	+	+	+	+	+	+	+	+	+	+	+	+
Dyrdals-vatn	Q_s	+	+	+	+	+	+	+	+	-	-	-	-
	αQ_s	+	+	+	+	+	+	+	+	-	-	-	-
	Q_N	+	+	+	+	+	+	+	+	-	-	-	-

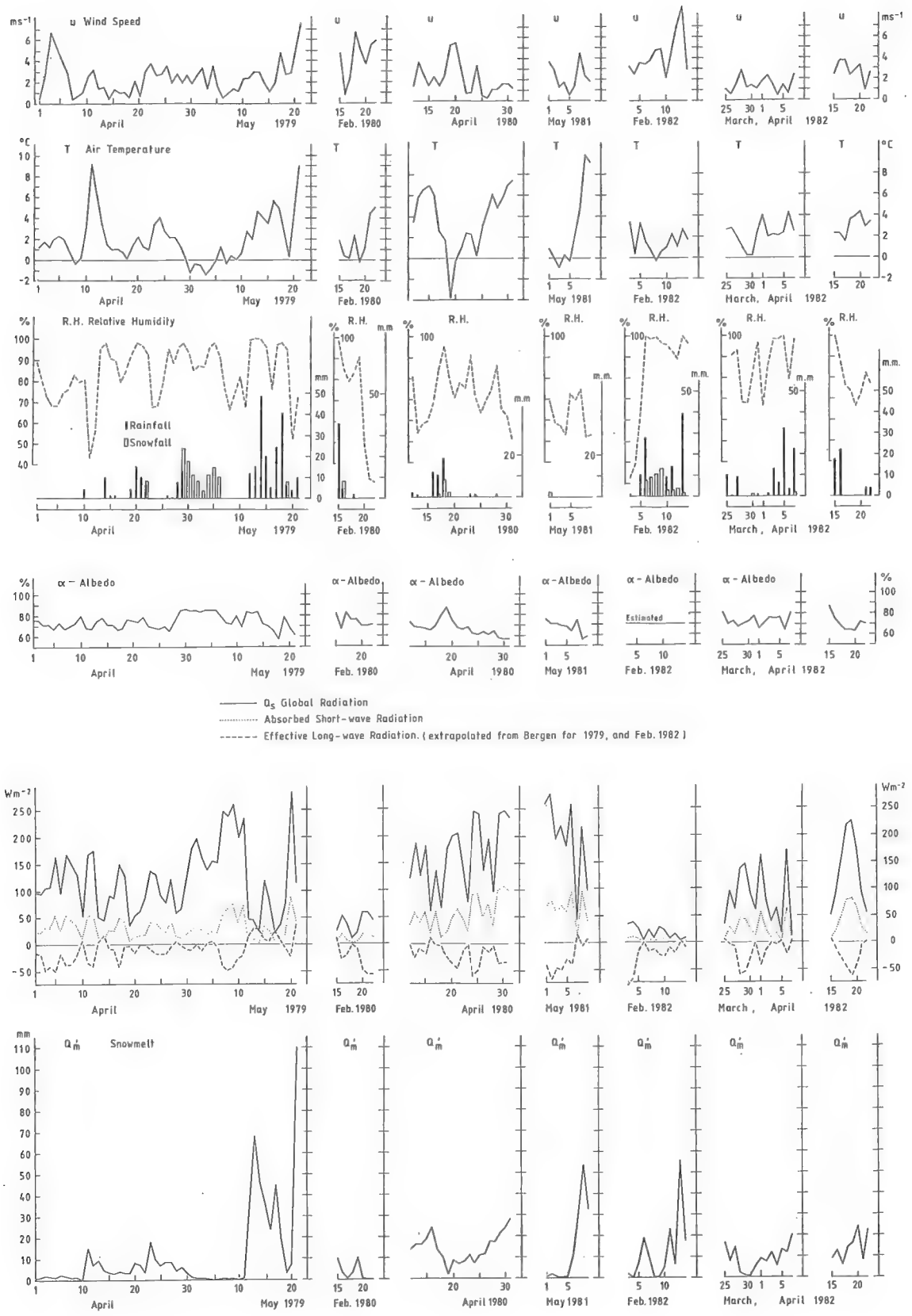

Fig. 4.1. Diurnal values of recorded data during snowmelt at Dyrdalsvatn 1979-82.

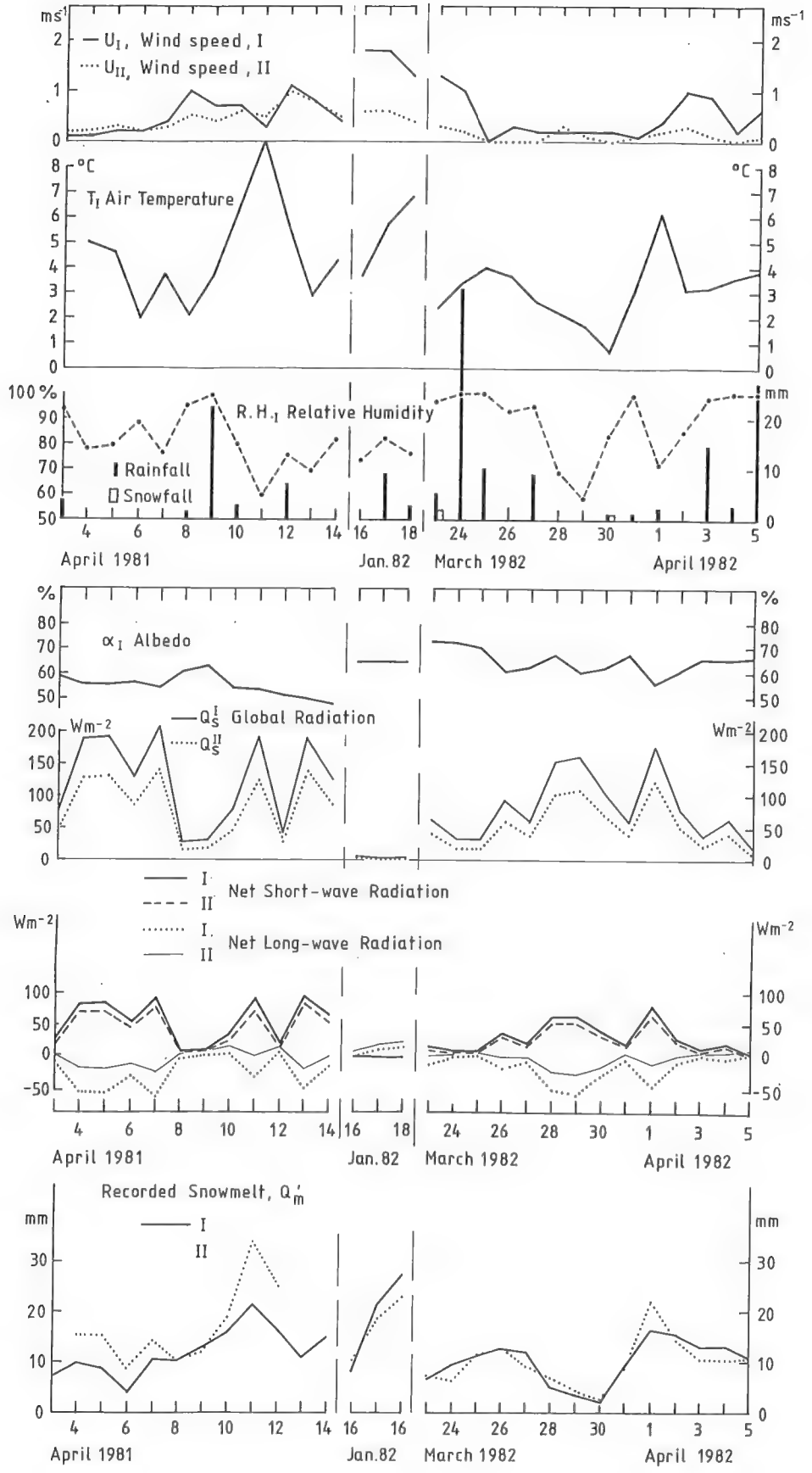

Fig. 4.2. Diurnal values of recorded snowmelt and meteorological data at the woodless (I), and wooded (II) sites at Frotveit 1981-82. (For 1982 and parts of 1981 (Table 4.3) the radiation fluxes are estimated (Chapt. 4.2.1) due to missing data.)

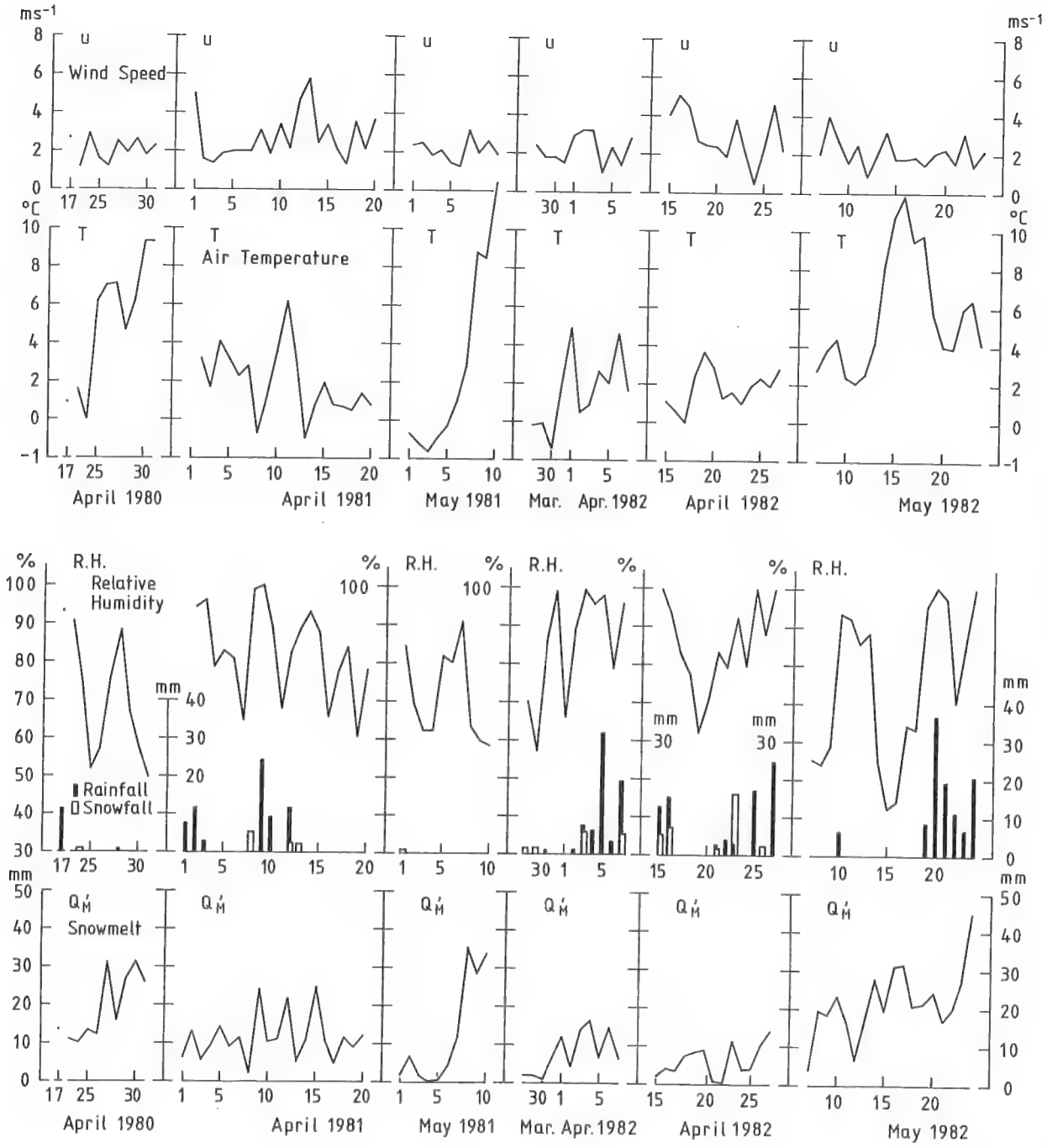

Fig. 4.3. Diurnal values of recorded data at Austlihylla during snowmelt 1980-82.

4.2. The Energy Balance of Recorded Snowmelt.

4.2.1. Modelling Radiation Fluxes.

The snow surface absorbs, reflects and emits short-wave as well as long-wave radiation. The net radiation of the snow surface is accordingly defined by

$$Q_N = Q_S(1-\alpha) + Q_{L\downarrow} - Q_{L\uparrow} \quad , \qquad (4.2.1)$$

where Q_S is the global radiation, α is the albedo of the surface, $Q_{L\downarrow}$ the incoming and $Q_{L\uparrow}$ the outgoing long-wave radiation.

Global radiation

Global radiation, Q_S , is an important and highly variable energy flux, varying regularly with season and hour, and more irregularly with cloudiness. The most precise determination of Q_S is by direct measurements. However, estimates of snowmelt are frequently needed in areas where records of global radiation are missing.

Global radiation data observed in Bergen, Q_{SB} , and at Dyrdalsvatn, Q_{SD} , during the periods of snowmelt discussed, are compared here. Daily mean values from 102 days yielded the regression

$$\frac{Q_{SD}}{Q_{ex}} = 0.85\left(\frac{Q_{SB}}{Q_{ex}}\right) + 0.06 \quad , \qquad (4.2.2)$$

where Q_{ex} is the extraterrestrial global radiation. The correlation coefficient is 0.94 and the mean values of $\left(\frac{Q_S}{Q_{ex}}\right)$ are 0.40 for both sites. This indicates that the global radiation flux in this area is fairly invariant within distances of 10-20 km.

The equation (4.2.2) predicts $\frac{Q_{SD}}{Q_{ex}} = 0.70$ when $\frac{Q_{SB}}{Q_{ex}} = 0.75$. The average value of $\frac{Q_{SB}}{Q_{ex}}$ for all days with values exceeding 0.60 is 0.69, while $\frac{Q_{SD}}{Q_{ex}}$ is 0.63 when averaged over the same days. Since the station at Dyrdalsvatn is more screened by the mountains this is to be expected.

Eq. (4.2.2) also indicates that the highest values of $\frac{Q_S}{Q_{ex}}$ during cloudy weather are found at Dyrdalsvatn. The average value of $\frac{Q_{SB}}{Q_{ex}}$ for all days with $Q_{SB} < 0.30$ is 0.17, while the average value of $\frac{Q_{SD}}{Q_{ex}} = 0.19$ for the same days. This can be explained by increased diffuse radiation due to multiple reflection between the snow cover and the clouds.

In accordance with these systematic differences, the standard deviation of the data from Bergen is 0.22, and 0.20 for Dyrdalsvatn. Some of the deviation from the line 1:1 by eq. (4.2.2) may, however, also be due to differences in cloud cover at the two sites.

The cloud cover and the relative sunshine duration may both be used for estimating global radiation. These two variables are closely related. For the 102 days used for determination of eq. (4.2.2), the regression

$$\frac{s}{S} = 1.18\ (1-C) - 0.02\ ;\quad r = 0.91 \qquad (4.2.3)$$

is found. C is the cloud cover, defined in this chapter as a fraction of unity, and $\frac{s}{S}$ is relative sunshine duration, defined as the ratio of actual to possible sunshine duration (all data from Bergen-Florida). Some of the unexplained variance may be due to inaccuracies in observed cloud cover. The slope of the line (4.2.3) deviates from unity, which is probably due to systematic differences during fine weather. Thin clouds, or clouds not covering the sun will lower the values of $1-C$, but not those of $\frac{s}{S}$. Besides, C is reported as 1/8 at the slightest trace of clouds, partly explaining why (4.2.3) predicts $\frac{s}{S} \approx 1.0$ at $C = 1/8$.

Different authors (Kimball (1914), Prescott (1940), Penmann (1948), McCay (1970), Bayne (1978)) found good estimates of relative global radiation, $\frac{Q_S}{Q_{ex}}$, from $\frac{s}{S}$ or C. Skartveit (1976) used the regression model

$$\frac{Q_S}{Q_{ex}} = s_1 C_s + s_2 C_s^{\frac{1}{2}} + s_3\ , \qquad (4.2.4)$$

where $C_s = \frac{s}{S}$, and s_1, s_2, and s_3 are regression coefficients. This model is optimized on a daily basis for the 102 days used for determination of eq. (4.2.2), using both $\frac{s}{S}$, and $1-C$ for C_s. Results from the analysis made by Skartveit (1976) and the coefficients found in this investigation are listed in Table 4.4. Note that s/S and C are observed in Bergen only, while the computation is made for global radiation recorded both in Bergen and at Dyrdalsvatn. From the table it can be deduced that $\frac{Q_{SB}}{Q_{ex}}$ is predicted higher by using the present coefficients than by using those found by Skartveit (1976). The difference is, however, hardly statistically significant. When using global radiation data from Dyrdalsvatn, a slightly lower correlation is found, as expected due to the distance between the sites. The regression coefficients differ somewhat, in accordance with the differences in global radiation (4.2.2). Use of relative clearness, $1-C$, for C_s yields a somewhat lower correlation. This is partly due to the mentioned inaccuracies in the cloud cover data, and partly due to $\frac{s}{S}$ being a more adequate physical indicator.

We may conclude that rather good Q_S-estimates can be derived from cloud cover or relative sunshine data. This is a fact of practical importance since the cloud cover is observed at weather stations on a routine basis, so that fairly reliable data are available for most areas. The equation (4.2.4d) (Table 4.4) is then recommended.

For comparing global radiation at Dyrdalsvatn and Frotveit (open site) only 8 days are available. The mean values were $\bar{Q}_{SD} = 119\ Wm^{-2}$, and $\bar{Q}_{SI} = 116\ Wm^{-2}$ with a correlation coefficient, $r = 0.96$. By excluding a single day with fog at Frotveit (no fog at Dyrdalsvatn on that day), $Q_{SD} = 112\ Wm^{-2}$, $Q_{SI} = 114\ Wm^{-2}$, and $r = 0.99$. This confirms the high quality of our data and shows that global radiation records from Dyrdalsvatn can be used as high quality estimates for the open site at Frotveit, FI, when data are missing.

Table 4.4. Correlation coefficients and regression coefficients computed by the regression model $\frac{Q_S}{Q_{ex}} = s_1 C_s + s_2 C_s^{\frac{1}{2}} + s_3$ (4.2.4), where $\frac{Q_S}{Q_{ex}}$ is relative global radiation. Relative clearness, 1-C (fraction of unity), and relative sunshine duration, $\frac{s}{S}$, observed in Bergen are used for C_s.

Recording station for global radiation, Q_S		Variable	Regression coefficients			Multiple corr.coeff.	Reference
		C_s	s_1	s_2	s_3	R	
Bergen	March 1965-70	s/S	-0,03	0,55	0,13	0,95	Skartveit (1976)
"	April "	s/S	0,18	0,36	0,15	0,97	"
"	May "	s/S	0,18	0,38	0,13	0,97	"
"	102 days during March-May 1979-82	s/S	0,17	0,43	0,15	0,95	(4.2.4a)
"	"	1-C	0,07	0,66	0,07	0,88	(4.2.4b)
Dyrdalsvatn	"	s/S	0,00	0,52	0,17	0,92	(4.2.4c)
"	"	1-C	-0,16	0,81	0,07	0,88	(4.2.4d)

Snow albedo

The albedo of snow is generally high, but is shows quite substantial and very important variations. The crystal structure, the liquid water content of the snow cover, and litter, dust, etc. at the surface all influence the albedo. These parameters change with time, and Fig. 4.4 (from U.S.A.C.E., 1956) exemplifies how the resulting time dependency of snow albedo may be parameterized in terms of time since last snowfall or in terms of accumulated daily maximum air temperature. A regression analysis between the albedo, α , and the time since last snowfall (days) during spring snowmelt at Dyrdalsvatn 1979-82 (91 days, days with snowfall excluded) yields a correlation coefficient, r , of only -0.24. We now define the time, t , of open air exposure of the snow at the surface by

$$t = \begin{cases} n + 1 - \Sigma T_i & \text{when the old surface is exposed to open air} \\ n_i + 1 & \text{when the old surface is covered by a new snowfall,} \end{cases} \quad \text{(days)} \quad (4.2.5)$$

where n is the number of days since the last day of snowfall before spring snowmelt, and n_i the number of days since the last snowfall. T_i is the number of days when a new snowfall is covering the old surface, estimated from totals of snowfall and a first order estimate of snowmelt. The definition is illustrated in Fig. 4.5. It should be noted that this is a very rough parameterization of the surface conditions. Nevertheless, the correlation coefficient between α and t was -0.50 for the 91 days at Dyrdalsvatn 1979-82, indicating that the sudden changes in the albedo due to the covering and uncovering of the old surface affects the albedo significantly.

The relation between α and t is illustrated in Fig. 4.6. The figure indicates a more rapid albedo decrease for the first days after a snowfall. By exchanging t with $\ln t$ the correlation coefficient, r , increases to -0.55. As can also be seen, the albedo decrease with time is slower than suggested by U.S.A.C.E

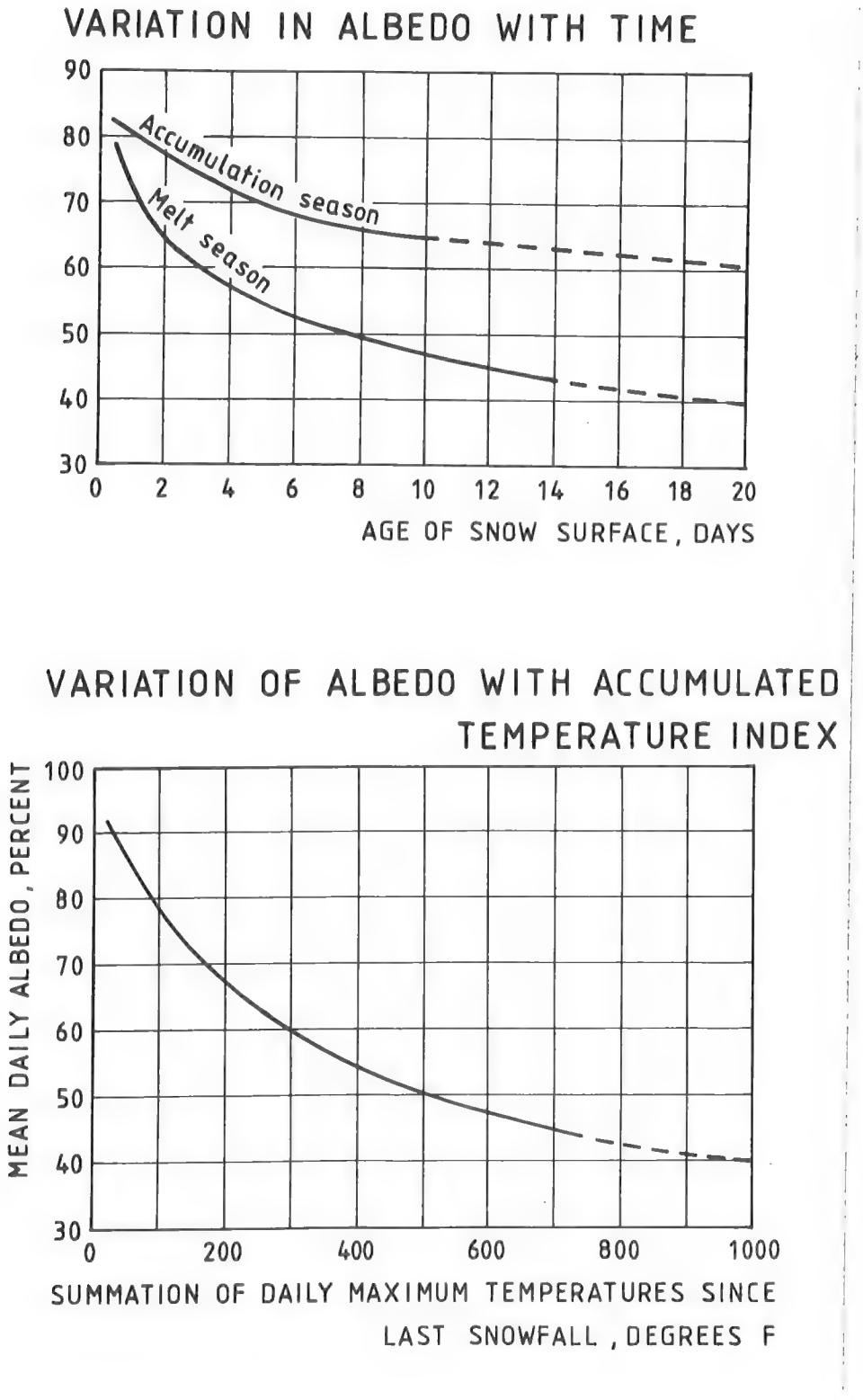

Fig. 4.4. Variation of albedo (after U.S.A.C.E., 1956).

(Fig. 4.4). However, that result was based on data from Centra Sierra, situated at about 39°N, and with a continental climate. Due to the lower latitude, the crystal transformations are expected to work faster in that area.

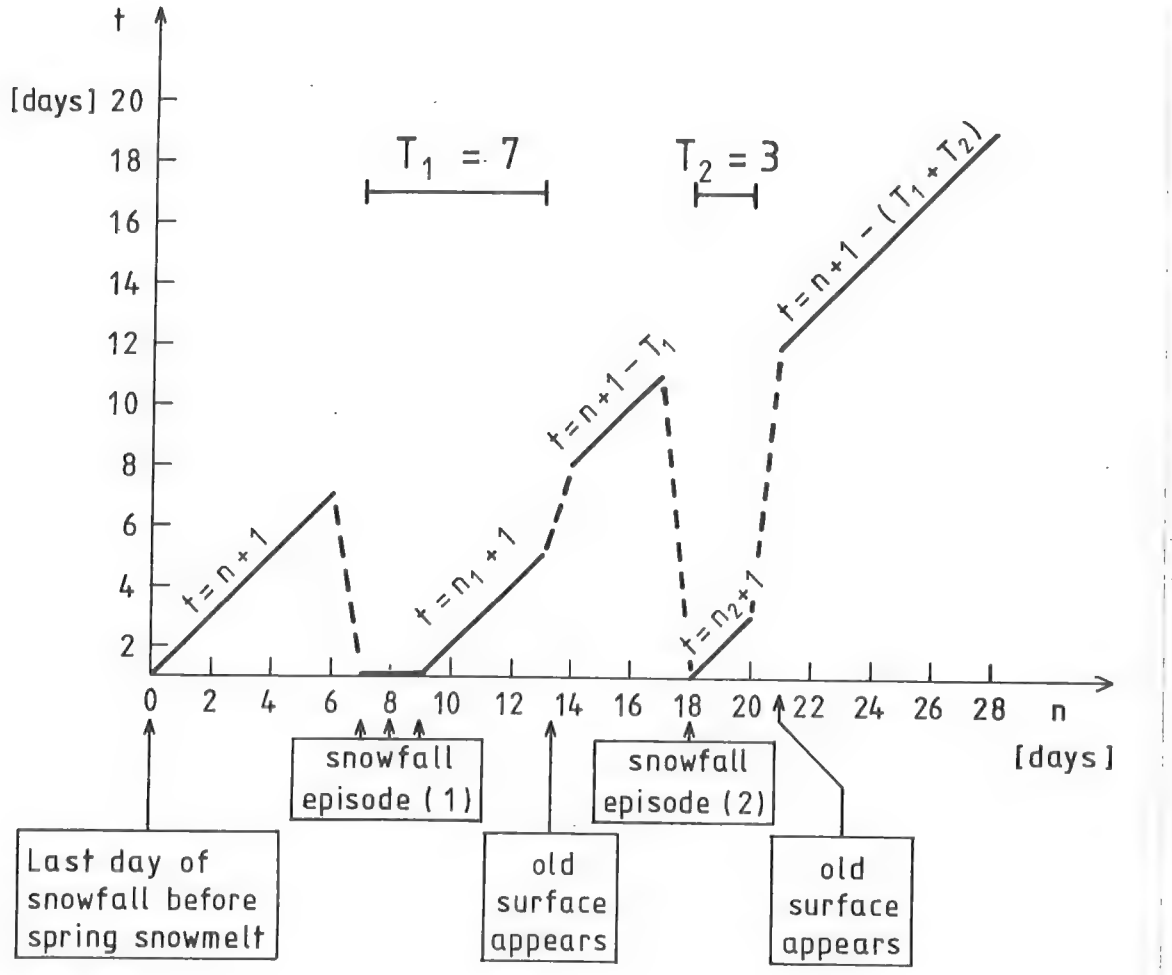

Fig. 4.5. Illustration of the definition (4.2.5) of the time, t (days), of open air exposure of the snow at the surface.

Fig. 4.7 shows the regression line between the albedo and the relative clearness, 1-C . The correlation coefficient is -0.42 which is rather high considering the neglection of variations in snow surface age. An increase in snow albedo with increasing cloud cover is also reported by Kondratjev (1969, pp. 426),

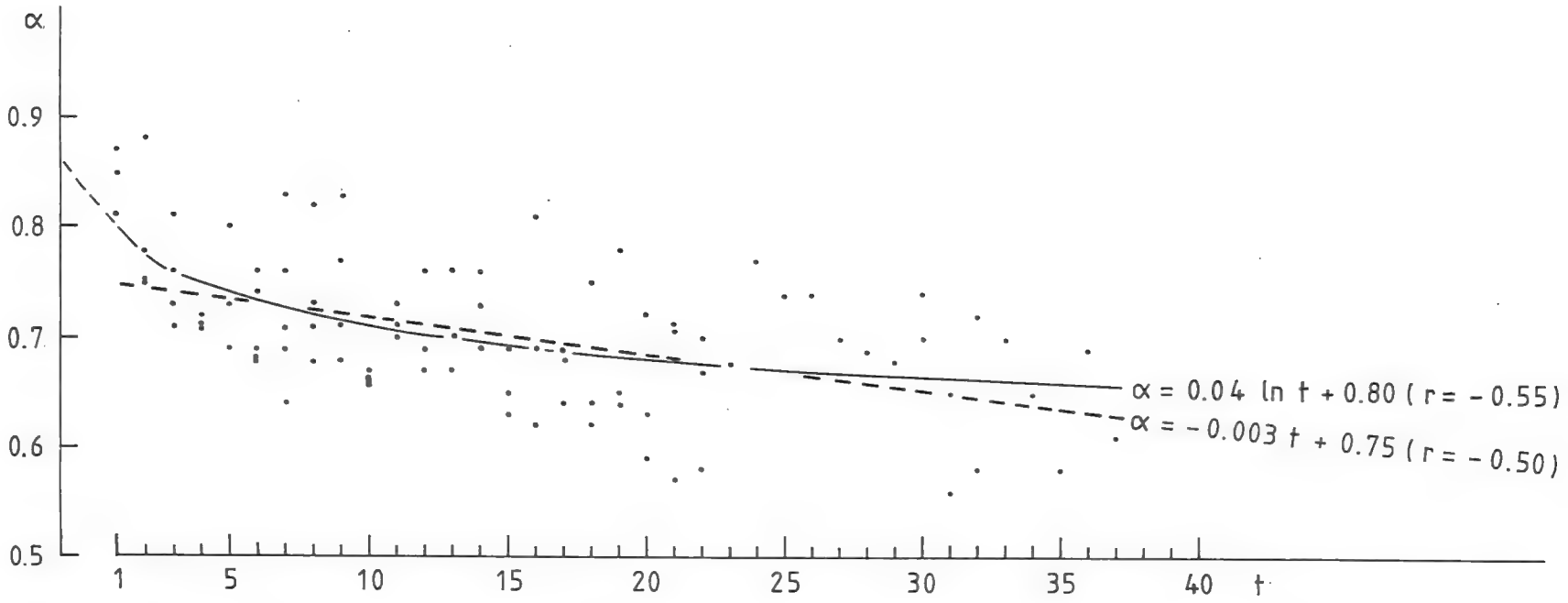

Fig. 4.6. Relation between the time, t , of open air exposure of the snow at the surface (pp. 53) and the albedo, α , during spring snowmelt at Dyrdalsvatn 1979-82.

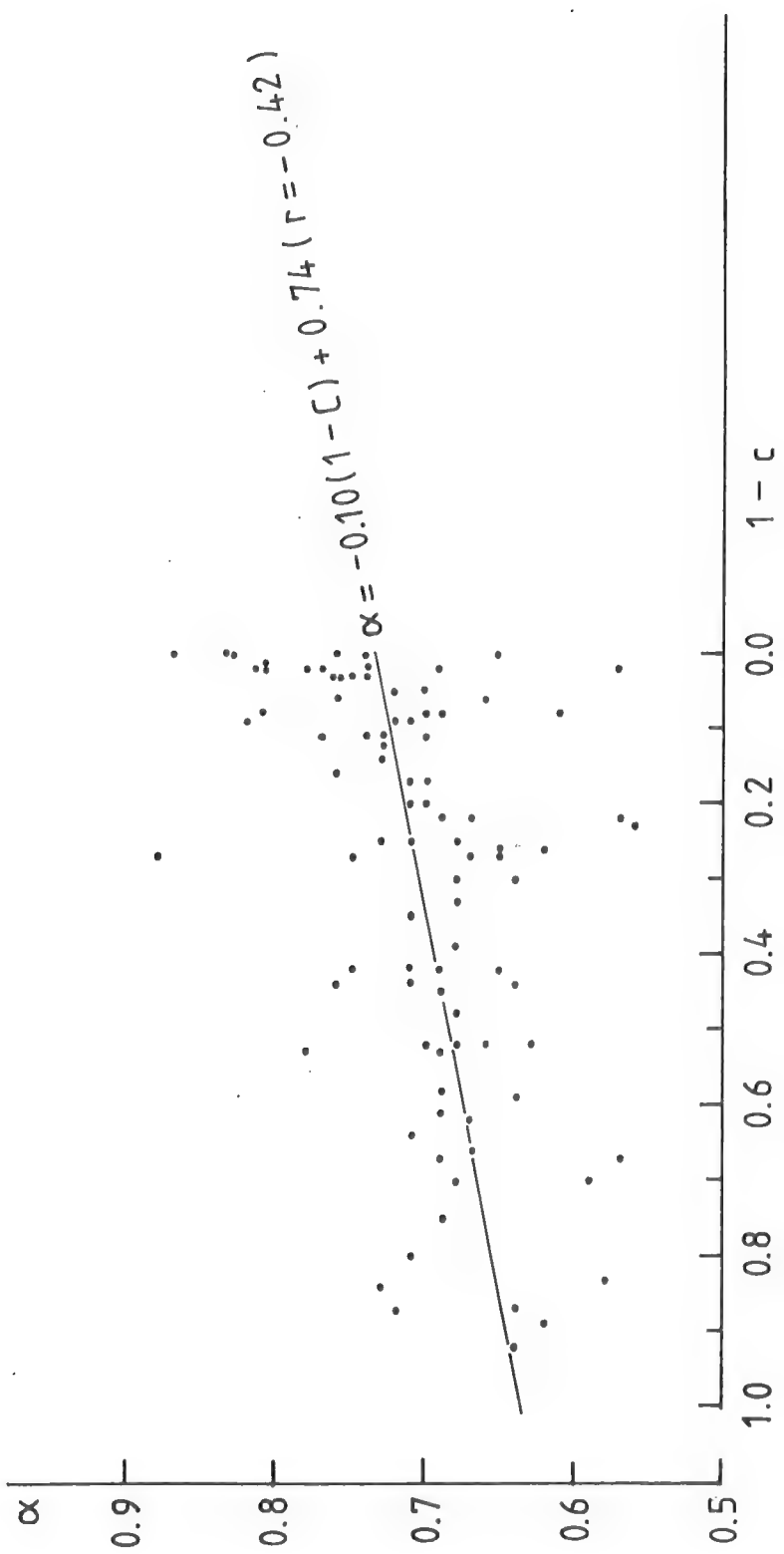

Fig. 4.7. Relation between the albedo, α , during spring snowmelt at Dyrdalsvatn, 1979-82, and relative clearness, 1-C , observed at Bergen.

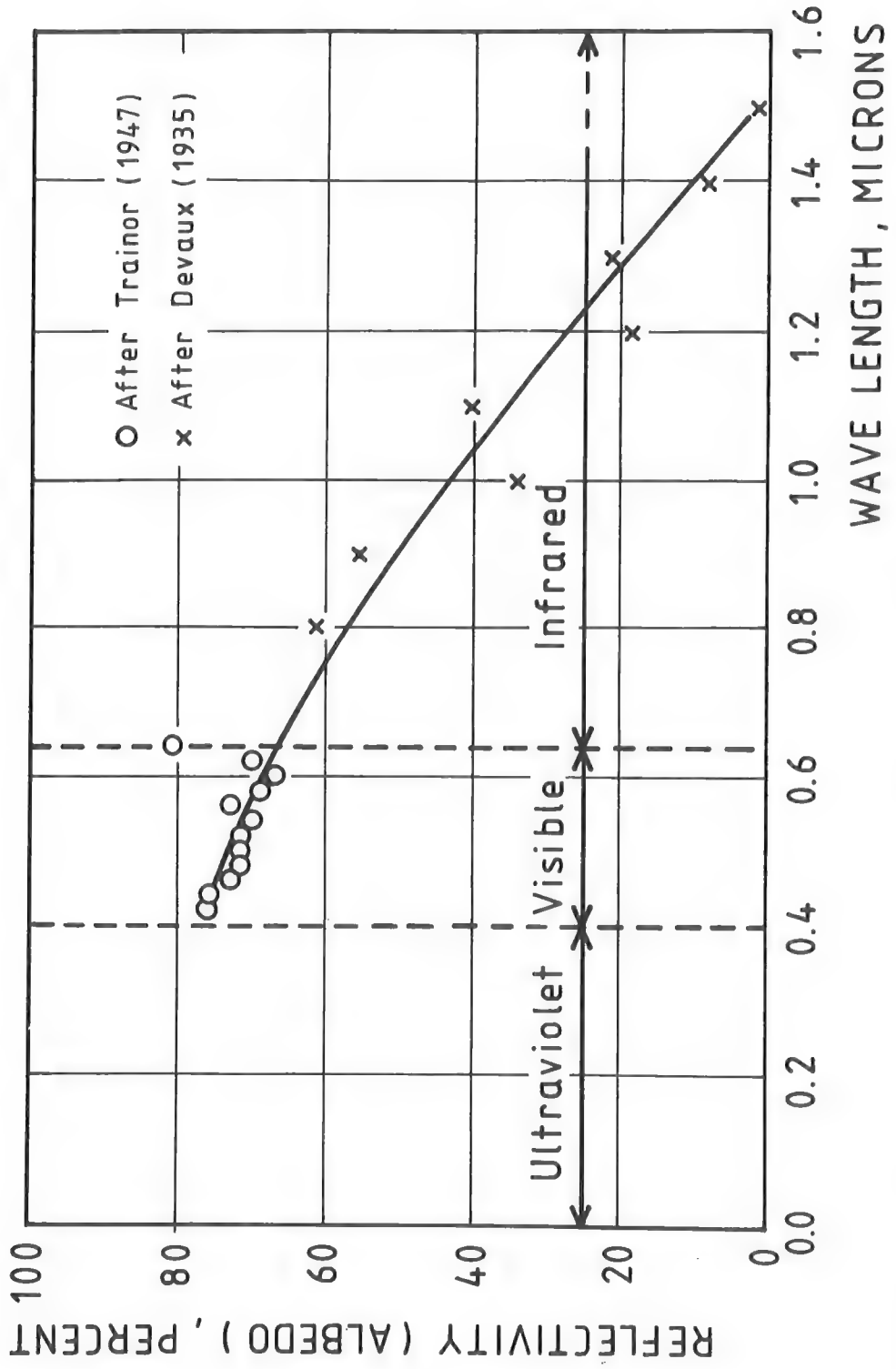

Fig. 4.8. Approximate spectral reflectivity of melting snow (after U.S.A.C.E., 1956).

and Liljequist (1956-57). The line in Fig.4.7 should perhaps be curved towards high values of α for dense cloud cover, a tendency also reported by Kondratjev (1969, pp. 426). The scattering process in clouds is only slightly spectrally dependent in the shortwave band (Robinson, 1966, pp. 173), and the transmission through the pyranometer glass bulb is nearly independent of the wavelength between 0.3μ and 2μ (Robinson, 1966, pp. 265; Sonntag, 1964).

The spectral albedo of snow, however, increases with decreasing wavelength (Fig. 4.8). Multiple reflections between the snow surface and the clouds therefore simultaneously enhance the global radiation and cause a "blue-shift" in its spectral distribution. Such a "blue-shift" in turn enhances the integral snow albedo, given the above-mentioned correlation between spectral albedo and wavelength.

A multiple correlation analysis albedo and the relative clearness, $1-C$, and $\ln t$ (pp.53) yields a regression model (91 days) for the albedo, α (in fraction of unity):

$$\alpha = -0.13(1-C) - 0.05 \ln t + 0.87 \quad , \qquad (4.2.6)$$

where C is observed in Bergen. The correlation coefficient is $R = 0.75$, which means that 56% of the variation of α is explained. A slightly better model is found by replacing relative clearness with relative global radiation, $\frac{Q_{SD}}{Q_{ex}}$, where Q_{SD} is global radiation observed at Dyrdalsvatn:

$$\alpha = -0.18 \frac{Q_{SD}}{Q_{ex}} - 0.05 \ln t + 0.90 \quad , \qquad (4.2.7)$$

where $R=0.77$. Both models predict a 12% decrease of the albedo 10 days after last snowfall if older surfaces are not exposed, and a corresponding decrease during the transition from overcast to clear weather. The unexplained variance is rather high, as should be expected considering the many factors which influence the albedo. If possible, these models should be optimized when used at other sites. This is especially important when regional climate, height

above sea level, snowmelt season, vegetation or pollution of the snow surface deviate significantly from those of Dyrdalen.

By comparing the albedo recorded at Dyrdalsvatn and the open site, FI , at Frotveit, the values at FI are found to be some 10% lower than at Dyrdalsvatn, on the average. The correlation coefficient is 0.79, but the sample is not large enough to allow a discussion of the difference. Falls from the vegetation in the area, and the lower altitude (higher temperature) probably account for most of the albedo decrease. When missing at Frotveit, α_I is therefore extrapolated from Dyrdalsvatn by subtracting 10%. The exact value of the albedo at the wooded site, α_{II} , is somewhat less critical due to the lower incoming short wave radiation, and was not recorded. This value is put at 10% lower than α_I , since the surface within the wood appeared darker to the eye due to more fall from the trees.

Longwave radiation

In contrast to the case of shortwave radiation, the absorbitivity of a snow cover is approximately unity for longwave radiation. This fact enhances the importance of downward longwave radiation, $Q_{L\downarrow}$, relative to that of global radiation in connection with snowmelt. When not recorded, incoming longwave radiation during cloudy weather is frequently estimated from formulae of the following type:

$$Q_{L\downarrow} = Q_{oL\downarrow} (1 + L_1' C + L_2' C^2) , \qquad (4.2.8)$$

where C is cloud cover (Ångström (1913), Bolz (1949), Paulsen and Torheim (1964), and others). The coefficients L_1' and L_2' are sometimes assumed to be functions of cloud type (Monteith, 1975, pp. 37). $Q_{oL\downarrow}$ is the atmospheric radiation during clear weather at the same air temperature (and humidity). For Bergen, Paulsen and Torheim (1964) arrived at an equation for recorded hourly values during clear weather, given by Paulsen (1967) as

$$Q_{oL\downarrow} = 0.895 \sigma T^4 - 29.3 \quad (Wm^{-2}) , \qquad (4.2.9)$$

where T is the air temperature (°K), and σ is Stephan-Bolzmann's constant. The correlation coefficient was $r = 0.949$. Now, the formula (4.2.8) prescribes $Q_{oL\downarrow}$ to be multiplied by a cloud factor to obtain actual atmospheric radiation, $Q_{L\downarrow}$. Paltridge and Platt (1976, pp. 138-140) argue that the radiation outside the atmospheric window (8-13μm) is of a black body character, and is independent of the cloud cover. The extra radiation from clouds must therefore occur in the window region. They then suggest the equation

$$Q_{L\downarrow} = Q_{oL\downarrow}' + (1-0.7)\varepsilon_c \; T_c^4 \cdot C \quad , \qquad (4.2.10)$$

where $Q_{oL\downarrow}'$ is the radiation outside the window region, ε_c is cloud emissivity (0.3 for cirrus; 1.0 for low clouds), and T_c cloud base temperature. The factor (1-0.7) is the approximate part of blackbody radiation which occurs between 8 and 13 μm. Fig. 4.9 shows an approximately linear increase of the incoming longwave radiation, $Q_{L\downarrow}$ with the cloud cover, C. A regression model like

$$Q_{L\downarrow} = L_1\sigma T^4 + L_2 C_L + L_3 \quad , \qquad (4.2.11)$$

should then be reasonable. σT^4 is blackbody radiation at air temperature, and C_L is a cloud variable which may include cloud type and height of cloud base. L_1, L_2, and L_3 are the regression coefficients.

Table 4.5 shows the results of the multiple regression analysis using C, C^2, and $(\frac{Q_{SD}}{Q_{ex}})^2$ for C_1. $C_1 = C$ is also applied to 150 monthly mean values (1965-1979) from Bergen. When the coefficients of the various formulae is compared it should be remembered that when C increases from 0 to 1, $(Q_S/Q_{ex})^2$ declines from about 0.5 to 0. The predicted contribution to atmospheric radiation, $Q_{L\downarrow}$, from clouds during completely overcast weather should then be 80, 66, 59, and 71 (Wm^{-2}) for the four versions, respectively. This is reasonably close to the value 60 Wm^{-2} found by Paltridge and Platt (1976, pp. 140) for Aspendale, Australia, " a fairly typical mid latitude station."

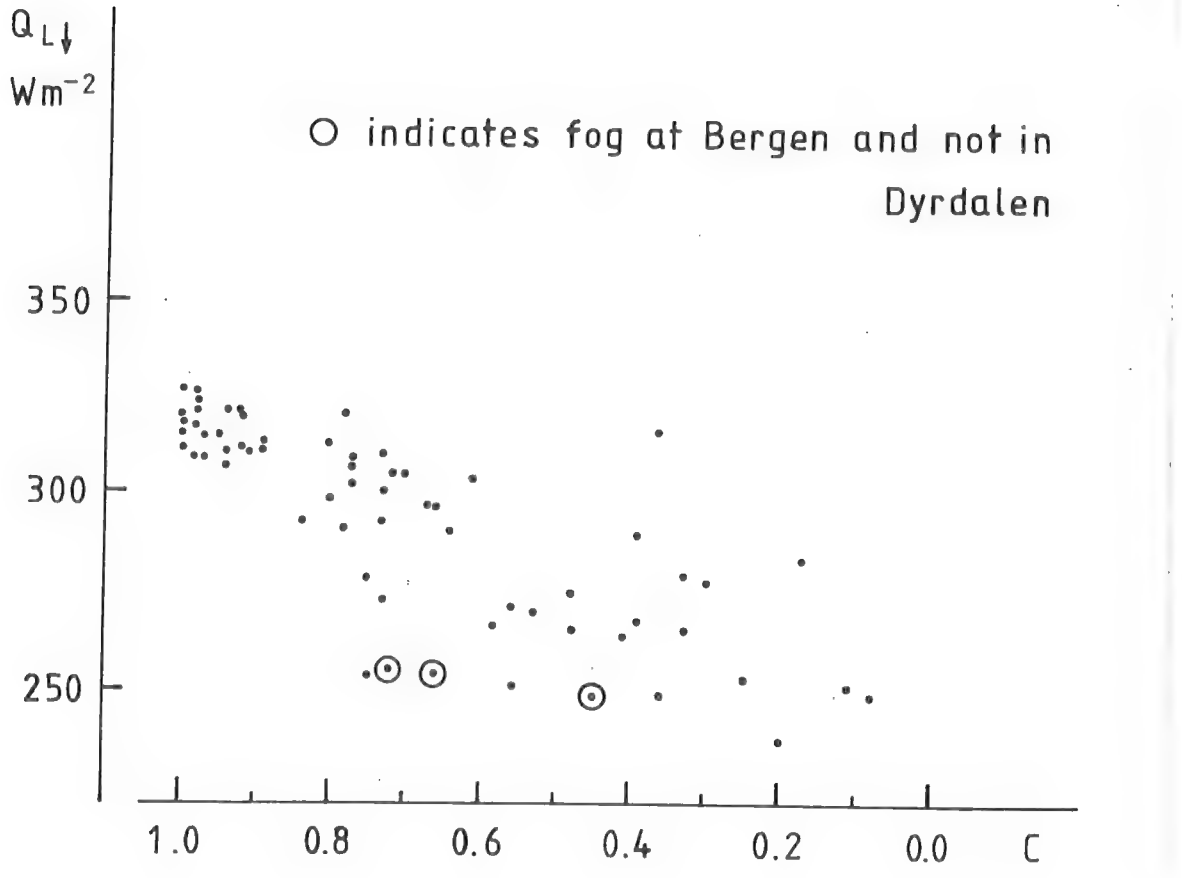

Fig. 4.9. Relation between cloud cover, C , from Bergen, and incoming longwave radiation, $Q_{L\downarrow}$, at Dyrdalsvatn during 65 days of spring snowmelt 1980-82.

Table 4.5. Coefficients from the regression analysis $Q_{L\downarrow} = L_1\sigma T^4 + L_2 C_L + L_3$ (Wm^{-2}) for Bergen and Dyrdalsvatn. σ is Stephan-Bolzmann's constant and T air temperature (°K); and C_L a cloud variable for which the cloud cover, C (in fractions of unity), C^2, and the square of relative global radiation, $(\frac{Q_S}{Q_{ex}})^2$ are used. The cloud cover is observed at Bergen.

Recording station for incoming longwave radiation, $Q_{L\downarrow}$	Period	C_L	Regression coefficients L_1	L_2	L_3	Corr.coeff. R	Model version
Dyrdalsvatn	65 days during spring snowmelt 1980-82	C	0.70	79.7	6.2	0.87	M1
"		C^2	0.75	66.1	7.5	0.89	M2
"		$(\frac{Q_{SD}}{Q_{ex}})^2$	0.73	-117.8	77.8	0.92	M3
Bergen	150 months in 1965-79	C	1.020	70.7	-91.5	0.947	M4

In Fig. 4.10, predicted $Q_{L\downarrow}$ values for M1, M2, M3 and M4 during clear weather (C=0) are plotted against the well known formula derived by Swinbank (1963):

$$Q_{L\downarrow} = 5.31 \cdot 10^{-13} T^6 \quad (Wm^{-2}) \qquad (4.2.12)$$

and the formula found by Paulsen (1967) (M5). The formula based on the large set of monthly mean values from Bergen predict $Q_{L\downarrow}$ values under clear skies very close to those found by using the Swinbank formula, and notably lower values than by using the Paulsen formula. All the three model versions M1, M2, and M3 also predict lower clear weather values of $Q_{L\downarrow}$ than found by using the Paulsen formula.

The somewhat low increase in $Q_{L\downarrow}$ with increasing air temperature found in M1, M2, and M3 may be due to the relative narrow temperature interval used ($276.5 \pm 3.0°K$) compared to the rather high variance in the cloud cover data (Fig. 4.9). Therefore, these equations should not be applied too far outside the temperature interval mentioned. In that respect M4 should be more reliable. It is highly noteworthy that this equation yields a cloud cover term in accordance with Paltridge and Platt (1976) and a clear sky term in accordance with Swinbank (1963), a fact that strengthens our confidence in that particular model.

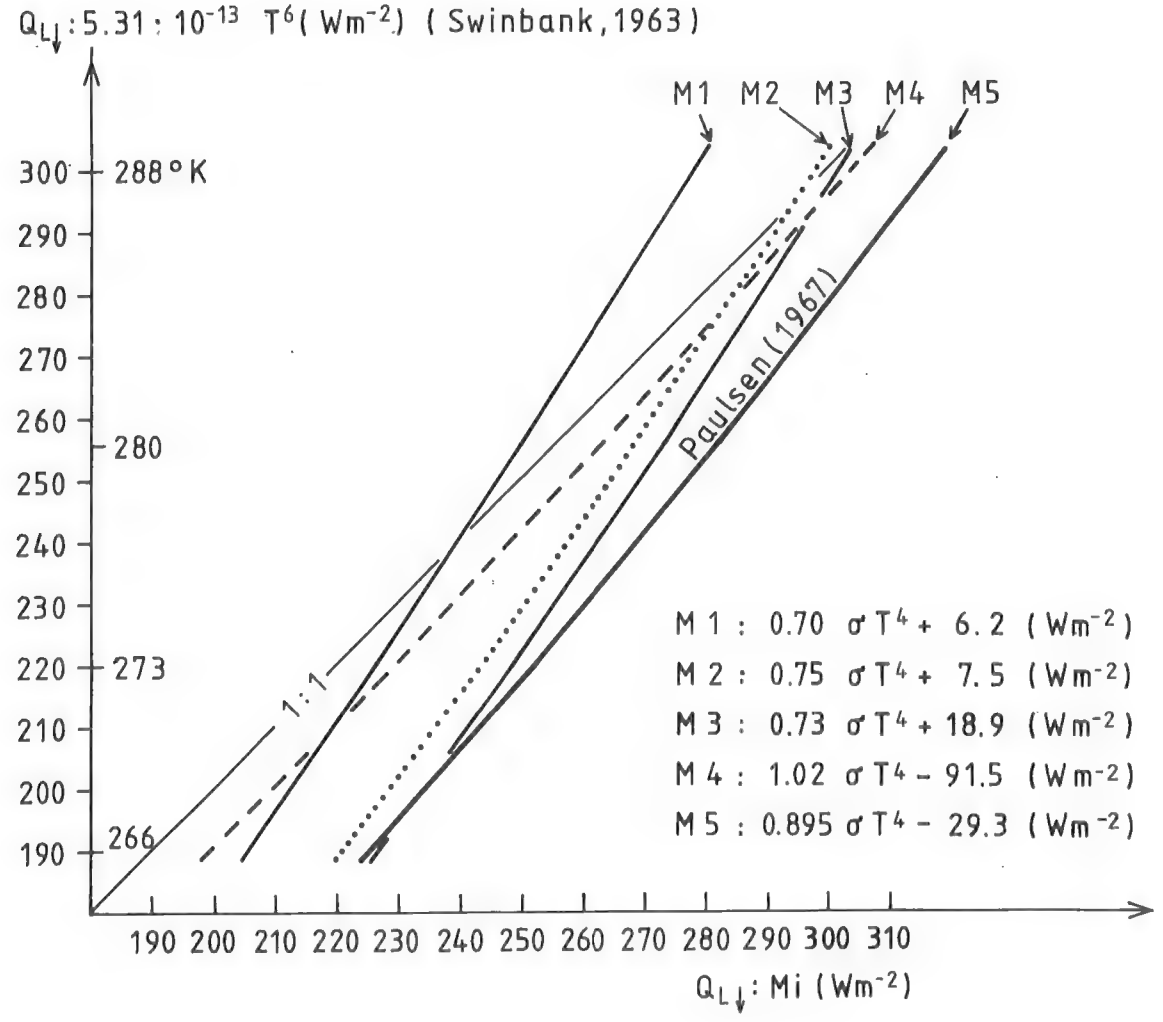

Fig. 4.10. Estimated longwave radiation, $Q_{L\downarrow}$ for clear weather using the model versions M1 to M4 (see table 4.5), and the Paulsen formula (M5) plotted against the Swinbank formula.

The effect of a leafless, deciduous wood canopy on downward radiation.

Any wood canopy affects all energy fluxes involved in snow melting. The observations at Frotveit make possible a rough quantification of how, in particular, a deciduous wood modifies the input of radiant energy to the melting process.

The downward longwave radiation, $Q_{L\downarrow}$, over a "black" surface of temperature, T_o, may be expressed from eq. (4.2.1) as:

$$Q_{L\downarrow} = Q_N - (1-\alpha)Q_S + \sigma T_o^4 \qquad (4.2.13)$$

where Q_N is the net radiation and Q_S is the global radiation at the snow surface, while α is the albedo and σ is the Stephan-Bolzmann's constant.

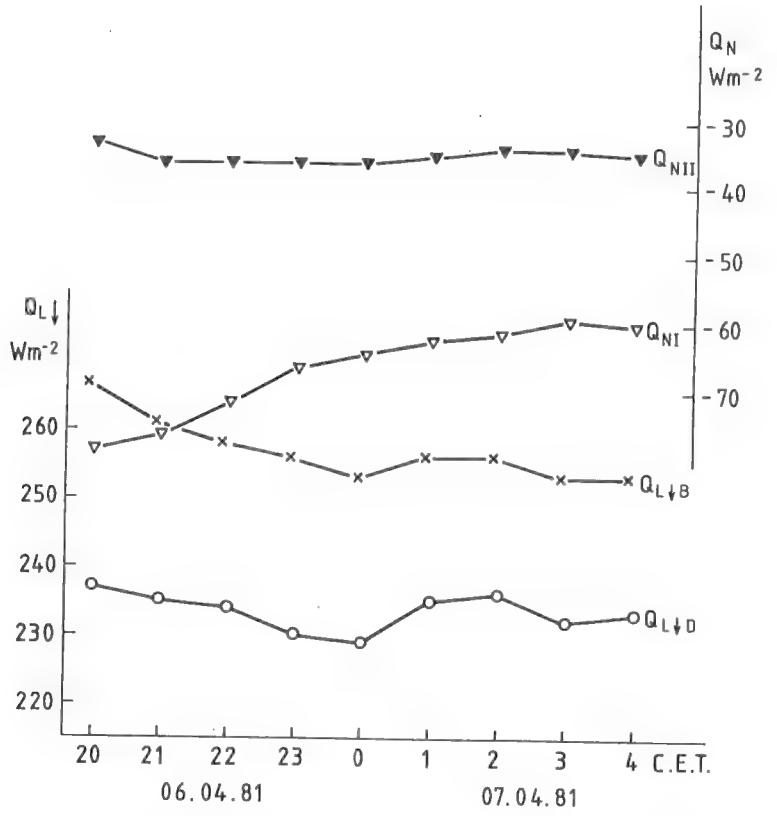

Fig. 4.11. Recorded net radiation, Q_N, at Frotveit (woodless (I), and wooded (II) site), and incoming longwave radiation, $Q_{L\downarrow}$, at Bergen-Florida (B) and Dyrdalsvatn (D) during the clear night of April 6-7 1981.

At Frotveit Q_N , Q_S and α were measured at the woodless site, and Q_N and Q_S at the wooded site. Due to fall from the trees the albedo is lower within the wood than outside. As discussed earlier, this difference is assumed to be 10%. Moreover, T_o=273°K whenever the snow is melting, and $Q_{L\downarrow}$ is readily obtained from eq. (4.2.13) in such cases. A comparison of daily means thus derived for the woodless Frotveit site and corresponding values measured at Dyrdalen, yields a correlation coefficient of 0.97 and a mean difference of only 0.9 Wm^{-2}. Considering the different ways by which these $Q_{L\downarrow}$ are obtained at the two sites, this data comparison is in remarkably good agreement with the small intersite difference expected ($\leq$ 5 Wm^{-2}) from the small horizontal and vertical distance between the sites. In the case of missing data at the woodless Frotveit site, $Q_{L\downarrow}$ values measured at Dyrdalsvatn are therefore used without corrections. When snowmelt does not occur, however, the surface temperature T_o may well drop substantially below 273°K. The cloudless night between 6 and 7 April 1981 provides one, not extreme, example of this. The available snowmelt data indicate that the surface temperature stayed at 273°K until 20 hr CET in the evening of 6 April at both Frotveit sites. $Q_{L\downarrow}$ at that hour is therefore known at both sites from eq. (4.2.13). Moreover, the recorded $Q_{L\downarrow}$ follow quite identical patterns at Dyrdalsvatn and at Bergen during this night (Fig. 4.11). This observation strongly corroborates that the changes in $Q_{L\downarrow}$ during the night are the same at the woodless Frotveit site as Bergen and Dyrdalsvatn. Furthermore, the excess $Q_{L\downarrow}$ at the wooded Frotveit site (relative to $Q_{L\downarrow}$ at the woodless site), due mainly to the downward "window" radiation ($\sim$8-13 μm wavelength) from the tree canopies, is assumed to remain at its 20 hr CET value (42 Wm^{-2}) throughout the night. This last assumption is reasonable since the downfacing canopy parts are close to the air temperature, which varies only slightly during the night (Fig. 4.12).

By the above assumptions we have estimates of $Q_{L\downarrow}$ throughout the night at both Frotveit sites (Fig. 4.12), and the corresponding surface temperature, T_o , is readily obtained from eq. (4.2.13).

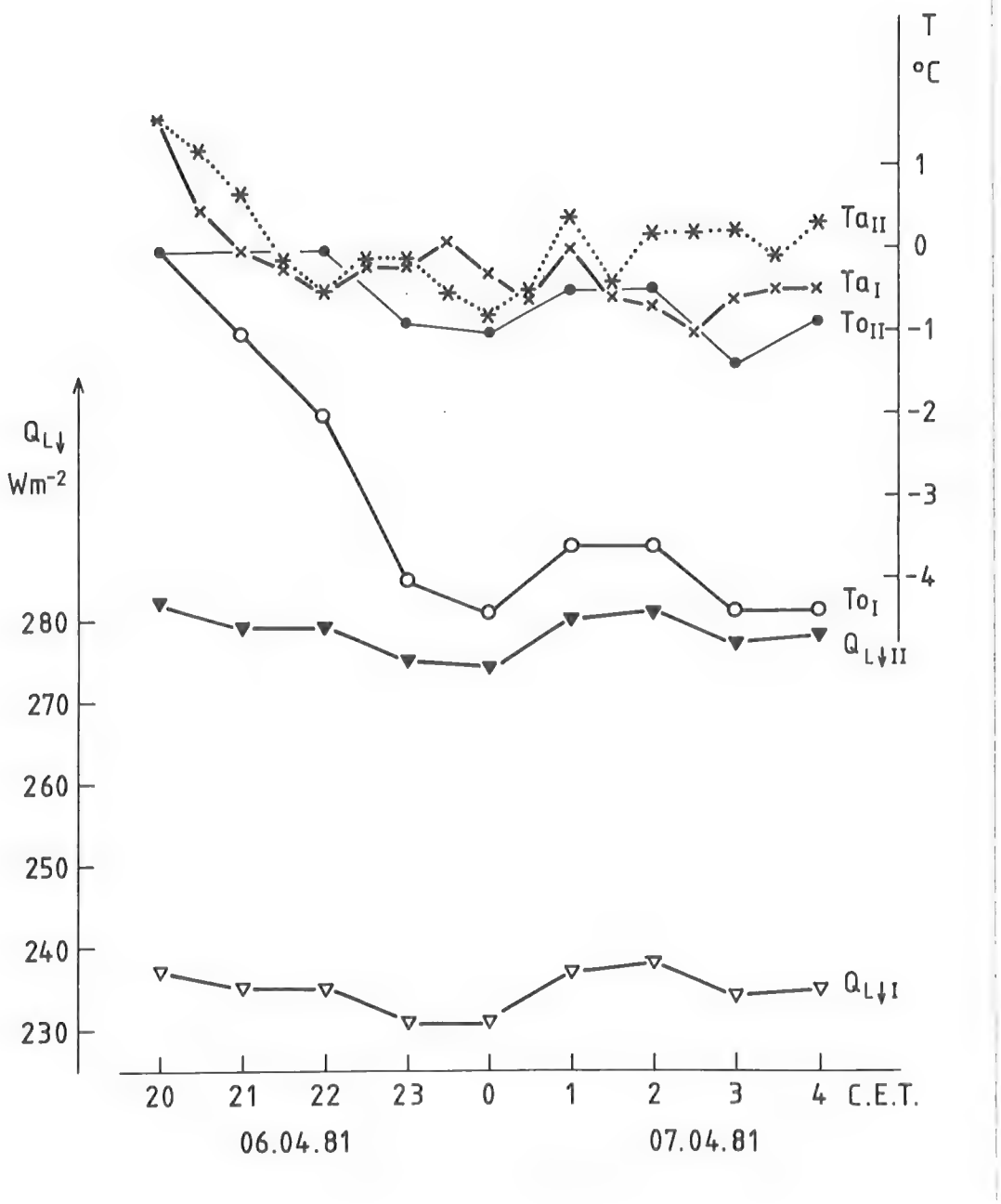

Fig. 4.12. Recorded air temperature, T_a , and estimated incoming longwave radiation, $Q_{L\downarrow}$, and snow surface temperature, T_o at Frotveit during the clear night of April 6-7 1981.

I : Woodless site

II: Wooded site

It is seen (Fig. 4.12) that T_o at the woodless site drops rapidly before midnight and then levels off at about -4°C, while the air temperature 1,8 m above the snow surface remains at about -0.5°C throughout the night. The existence of such a surface inversion is qualitatively corroborated by the observation that the air temperature at Austlihylla (Fig. 2.2) this night was above 0°C while it dropped to -7°C at Dyrdalsvatn. At the wooded site, on the other hand, the estimated surface temperature dropped only slightly below 0°C during this night, well in accordance with the common observation that during cold spring nights the snow surface crust forms far more rapidly in woodless areas than within a wood.

The difference in downward radiation at the wooded and at the woodless sites may be interpreted in terms of the canopy porousity (Hendrie and Price, 1978) or the sky obscuration factor (Perthu, 1982). The canopy porousity, P_c', for isotropic downward shortwave radiation may be measured accurately during overcast conditions. During two overcast days the ratio P_c' between the mean global radiation (Q_S) at the wooded site (II) and the woodless site (I) was:

$$P_c' = \frac{Q_{SII}}{Q_{SI}} = 0.58 \quad . \qquad (4.2.14)$$

Assuming again that the downfacing canopy parts radiate at air temperature, T_a, and that the downward longwave sky radiation is isotropic, we derive an alternative measure P_c'' of canopy porousity from the following equation, relating $Q_{L\downarrow}$ at the wooded (II) and the woodless (I) sites:

$$(1-P_c'')\sigma T_a^4 + P_c'' Q_{L\downarrow I} = Q_{L\downarrow II} \quad . \qquad (4.2.15)$$

During the cloudless night 6 - 7 April 1981 this P_c'' varied slightly about the value 0.47. Since the difference between black-body radiance at air temperature (≈canopy radiance) and clear sky radiance increases with decreasing zenith angle (Kondratjev, 1969) the above P_c'' is significantly biased towards the canopy porousity just overhead, which may by accident deviate considerably from an average value.

Since the sky radiance is far more isotropic in cloudy weather the following mean value is chosen, as a compromise, for the average porousity for downward longwave radiation at the wooded site:

$$P_c''' = \tfrac{1}{2}(P_c' + P_c'') = 0.53 \quad . \qquad (4.2.16)$$

It should be mentioned here that this canopy porousity is a single spot value of an obviously variable quantity.

A substitute of a canopy porousity of 0.53 into eq. (4.2.15) yields

$$Q_{L\downarrow II} = 0.47\sigma T_a^4 + 0.53\, Q_{L\downarrow I} \quad . \qquad (4.2.17)$$

If not available, $Q_{L\downarrow I}$ may be estimated from the empirical formula found for Dyrdalen (Table 4.5):

$$Q_{L\downarrow I} = Q_{L\downarrow D} = 0.73\sigma T_a^4 - 118\,(\frac{Q_{SD}}{Q_{ex}})^2 + 78 \quad (Wm^{-2}) \ , \qquad (4.2.18)$$

which yields by substitution into eq. (4.2.17):

$$Q_{L\downarrow II} = 0.86\sigma T_a^4 - 62\,(\frac{Q_{SD}}{Q_{ex}})^2 + 41 \quad (Wm^{-2}) \ . \qquad (4.2.19)$$

By comparing these formulae for $Q_{L\downarrow}$ at the wooded (II) and the woodless (I) sites, it is seen that the tree canopy reduces the sensivity of $Q_{L\downarrow}$ to variations in real cloudiness (parameterized in terms of the relative global radiation $\frac{Q_S}{Q_{ex}}$) and enhances its sensivity to air temperature. This merely reflects the analogy between the tree canopy and a constant partial cloud cover at air temperature.

The period of simultaneous registrations of shortwave radiation at I and II (Table 4.3) includes cloudy days as well as clear days. The line of regression is given by,

$$Q_{SII} = 0.71\, Q_{SI} - 4.7 \quad (Wm^{-2}) \quad , \qquad (4.2.20)$$

and the correlation coefficient is 0.994. The regression coefficients, reflecting the shading from the wood are, however, spot values

valid only for the actual site. The average values of Q_{SI} and Q_{SII} are 99 Wm^{-2} and 66 Wm^{-2}, respectively. The tree canopy thus reduces the downward solar radiation and simultaneously enhances the downward longwave radiation. During 6 days of parallel recordings, the net radiation, Q_N, was on average 17 Wm^{-2} higher at the wooded site than at the woodless site, which is qualitatively in agreement with the observations reported by Petzold and Wilson (1974) and by Hendrie and Price (1978). This difference between the wooded (II) and the woodless (I) sites, however, varies significantly with cloudiness. The following regression equations relating daily mean values were found:

$$\Delta Q_N = Q_{NII} - Q_{NI} = 31(1-C) + 5 \quad (Wm^{-2}) \qquad (4.2.21)$$

$$\Delta Q_N = Q_{NII} - Q_{NI} = 36\left(\frac{Q_S}{Q_{ex}}\right)^2 + 5 \quad (Wm^{-2}) \quad , \qquad (4.2.22)$$

with correlation coefficients of 0.67 and 0.79, respectively. Here C is fractional cloud cover observed in Bergen, while Q_S is the global radiation measured at Frotveit or Dyrdalsvatn. The lower correlation coefficient in the former case is thus at least partly explained from the fact that the cloud cover observed in Bergen may occansionally deviate from Frotveit/Dyrdalen. These two regression equations are based on 26 days, during more than half of which radiation records are missing at Frotveit and therefore extrapolated from data at Dyrdalsvatn as described above.

According to eqs. (4.2.21 - 4.2.22) net radiation is higher within than outside the wood, and this difference is most pronounced in cloudless weather. The contributions to this pattern from the various radiation fluxes are illustrated in Fig. 4.2 and Table 4.6. It is seen that the lower albedo within the wood counteracts the shading of global radiation. The increase in net radiation within the wood is thus largely controlled by the enhancement of downward longwave radiation due to "window" radiation from the tree canopies. Consequently, this net radiation increase is enhanced by reduced sky radiance within the "window" region, i.e. by reduced cloud cover in accordance with eqs. (4.2.21 - 4.2.22).

Table 4.6. Global radiation (Q_S), surface albedo (α), net shortwave radiation (K*), blackbody radiation (σT_o^4), downward longwave radiation ($Q_{L\downarrow}$), and net radiation difference (ΔQ_N) between wooded (II) and woodless (I) site at Frotveit. All data refer to close to snow surface level.

Period	Q_S^I	Q_S^{II}	α_I	α_{II}	K_I^*	K_{II}^*	σT_o^4	$Q_{L\downarrow}^I$	$Q_{L\downarrow}^{II}$	ΔQ_N
6 days Q_N recorded	136	92	0.59	0.49	56	46	315	276	303	17
26 days Q_N partly modelled	86	57	0.62	0.52	33	28	315	302	317	11

4.2.2. Turbulent Fluxes of Heat, and Model Fit to observed Data.

The energy consumed in snowmelt, Q_M , may now be estimated from the equation (3.2.4), i.e.

$$Q_M = Q_N + Q_H + Q_E \quad ,$$

where the net radiation, Q_N , is recorded or estimated as described in Chapt. (4.2.1), and the turbulent fluxes of sensible (Q_H) and latent (Q_E) heat are estimated from the equations (3.3.5) and (3.3.6). Half-hourly values of wind speed, u , air temperature, T_a , and vapour pressure, e_a , recorded at the height, Z_a , above the snow surface (1.3 m on the average) are used in calculating daily totals of the heat fluxes. The three wind functions (3.3.9), (3.3.10), and (3.3.11) are applied, and the optimal values of the adjustable constants (a, b) in those functions are found. This is done by comparing daily totals of computed and recorded snowmelt and determining the set of (a, b) values which yields the lowest residual error, σ_r , (3.3.12).

Results from Dyrdalsvatn snowmelt station.

The optimal values of a and b and the corresponding model efficiency, R2 (3.3.13), are given in Table 4.7. The three wind functions yield nearly identical efficiencies. Therefore, only the wind function, $f_1(u)$, (3.3.9), which contains a stability correction factor ($1-Ri_B Ri_c^{-1}$), and the more simple and widely used linear function, $f_2(u)$, (3.3.10) will be further discussed.

Following Anderson (1976), $Ri_c = 0.4$ is applied in $f_1(u)$. This yields by optimalization $a_1 = 4.05\ Jm^{-3}K^{-1}$, and, from eq. (3.3.16), $Z_o = 0.08$ cm . Optimizing with $Ri_c = 0.2$ gives $a_1 = 4.40\ Jm^{-3}K^{-1}$ and $Z_o = 0.11$ cm , indicating that the model is not very sensitive to Ri_c. Sverdrup (1936) arrived at $Z_o = 0.23$ cm by measuring wind profiles above a melting snow cover at West Spitsbergen, while Liljequist (1956-57) found values between 0.01 and 0.1 cm above an Antarctic snow field. Kuzmin (1961) suggests

Z_o=0.05 cm for a stable snow cover deeper than 10-20 cm. The investigation of Anderson (1976) indicated varying but evidently decreasing values of Z_o through the melt season, with a mean value of 0.15 cm. Accordingly, a value of 0.08 cm seems to be reasonable for Dyrdalsvatn during snowmelt.

Table 4.7. Model fit and optimal values of the adjustable constants (a, b) in the three wind functions during snowmelt at Dyrdalsvatn 1979-82.

Wind Function	Residual error σ_r mm day^{-1}Wm^{-2}		Model efficiency R2	a_i Jm^{-3}K^{-1}	b_i	Standard deviation mm day^{-1}Wm^{-2}	
$f_1(u)=a_1(1-Ri_c^{-1}Ri_B)^2u$	6.94	26.7	0.793	4.05	—		
$f_2(u)=a_2u+b_2$	6.88	26.5	0.797	3.65	0.0(Wm^{-2}K^{-1})		
$f_3(u)=a_3u^{b3}$	6.94	26.7	0.793	4.05	0.95		
Recorded snowmelt						15.3	58.8

The standard deviations in T_a, u, and Z_a lead to a standard deviation of 10% in the stability correction factor $(1-Ri_BRi_c^{-1})$. From Table 4.7, however, it can be seen that the introduction of this variable factor does not improve the model. Possible improvement may be masked by variation in Z_o, and/or noise in the records of net radiation and snowmelt. The deviation from ideal site conditions may also strongly affect the stability factor, which is explicitly related to ideal conditions.

The optimal wind functions adopted for the Dyrdalsvatn snowmelt station are:

$$f_1(u) = 4.05(1-Ri_BRi_c^{-1})^2u \qquad (Wm^{-2}) \qquad (4.2.23)$$

where $Ri_c = 0.4$, and

$$f_2(u) = 3.65\ u\ , \qquad (Wm^{-2}) \qquad (4.2.24)$$

where the wind speed, u, is given in ms^{-1}. During neutral conditions $Ri_B = 0$, which yields $f_1(u) = 4.05\ u$.

Since (4.2.24) is developed from all observations at Dyrdalsvatn, this indicates that stable conditions above the melting snow cover suppress the average turbulent exchange by some 10% from the expected value during neutral conditions.

The topography of the model efficiency, R2 , when $f_2(u)$ is applied, is illustrated in Fig. 4.13. The optimal area is rather wide, indicating that many combinations of (a, b) values are suitable. By extrapolating the "ridge" to a=0 , the wind function degenerates to a constant. The efficiency, R2 , however, then is notably lower than the optimal value. It therefore can be established that variations in the wind speed is important to model.

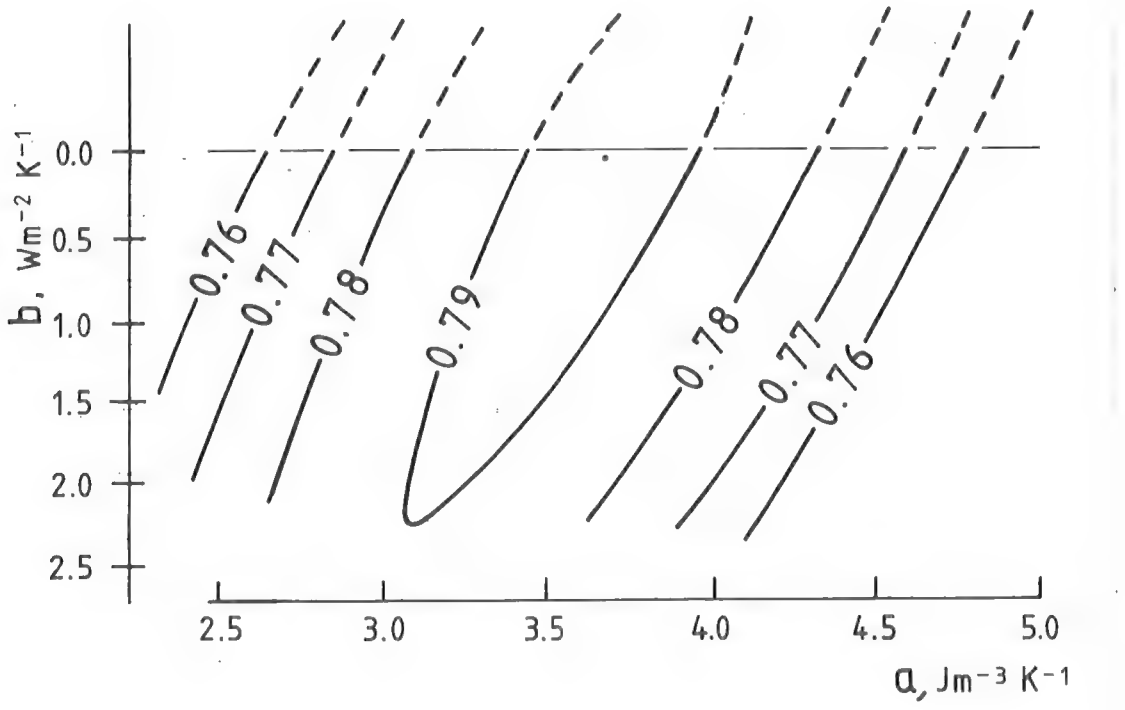

Fig. 4.13. Part of the R2 topography for the wind function $f_2(u) = a\,u + b$ for data from Dyrdalsvatn during snowmelt 1979-82.

For the linear wind function, $f_2(u) = a\,u + b$, Harstveit (1981) found the following (a, b) values: for April 1979 (3.1, 0.0), for May 1979 (3.85, 1.9), and for April 1980 (3.65, 1.15).

These values are slightly biased towards higher values, due to a systematic error in the incoming longwave radiation values, which has now been adjusted (Chapt. 3.1). Though there is some variation from one period to another, the constants are comparatively stable.

The figures 4.14 and 4.16 illustrate the fit of the energy balance model to recorded snowmelt when the optimal linear wind function (4.2.24) is applied. The fit is generally good. During the days May 12 - 15, 1979, however, large deviations are found. In the first part of this month, the old, coarse-grained snow pack was covered by a finer-grained layer, and the snow pack thus was strongly layered. Some of the melt water produced during the days May 1 - 11 was probably stored in the snow pack since the vertical flow of melt water is impeded by such a layering (Jordan, 1983). During the days of rapid snowmelt, May 12 - 15, the stored melt water percolated together with actual rain and melt water, thereby giving too high recorded melt rates. By excluding those days, the efficiency, R2, increases from 0.80 to 0.84.

Results from Frotveit.

The topography and local variations in the surface roughness at Frotveit make the application of the theory for deducing the wind functions rather doubtful. Nevertheless, an attempt was made to compute the constants in the linear wind function from the data set. The optimal function was:

$$f_I(u) = 3.1\ u + 2.3 \qquad (Wm^{-2}K^{-1}) \qquad (4.2.25)$$

for the woodless site, I, and

$$f_{II}(u) = 5.4\ u + 1.9 \qquad (Wm^{-2}K^{-1}) \qquad (4.2.26)$$

for the wooded site, II. The wind speed, u, is given in ms^{-1}. The efficiency, R2, is 0.71 at the woodless site and 0.83 at the wooded site. The difference could partly be explained by the different wind speed patterns at the two sites: At the wooded site the wind speed remained very low through all the days of snowmelt,

while at the woodless site it was relatively high during humid weather conditions (Table 4.10). This could result in a more variable turbulence mechanism at the open site. In addition, the net radiation is greater within the wood due to longwave radiation from the trees (Chapt. 4.2.1). The radiation estimates may be more precisely determined than the turbulent heat fluxes, and thus the total energy balance estimates may be of higher quality within the wood than outside. The samples are small, however, and the difference in R2 between the two sites may be insignificant.

The optimal wind functions, $f_I(u)$ and $f_{II}(u)$, are used in the further calculations. At a first glance, these functions may seem rather different. Both indicate, however, that the turbulent activity does not vanish for the very low wind speeds which prevailed at Frotveit during the recorded snowmelt periods. Businger (1973) suggests a "bursting" process during very stable conditions. The air near the snow surface is cooled, and small wind speed fluctuations mix the air when the layering becomes too strong.

The function $f_{II}(u)$ deviates from $f_I(u)$ mostly through the higher value of the slope constant, a. This could be explained by higher surface roughness values. However, the model fit is rather insensitive to variations of this adjustable constant due to the very low wind speed prevailing in the wood. By exchanging (4.2.26) for (4.2.25) at the wooded site, R2 drops only from 0.83 to 0.79.

Results from Austlihylla.

For Austlihylla, the optimal linear function is

$$f(u) = 3.1\ u \qquad (Wm^{-2}K^{-1}) \qquad (4.2.27)$$

where u is the wind speed (ms^{-1}). This function yields somewhat lower values of the heat fluxes than the optimal function at Dyrdalsvatn during identical weather conditions. The model efficiency, R2 = 0.47, which is a markedly poorer model fit than was found at Dyrdalsvatn.

Due to the large amount of snow at Austlyhylla a time lag between actual and recorded snowmelt/rain amount should be taken into account also on daily basis. The model improvement when using an optimal time lag (4 hours) between actual snowmelt/rain input and recorded discharge is small (Table 4.8), however, and cannot explain the low model efficiency found.

The data set is also separated in two parts according to the amount of daily precipitation, P : $P \leq 5$ mm (category I, 60 days), and $p > 5$ mm (category II, 22 days).

Table 4.8. Model efficiencies, standard deviations, and mean values of modelled and recorded snowmelt at Austlihylla during 1979-82.

No of days	Classification	Model	Model Efficiency R2	Standard Deviations mm day^{-1}	Wm^{-2}	Mean Values mm day^{-1}	Wm^{-2}
82	–	Energy Balance f(u)=3.1 u	0.47	11.6	44.7	13.3	51.2
82	–	Energy Balance f(u)=3.1 u and 4 hours time lag	0.50	11.5	44.3	13.3	51.2
60	$P \leq 5$ mm	Energy Balance f(u)=2.9 u	0.67	12.1	46.6	12.8	49.3
22	P>5 mm	Energy Balance f(u)=4.05 u	0.00	10.1	38.9	15.0	57.8
82	–	Recorded Snowmelt	–	9.9	38.1	13.5	52.0
60	$P \leq 5$ mm	Recorded Snowmelt	–	9.7	37.3	12.8	49.3
22	P>5 mm	Recorded Snowmelt	–	10.0	38.5	15.5	59.7

The data in category II (P > 5 mm) yield no model fit, which suggests that the deviation between recorded and computed snowmelt is due to errors in the snowmelt data during heavy rain. Austlihylla is a rather flat mountain plateau, but on a larger scale the terrain is sloping some 45% (Fig. 2.2). During winter a deep snow-drift builds up along the plateau. Water movements parallel to the snow surface may occur, especially during heavy rain. These movements, however, have a random character depending on physical properties of the snowpack, e.g. ice layers and other density barriers, as well as on the rainfall and snowmelt rates (Wankiewicz, 1978). The vertical movements of the liquid water through the snow will have a corresponding random character. It should, however, also be noted that the standard error in the rain records is high (Chapt. 3.1). Nevertheless, the conclusion must be that during rain-on-snow events a net flow of liquid water has passed across the lysimeter edges. Unfortunately, no measurements of water equivalent on the lysimeter for discharge verification exist.

By using the 60 days of category I ($P \leq 5$ mm), a significant model improvement was achieved (Table 4.8). The wind function then found was

$$f(u) = 2.9\ u \qquad (Wm^{-2}K^{-1}) \quad , \qquad (4.2.28)$$

where u is the wind speed (ms^{-1}).

These 60 days largely coincide with a group of days with small cloud amounts. During such days the energy balance model at Dyrdalsvatn yields higher values than recorded snowmelt, indicating that the turbulent heat supply to the snow surface is overestimated. It is therefore to be expected that the a-value of the wind function, a_u, during fine weather at Austlihylla is lower than the value 3.65 valid during average weather conditions at Dyrdalsvatn.

Conclusions regarding the wind function.

The linear wind function (4.2.25)

$$f(u) = 3.1\ u + 2.3 \quad ,$$

derived at the open site at Frotveit is not far from optimal at

the wooded site as well. Fig. 4.13 illustrates that it is also very close to optimal at Dyrdalsvatn (R2=0.79). In addition, considering the inaccuracies connected to the deduction of eq. (4.2.27), the function (4.2.25) is nearly optimal for the data set at Austlihylla,too. For making the heat flux calculations and drawing the figures, the wind function optimal to the respective site is used. By exchanging the optimal function with eq. (4.2.25), however, very small deviations would occur. The validity of eq. (4.2.25) is thus confirmed at several sites, which differ in wind exposure and vegetation, and should therefore be suitable in the whole maritime region of Western Norway.

By comparing the wind function (4.2.25) to functions found in other investigations, it is essential that the wind speed records refer to the same height above the surface. Records at different heights can be made comparable by using the formula,

$$\frac{u_2}{u_1} = \left(\frac{z_2}{z_1}\right)^n , \qquad (4.2.29)$$

where the indices represent two different levels at the same site. n varies with such conditions as surface roughness, height, and stability. However, the value 0.17 suggested by Anderson (1976) at a melting snow cover is adopted here as an average value.

In Table 4.9 linear wind functions found in different studies are reduced to the reference height, 1.0 m. The adjustable constants a and b found in this study are in reasonable agreement with the three most reliable investigations (Kuzmin (1961), U.S.A.C.E. (1955), Anderson (1976)) listed.

Table 4.9. Comparison of linear wind function constants found in different investigations.

Reference	Value of coefficents for a measurement height of 1.0 m	
	a($Jm^{-3}K^{-1}$)	b($Wm^{-2}K^{-1}$)
Kuzmin (1961) based on data from the USSR plus measurements by Kohler (1950)	3.2	4.0
Snow investigations (U.S.A.C.E., 1955), Central Snow Laboratory	4.0	0.0
Meiman and Grant (1974), Colorado	7.2	0.0
Anderson (1976), using an optimizing routine	3.4	0.0
Present study	3.2	2.3

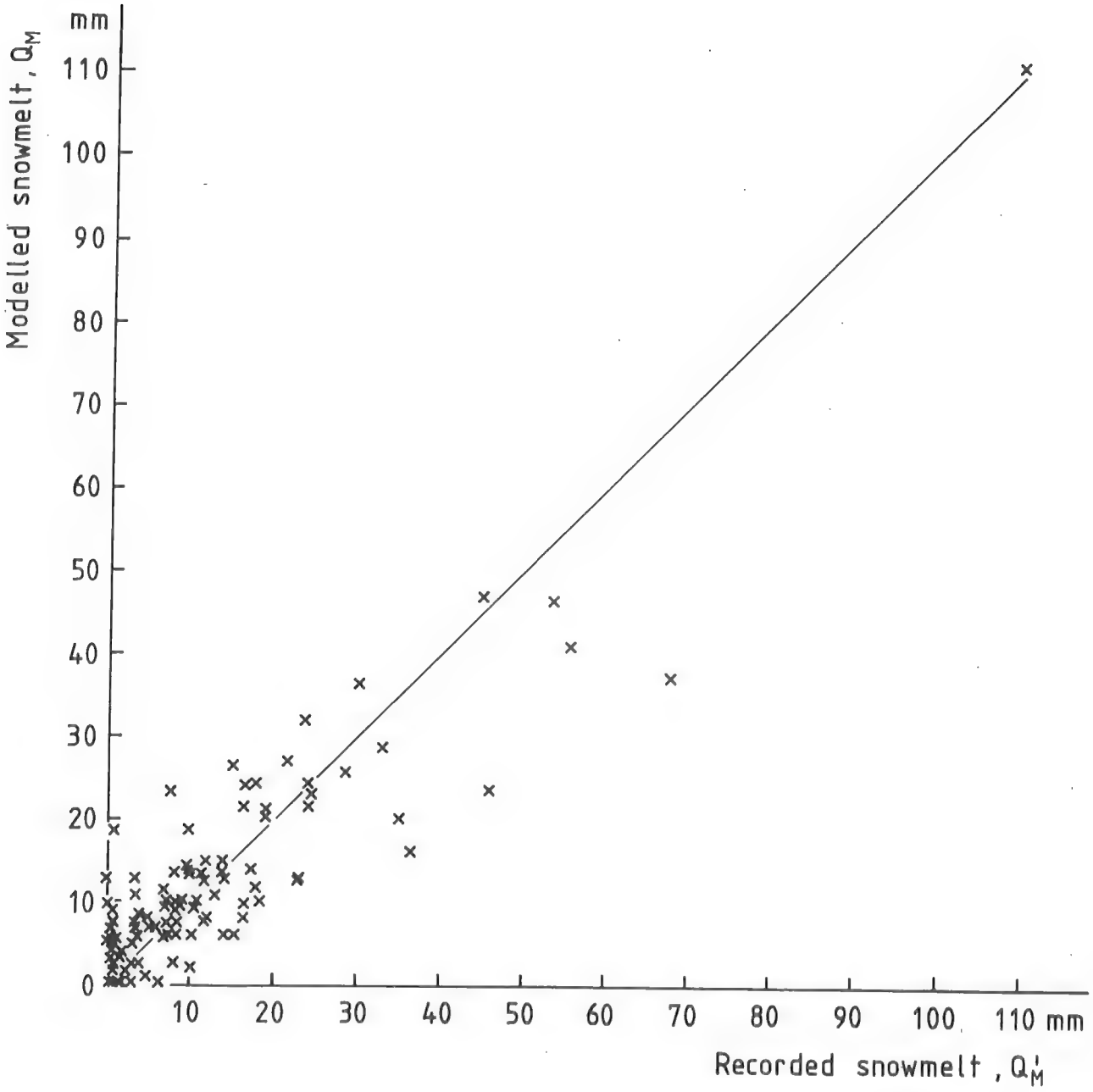

Fig. 4.14. Scatter diagram of recorded/estimated daily snowmelt at Dyrdalsvatn 1979-82 using the energy balance model with the optimal wind function $f(u) = 3.65u$ ($Wm^{-2}K^{-1}$).

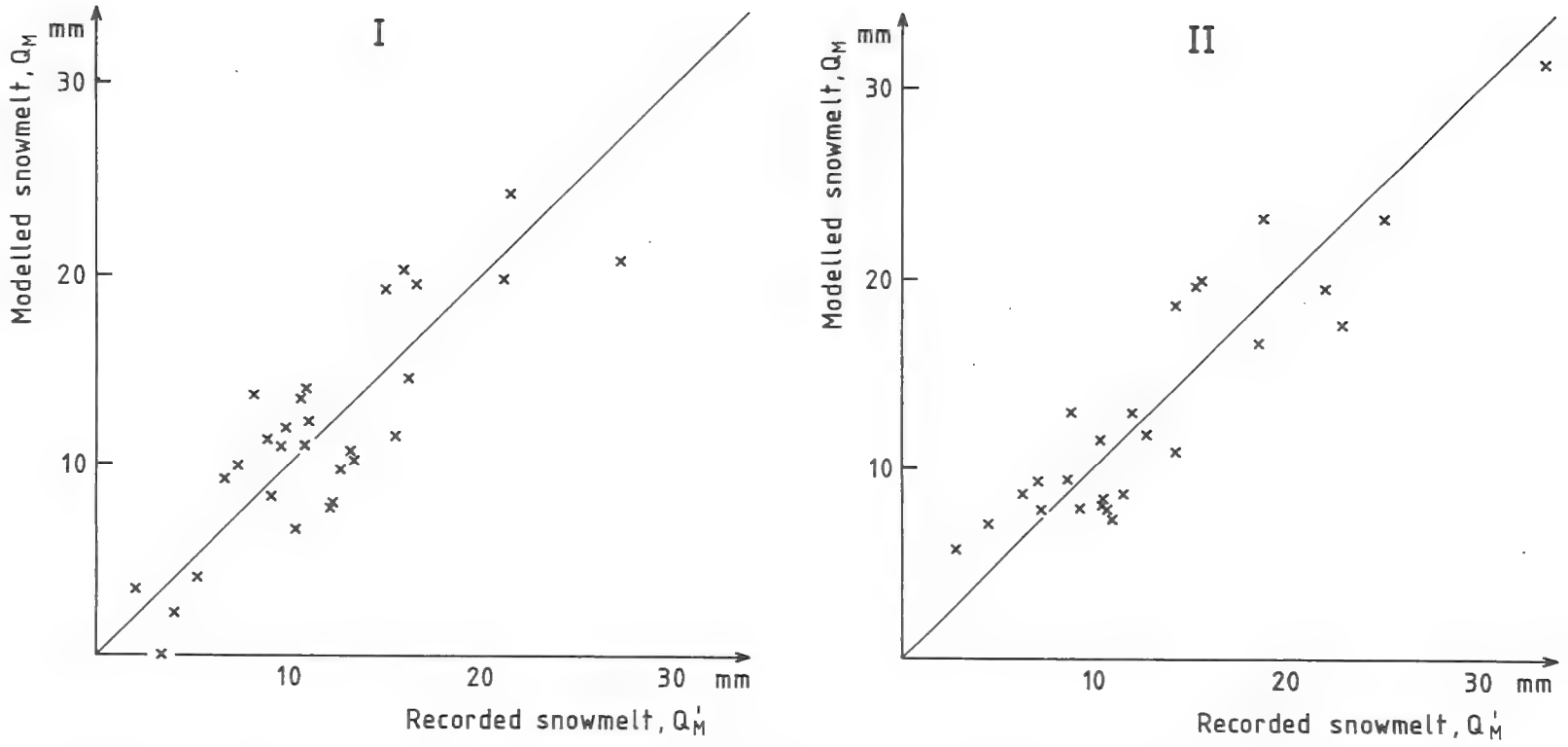

Fig. 4.15. Scatter diagram for recorded and modelled daily snowmelt using the energy balance model (with optimal wind functions) at the woodless (I) and wooded (II) site at Frotveit, 1981-82.

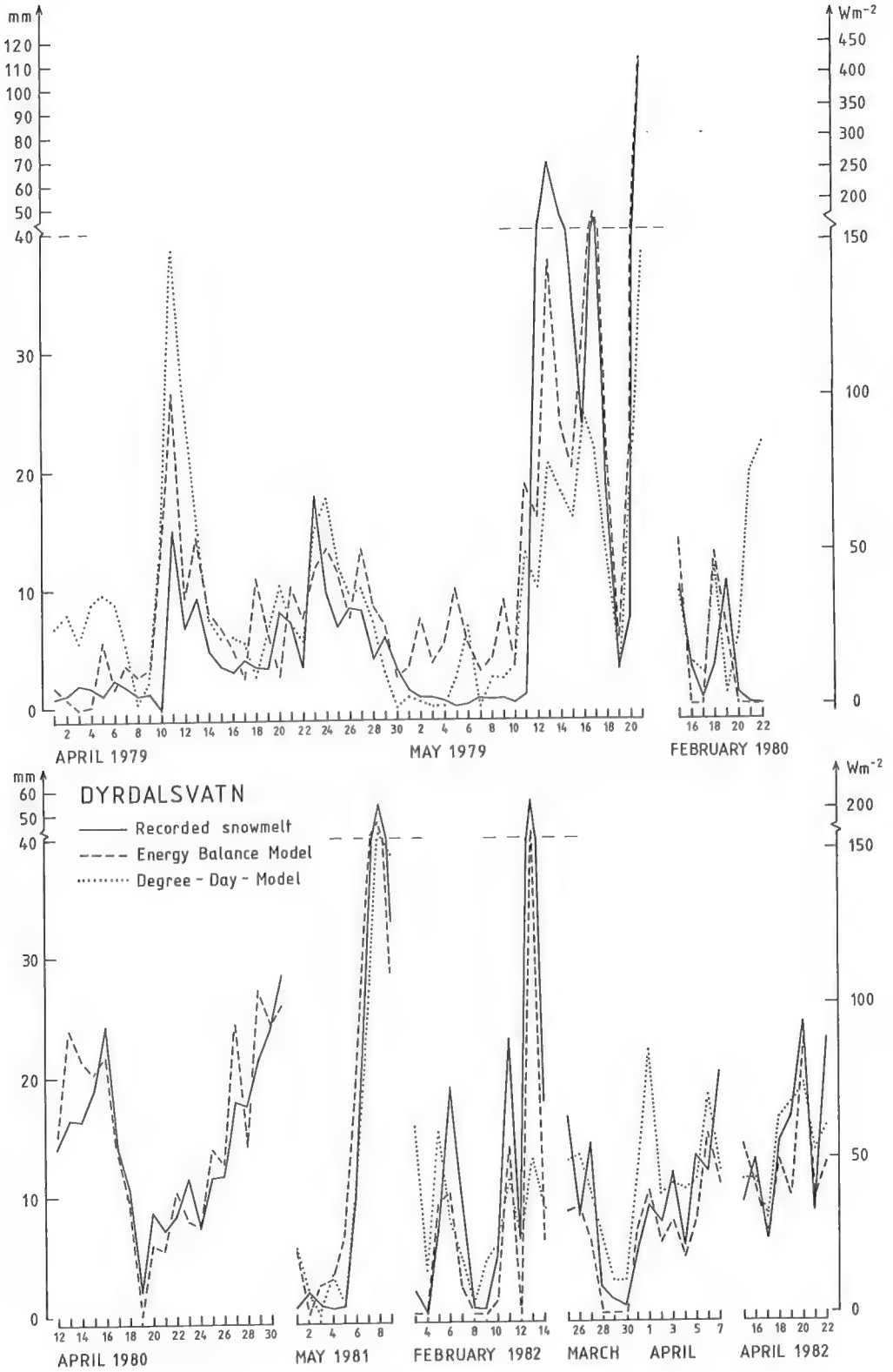

Fig. 4.16. Daily totals of recorded and modelled snowmelt at Dyrdalsvatn during 1979-82.

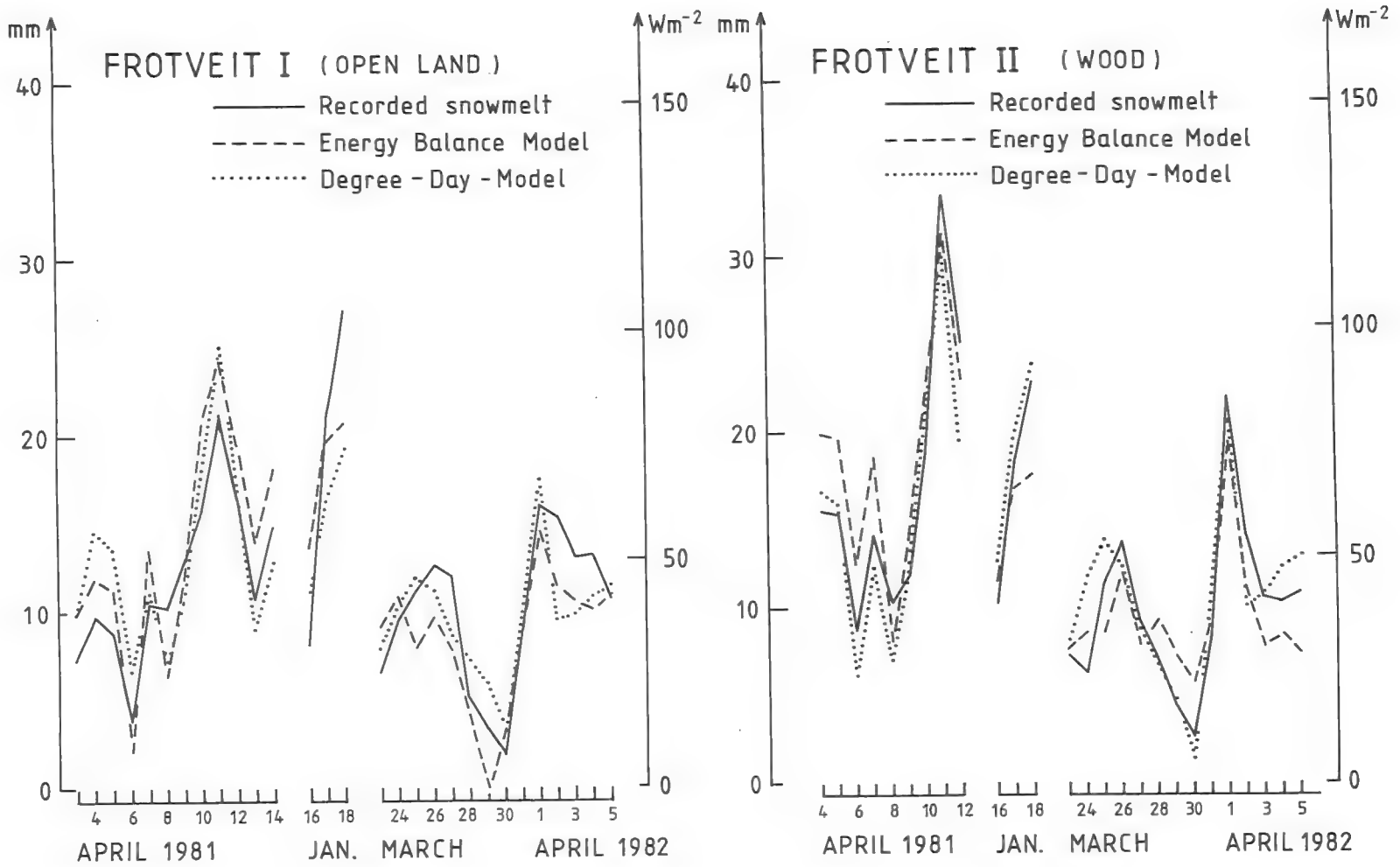

Fig. 4.17. Recorded and computed daily totals of snowmelt at Frotveit 1981-82.

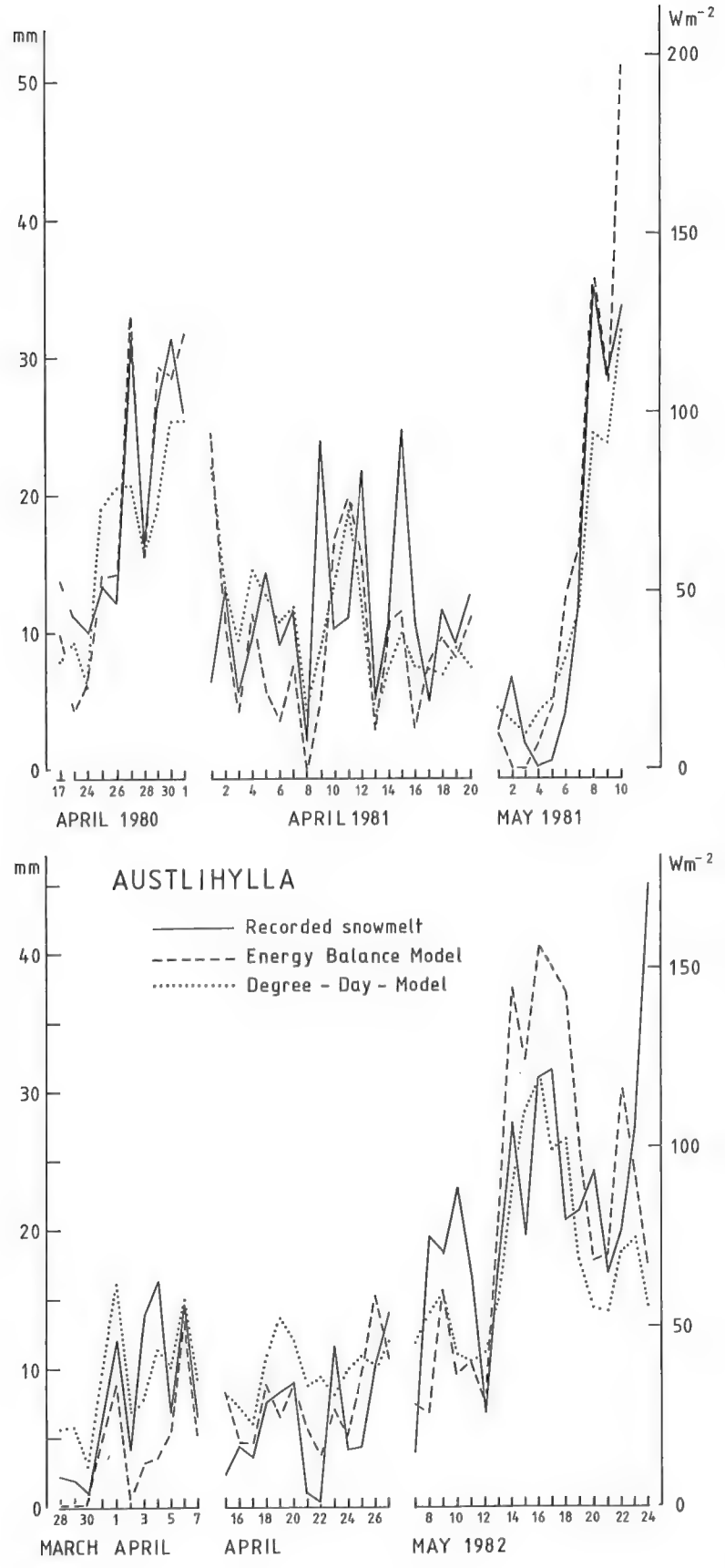

Fig. 4.18. Daily totals of recorded and modelled snowmelt at Austlihylla 1980-82. The wind function f(u)=3.1 u is used for the energy balance model.

The relative importance of the different heat sources in snowmelt.

The recorded net radiation, Q_N , and computed sensible (Q_H) and latent (Q_E) heat (using the optimal linear wind function (4.2.24) during snowmelt at Dyrdalsvvatn 1979-82 are shown in Fig. 4.19. On the average, Q_H represented 68%, and Q_N 36% of the total energy used in melting the snowpack, while Q_E represented a heat sink of 4%. The data are also separated into two groups according to the cloud cover (observed every 3 hour in Bergen) (Table 4.10). Cloudy weather often reflects maritime influence, while clear or light cloudy weather reflects continental influence. Q_H ususally provides the highest contribution to the snowmelt in both weather types, and is rather independent of the cloud cover. Q_N is also rather independent of the cloud cover, the gain of short-wave radiation during clear weather being counteracted by a longwave radiation loss (Table 4.10). During the spring of 1979, when the albedo values were high (74%, Fig.4.1), Q_H was notably higher than Q_N (Fig. 4.19). On the other hand, during the last part of the spring of 1980 snowmelt season - with high global radiation, Q_S , low albedo, α (60%), and low wind speed, u - the net radiation, Q_N , exceeded the sensible heat flux, Q_H .

The small size of the latent heat flux, Q_E (on the average a heat sink of 4% of Q_M), is a consequence of averaging over all weather conditions. During 47 days net condensation occurred, making a total energy source of 14% of Q_M (averaged over the 122 days). Net evaporation occurred in 75 days, representing a heat sink of 18%. Table 4.10 shows that snowmelt rates on overcast days are markedly higher than the rates on less cloudy days. Computed energy fluxes suggest that this is mainly due to differences in the latent heat flux, Q_E . When the weather is cloudy, $Q_E>0$ (condensation), while evaporation ($Q_E<0$) dominates in less cloudy weather. Evaporation and condensation contribute significantly to the energy budget of the snowpack, while the contributions to the mass budget are negligible (Table 4.11).

At Frotveit the melting rate was, as a rule, higher at the wooded site than at the woodless (Fig. 4.21, Table 4.10). During days with light cloud cover ($c<0.90$), this difference is pronounced, while the snow melts somewhat faster at the woodless site during overcast weather ($c\geq 0.90$). The correlation coefficient, r , between recorded daily snowmelt totals at the two sites was 0.82, while $r = 0.96$ using only overcast days ($c\geq 0.90$), and $r = 0.91$ using only days when $c<0.90$. These differences are mainly caused by enhanced net radiation, Q_N , at the wooded site during clear weather (Table 4.10) due to the high contribution of longwave radiation from the trees (pp. 67). Moreover, the fluxes of Q_H and Q_E are higher at the woodless site than in the wood during humid (overcast) weather.

The percentage contributions of the fluxes to the total energy input at the wooded site are 59% (Q_N), 32% (Q_H), and 9% (Q_E) while the corresponding values at the open place are 43%, 43%, and 14% during the 26 days of simultaneosly recorded snowmelt at the two sites.

Table 4.10 also illustrates that the modelled snowmelt at Frotveit and Dyrdalsvatn is overestimated during clear weather, and underestimated during overcast weather. This will not, however, be further discussed due to the rather small samples.

Table 4.10. Average daily values of wind speed, u , air temperature, T , vapour pressure, e , energy fluxes, and recorded snowmelt at Dyrdalsvatn (1979-82), Frotveit (1981-82), and Austlihylla (1980-82). The linear wind functions optimal to each of the stations, and half hourly values of u, T , and e are used in the calculations. Also shown are the results for Frotveit and Dyrdalsvatn for overcast days ($c \geq 0.90$), and days with less cloud cover ($c < 0.90$).

Station	No of days	Cloud Cover (Bergen)	$\bar{u}$, ms^{-1}	$\bar{T}$, °C	$\bar{e}$, mb	Latent Heat Q_E	Sensible Heat Q_H	Absorbed Shortwave Radiation	Effective Longwave Radiation	Net Radiation Q_N	Modelled Snowmelt Q_M	Recorded Snowmelt Q'_M (Wm^{-2})
	84	$c<0.90$	2.5	2.2	5.2	-10	29	42	-27	15	34	30
Dyrdalsv.	38	$c\geq0.90$	2.8	2.6	6.9	16	34	12	4	16	66	75
	122	$\bar{c}=0.71$	2.6	2.3	5.7	- 2	30	33	-17	16	44	44
	15	$c<0.90$	0.5	4.0	6.3	2	18	52	-29	23	43	40
Frotveit Woodl., I	11	$c\geq0.90$	0.8	3.9	7.6	12	20	12	- 1	13	45	52
	26	$\bar{c}=0.79$	0.6	3.9	6.9	6	19	35	-16	19	44	45
	15	$c<0.90$	0.3	3.8	6.5	2	18	42	- 3	39	59	54
Frotveit Wooded,II	11	$c\geq0.90$	0.2	3.8	7.6	8	13	10	9	19	40	47
	26	$\bar{c}=0.79$	0.3	3.8	7.0	5	16	28	2	30	51	51
Austlih.	82		2.4	3.3	6.0	0	25			26	51	52

Table 4.11. Totals of snowmelt, evaporation and condensation (mm water equivalent) at Dyrdalsvatn during 1979 and 1980.

Period	Recorded Snowmelt	Computed (Net Daily Values added)	
		Evaporation	Condensation
April 1, - May 21, 1979	550 mm	10.3 mm	13.4 mm
April 12, - May 1, 1980	291 mm	4.4 mm	1.2 mm

To conclude, net radiation, Q_N , and sensible heat, Q_H , on the average yielded some 50% of the energy consumed in melting the snowpack in this area, while the contribution from the latent heat flux, Q_E , was minor. However, the contributions of these three principal energy fluxes varied both in space and time. Moreover, it should be stressed that the low value of Q_E is an average value. During shorter periods much heat may be released by condensation or lost by evaporation.

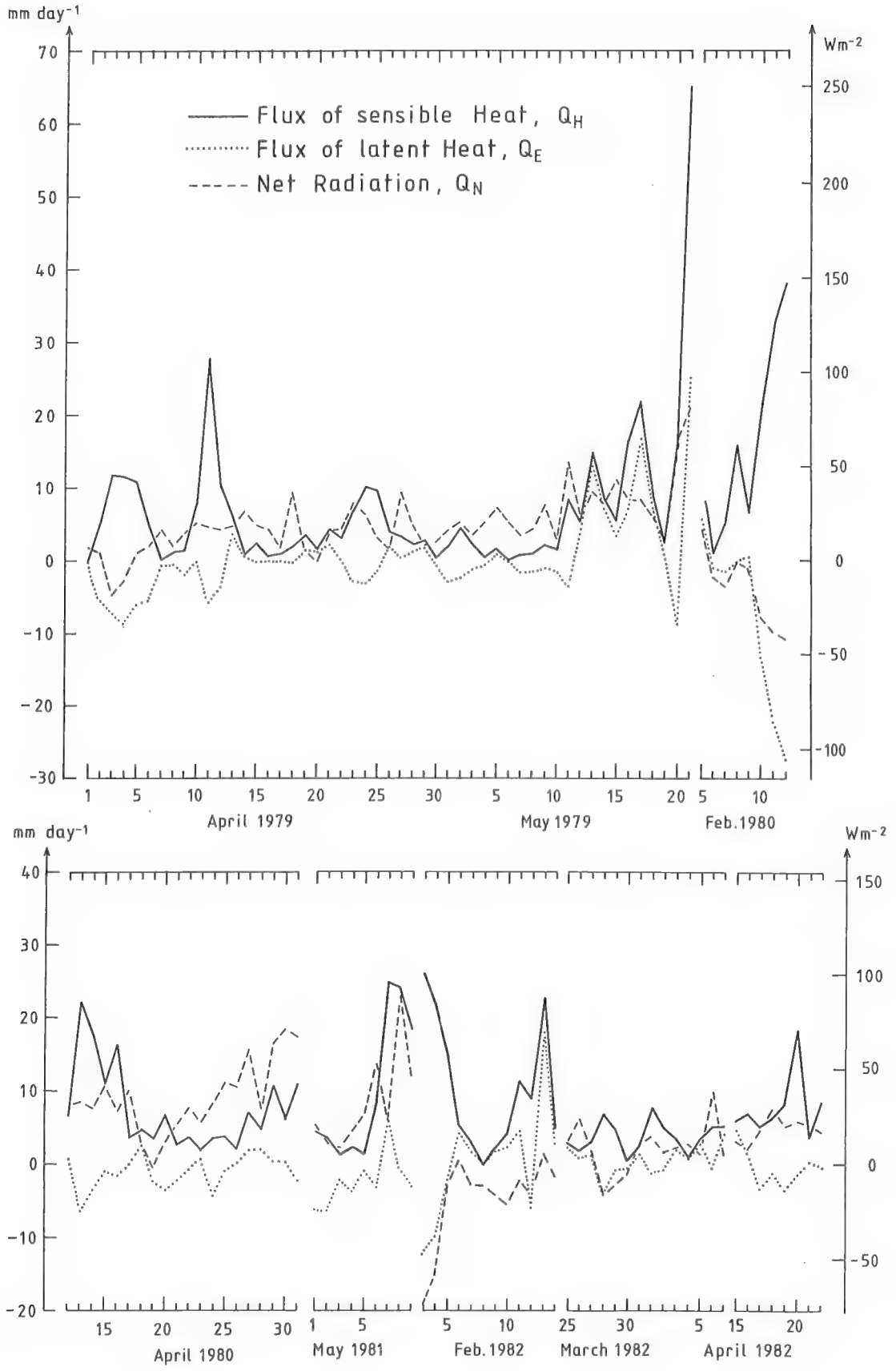

Fig. 4.19. The variation of the computed energy fluxed, Q_H , Q_E , and Q_N , at Dyrdalsvatn during snowmelt 1979-82.

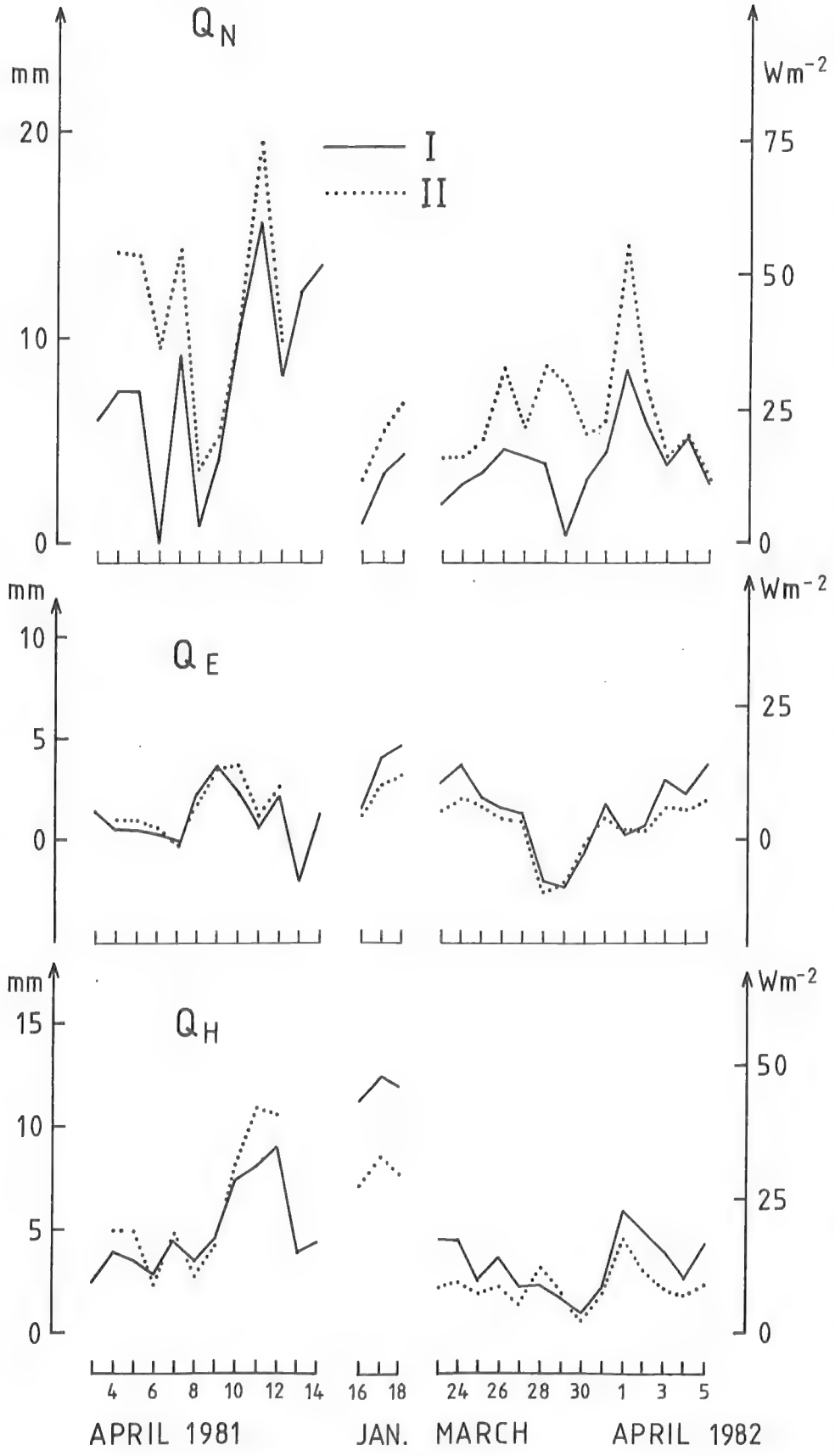

Fig. 4.20. Daily mean fluxes of net radiation, Q_N , latent heat, Q_E , and sensible heat, Q_H , at the woodless (I), and wooded (II) site at Frotveit during the periods of recorded snowmelt 1981-82.

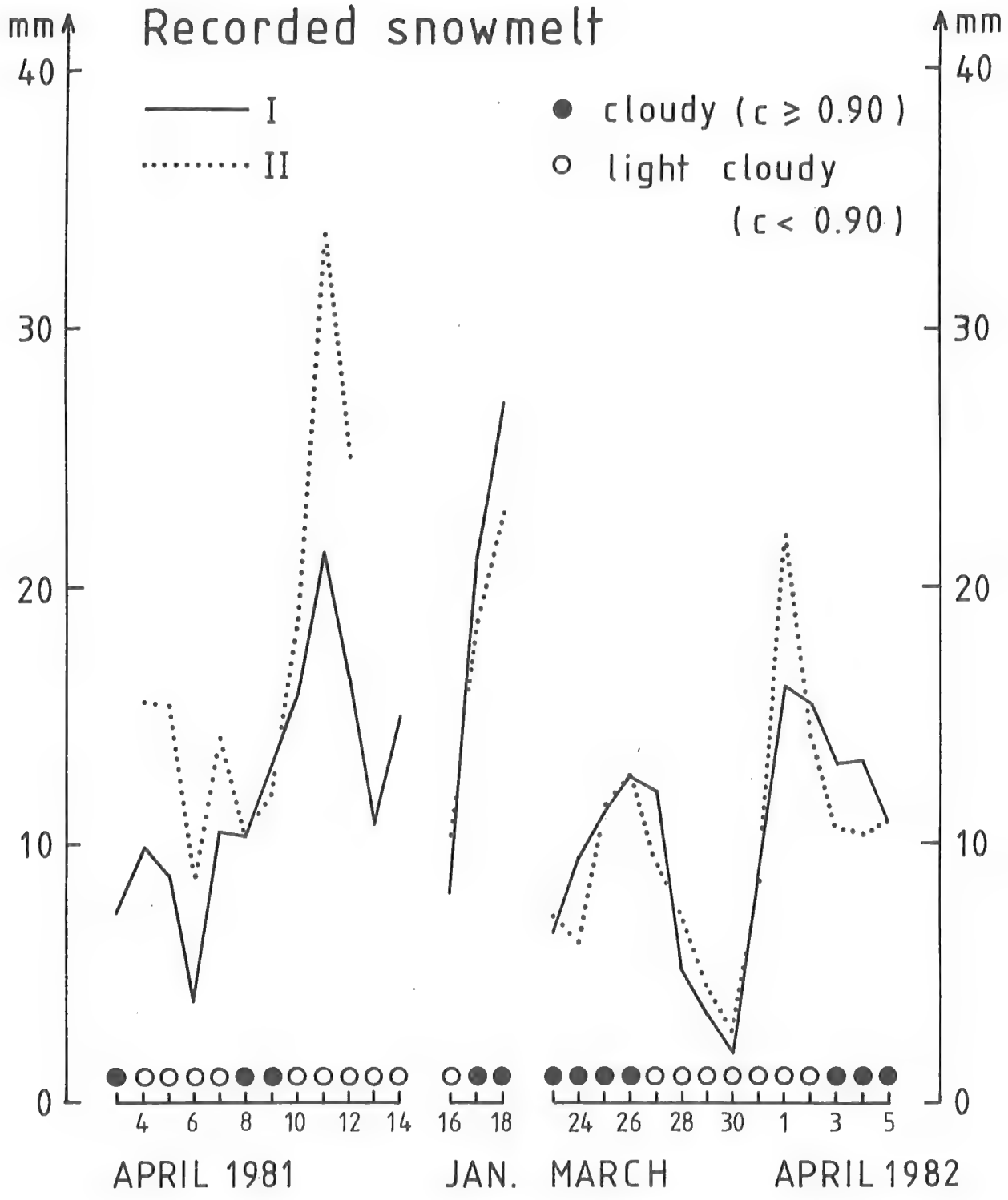

Fig. 4.21. Daily totals of recorded snowmelt at the woodless (I), and wooded (II) site at Frotveit 1981-82. Also indicated is the cloud cover, c , observed in Bergen.

Extreme events

On May 21, 1979 a snowmelt total of 110 mm was recorded. The melting rate was 8 mm hour^{-1} in the middle of the day (Fig. 4.22b). Fig. 4.22a shows that air temperature, T , and wind speed, u , varied throughout the day, but both remained high. The air was moist, the albedo low, and the weather cloudy except in the middle of the day, yielding a significant contribution from the absorbed global radiation, and an effective longwave radiation gain (Table 4.12). The rainfall total was markedly lower than the snowmelt total, the snowpack in the collection vats was rather small, and the physical properties of the snow did not change on this day. The snowmelt measurements should therefore be fairly accurate. When using the wind function $f_2(u) = 3.65\ u$, the efficiency, R2 , was 0.79 for 24 hourly observations on that day. Adjusting for the phase lag related to the percolation of the meltwater, yields an even better fit. Fig. 4.22b suggests a lag of 1 hour, which gives R2=0.88.

On some days (April 3-4, 1979; Feb. 20-22, 1980; Feb. 3-4, 1982) when net radiation loss, rather strong wind, and dry air conditions prevailed, no snowmelt was recorded, in spite of diurnal air temperatures exceeding 0°C. Since the snowpack was approximately ripe and isothermal those days, it can be concluded that no snowmelt occurred. The situation may be described as follows: The snow surface gains heat through the sensible heat flux, Q_H , and gives off heat through the net radiation, Q_N , and the latent heat flux, Q_E (evaporation). By suggesting the surface temperature, T_o , to be 0°C (T_o was not recorded), the net energy calculated, Q_M , is negative, and T_o must decrease. The energy balance method thus predicts no snowmelt. When T_o decreases, however, Q_H increases, and the net radiation loss as well as the evaporation loss decreases, and a balance probably occurs ($Q_M \approx 0$). The days of February 21-22 may serve as an example (Table 4.12). If T_o decreases to -1.6°C, a balance is established. It should be noted that such a small surface temperature decrease only slightly lowers the internal energy of the snow because of its poor heat conduction properties.

These extreme situations illustrate some of the problems in using the air temperature as a single snowmelt indicator, and strengthen the reliability of the energy balance method.

Table 4.12. Meteorological variables, energy fluxes, and recorded snowmelt at Dyrdalsvatn May 21, 1979, and February 21-22, 1980. Legend, see Table 4.10.

Date	$\bar{T}$, °C	$\bar{u}$, ms^{-1}	$\bar{e}$, mb	α (albedo)	Rain-fall, mm	Energy Fluxes (Wm^{-2}) Q_H	Q_E	Absorbed Shortwave Radiation	Eff. Longw. Rad.	Q_N	Q_M	Recorded Snowmelt Q'_M
May 21, 1979	9.0	7.6	8.2	0.61	9.6	250	96	42	39	81	427	424
Feb 21-22, 1980	4.7	5.7	2.8	0.70	0	131[x]	-93[x]	15	-54[x]	-39[x]	-1[x]	0

[x] For $t_o = -1.6$°c

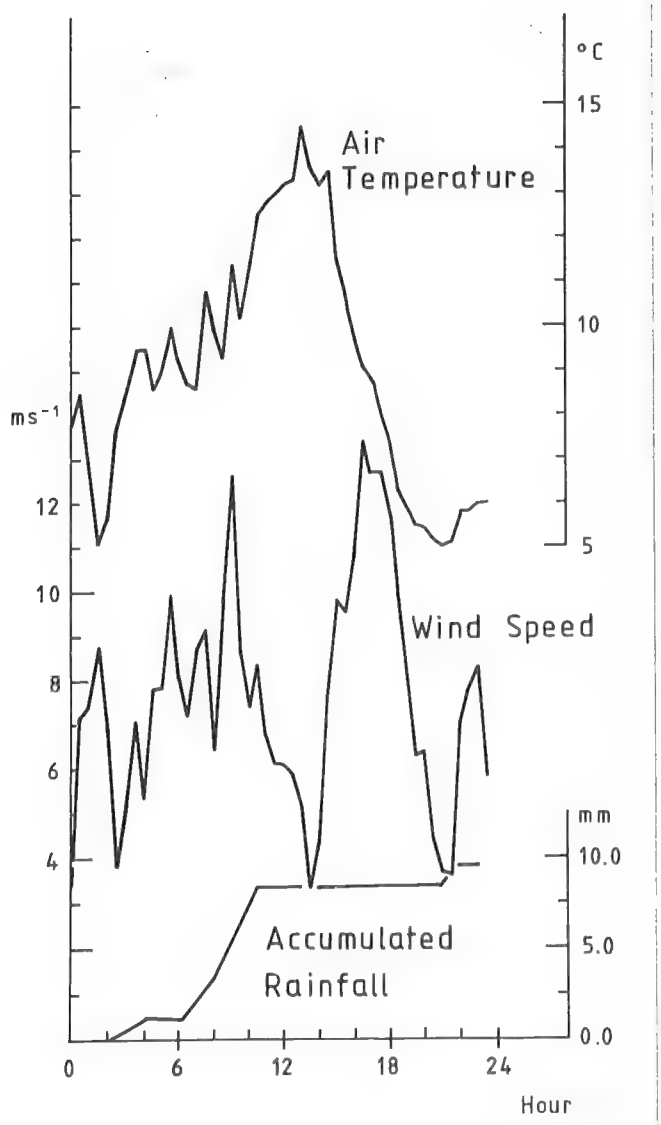

Fig. 4.22a. Recorded wind speed, air temperature and precipitation at Dyrdalsvatn on May 21, 1979.

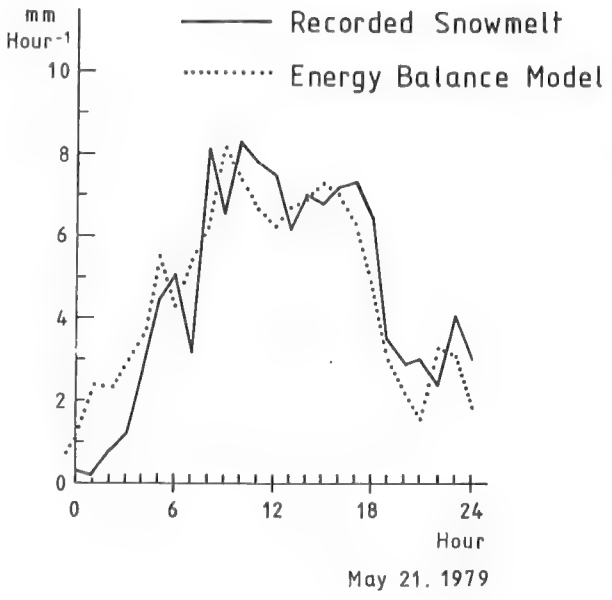

Fig. 4.22b. Computed and recorded snowmelt at Dyrdalsvatn on May 21, 1979.

4.2.3. Model Sensivity to Data Accuracy.

Snowmelt modelling is of special interest in outlying catchment areas for water reservoirs used in hydroelectrical power production. Meteorological stations are seldom situated near those areas, and the input data to the model therefore have to be extrapolated from observations at some distance from the actual site. It is of interest to see how sensitive the model is to errors of the size thereby introduced.

Daily mean values of air temperature, $\bar{T}$, water vapour, $\bar{e}$, and wind speed, $\bar{u}$, are replaced in turns by records from adjacent weather stations operated by the Norwegian Meteorological Institute. $\bar{T}$ are taken from Bergen-Florida, B (40 m a.s.l.), and Kvamskogen, K (408 m a.s.l.), $\bar{e}$ from Bergen-Florida, and $\bar{u}$ from Flesland, F (50 m a.s.l.) (Fig. 2.1). The radiation terms Q_S (global radiation), and $Q_{L\downarrow}$ (incoming longwave radiation) are taken from Bergen-Florida.

When comparing the data of $\bar{x}$ ($\bar{e}$, $\bar{T}$, Q_S, and $Q_{L\downarrow}$) recorded at Dyrdalsvatn and Bergen-Florida the daily mean difference is given by,

$$\Delta\bar{x}_1 = \bar{x}_B - \bar{x}_D \quad . \qquad (4.2.30)$$

Flesland is chosen as wind station since it is relatively exposed. The relation between observed wind speed at Dyrdalsvatn and Flesland is given by,

$$\Delta\bar{u}_1 = \frac{\bar{u}_D}{\bar{u}_F} \qquad (4.2.31)$$

The index 1 indicates the method of determining the systematic deviations of the data when recorded at different stations. In a second method (2) the height corrections are determined without using the data from Dyrdalsvatn. $\bar{T}$ and $\bar{e}$ are thus reduced according to the mean height gradients in the area. Fig. 4.23 illustrates the height gradients in Hordaland, found by using all weather stations except the lighthouses, for April 1979. The temperature gradient of -0.8°C/100 m is stronger than the accepted annual mean climatological value in the area (-0.6°C/100 m,

Lundquist, 1981). A gradient of -0.8°C/100 m, however, is also obtained by using standard normal values (1931-60) for April. The reason for the stronger gradient probably is that the more elevated station sites are snow covered, the lower ones are not.

The wind speed recorded at Flesland at a height of 10 m is reduced to a level of 1.3 m to be comparable with the records from Dyrdalsvatn. A surface roughness of 0.15 cm for melting snow (Anderson, 1976), and a logarithmic wind profile are assumed. It should be remarked that this theoretical reduction is rather speculative because of the differences in site characteristics, temporal variations in surface roughness, and the concept of logarithmic wind profile. The rough terrain in the area and the prevailing stable stratification above a snow surface make the last concept particularly questionable.

Any systematic difference in the cloud cover, and clear weather global radiation between Bergen and Dyrdalsvatn are neglected. For method 2, Q_S observed in Bergen is therefore used without corrections as model input at Dyrdalsvatn, and $\Delta Q_{S2} = 0$. Correspondingly, the incoming longwave radiation, $Q_{L\downarrow}$, is only corrected according to the differences in average air temperature by use of Swinbank's formula (4.2.12), and

$$\Delta Q_{L\downarrow} = 5.31 \cdot 10^{-13} (\bar{T}_B^6 - \bar{T}_D^6) \quad (Wm^{-2}) \qquad (4.2.32)$$

Here the air temperature recorded in Bergen, $\bar{T}_B$, is corrected according to the height gradient (Fig. 4.23) to obtain an estimate valid for Dyrdalsvatn, $\bar{T}_D$.

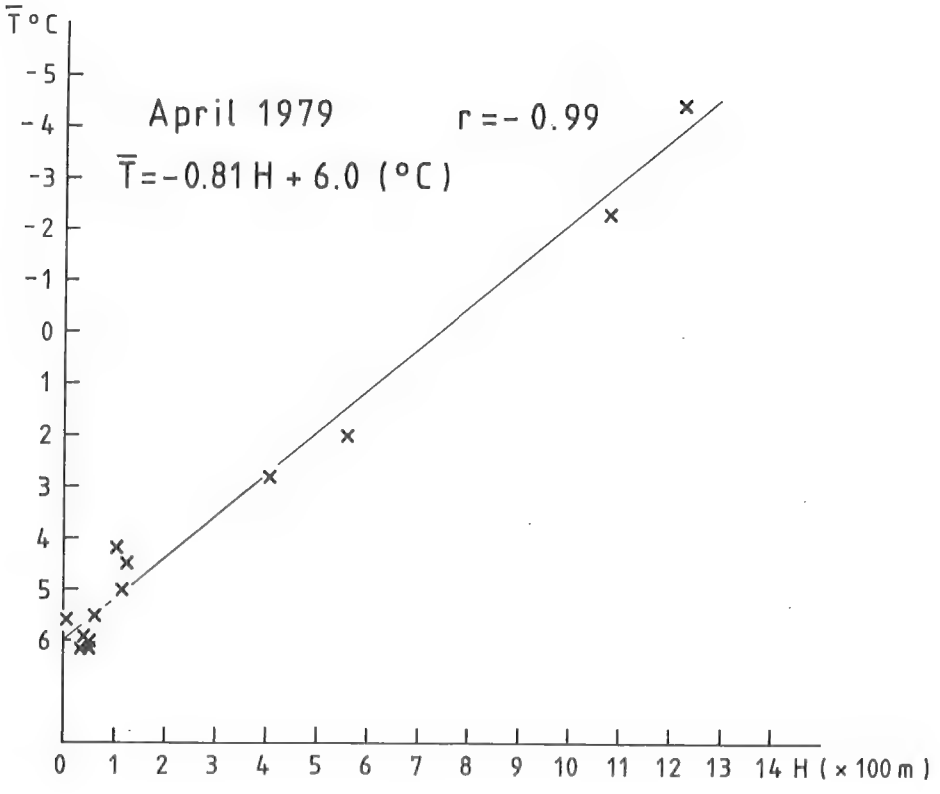

Fig. 4.23a. Relation between average air temperature of April 1979 and altitude based on 13 weather stations in Hordaland.

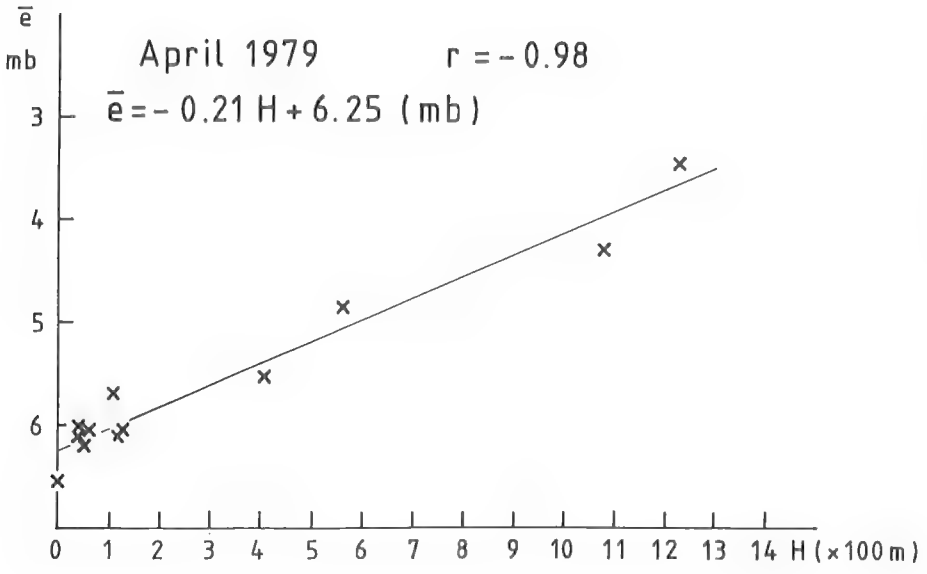

Fig. 4.23b. Relation between average vapour pressure of April 1979 and altitude based on 13 weather stations in Hordaland.

Table 4.13. Observed (1) and estimated (2) differences in diurnal air temperature, ΔT (°C), humidity, $\Delta \bar{e}$ (mb), global radiation, ΔQ_s (Wm^{-2}), incoming longwave radiation, $\Delta Q_{L\downarrow}$ (Wm^{-2}), and reduction factor for the wind speed, $\Delta \bar{u}$, between Dyrdalsvatn and adjacent weather stations at horizontal distance, hd . Standard deviations of the observed differences (reduction factor) are given in paranthesis.

Number of days :		n = 122		n = 122		n = 122		n = 122		n = 53	
Adjacent weather station	hd km	$\Delta \bar{T}_I$	$\Delta \bar{T}_2$	$\Delta \bar{e}_1$	$\Delta \bar{e}_2$	$\Delta \bar{u}_1$	$\Delta \bar{u}_2$	ΔQ_{s_1}	ΔQ_{s_2}	$\Delta Q_{L\downarrow 1}$	$\Delta Q_{L\downarrow 2}$
Bergen-Florida	11	4.0 (0.9)	3.2	0.83 (0.8)	0.84			0 (25)	0	17 (11)	17
Kvamskogen	23	0.9 (1.3)	0.3								
Flesland	18					0.70 (0.36)	0.77				

Method 2 is more general than method 1, since it does not presume any measurement of the average difference of the parameters between the actual site (Dyrdalsvatn) and the adjacent stations. As can be seen from Table 4.13, however, nearly identical corrections are obtained by the two methods. The further analysis based on method 1 is therefore valid for method 2 as well. (For Kvamskogen, no correction is applied in the analysis.)

Optimal modelled radiation estimates are also used. The global radiation, Q_s , is modelled according to Table 4.4, where 1-c is the cloud parameter. The incoming longwave radiation, $Q_{L\downarrow}$, is modelled according to Table 4.5, where c^2 is the cloud parameter, and the albedo, α , is estimated according to eq. (4.2.6). A constant value usually proposed, $\alpha = 0.70$, is also tried.

Table 4.14a. The efficiency, R2 , of the energy balance model when using data from Dyrdalsvatn, D, Bergen-Florida, B, Flesland, F, and Kvamskogen, K, for 122 days of recorded snowmelt at Dyrdalsvatn 1979-82. Index, M , specifies modelled radiation terms.

Station for recording							
Global Radiation, Q_s	Albedo α	Incoming Longwave Radiation $Q_{L\downarrow}$	Air Temp. T	Air humidity e	Wind Speed u	Average time of T, e, u	R2
D	D	B	D	D	D	½ h	0.79
D	D	B	D	D	D	24 h	0.79
D	D	B	D	D	F	24 h	0.81
D	D	B	B	D	D	24 h	0.79
D	D	B	K	D	D	24 h	0.78
D	D	B	D	B	D	24 h	0.83
D	D	B	D	B	F	24 h	0.81
D	D	B	B	B	D	24 h	0.84
D	D	B	B	B	F	24 h	0.83
D_M	D_M	D_M	D	D	D	½ h	0.78
D_M	0.70	D_M	D	D	D	½ h	0.77

Table 4.14b. Same as Table 4.14a for 53 days of snowmelt 1980-82 when $Q_{L\downarrow}$ was recorded at Dyrdalen.

Station for recording							
Q_s	α	$Q_{L\downarrow}$	T	e	u	Average time of T, e, u	R2
D	D	D	D	D	D	½ h	0.81
D	D	D	D	D	D	24 h	0.81
D	D	D	D	D	F	24 h	0.83
D	D	D	D	B	D	24 h	0.81
D	D	D	B	B	F	24 h	0.80
D	D	B	D	D	D	½ h	0.73
B	D	D	D	D	D	½ h	0.77
B	0.70	B	D	D	D	½ h	0.69
D_M	D_M	D_M	D	D	D	½ h	0.76
D_M	0.70	D_M	D	D	D	½ h	0.70

Tables 4.14 a and b give computed model efficiencies for different input data sets. The first two rows of Table 4.14 a, b differ only in the averaging period, ½ h and 24 h, respectively. For both data sets R2 is the same. Surprisingly, slightly better model fit is found using $\bar{u}$, $\bar{T}$, and $\bar{e}$-data from stations at a distance of some 10-20 km from the lysimeter. The difference, however, is not statistically significant.

The conclusion must be that the energy balance model is rather insensitive to errors in the input data, $\bar{u}$, $\bar{T}$, and $\bar{e}$ of the size introduced by extrapolating data 10-20 km away when a reasonable choise of the wind station is made, and necessary height corrections are made. These errors ($\Delta\bar{u} = 0.36\ \bar{u}$, $\Delta\bar{T} = 0.9°C$, $\Delta\bar{e} = 0.8$ mb, Table 4.13) are, however, large compared to the standard errors of the data recorded at the actual site (within 0.3 ms^{-1}, 0.2°C, and 0.1 mb, Chapt. 3.1). Since the first-mentioned errors have no effect on the model efficiencies, the last-mentioned have none either. The accuracy of the measurements of u, T, and e therefore are not critical.

Table 4.14 shows that the energy balance model is more sensitive to extrapolation errors in the radiation input data. The standard error of the net radiation, Q_N, recorded at Dyrdalsvatn (10 Wm^{-2}, Chapt. 3.1) is comparable to the error introduced by substituting incoming longwave radiation, $Q_{L\downarrow}$, from data recorded in Bergen (11 Wm^{-2}, Table 4.13). Improvements of the radiation data therefore are significant in endeavouring to improve the snowmelt estimates.

Table 4.14a indicates less sensitivity than 4.14 b, probably because the data in the former table also include several large snowmelt floods when moist and rainy weather invaded the area. In such situations, Q_S is very low and $Q_{L\downarrow}$ may be rather precisely estimated from the air temperature. This implies that during cloudy and rainy weather data from the regular network of meteorological stations can give fairly accurate snowmelt estimates assuming that representative surface wind values can be found.

However, during less cloudy and rainy weather, good estimates of net radiation are essential in producing reliable snowmelt estimates. Table 4.14 b indicates that the albedo should be estimated by a reasonable model if records are missing.

These results indicate that the rather poor energy balance model fit found by Kuusisto (1978) in Finland most certainly was due to unrepresentative net radiation records, a point mentioned by the author as a possible explanation.

4.3. The Degree-day Model.

In the simple degree-day model (3.4.1) the snowmelt is assumed proportional to the daily mean air temperature exceeding a threshold value. The model is widely used due to its simplicity, and is sometimes refined by allowing the proportionality factor (degree-day factor) to be a function of physical variables.

For the 122 days of recorded snowmelt at Dyrdalsvatn (1979-82), the average value of k in eq. (3.4.1) is 4.0 mm $day^{-1}{}^{\circ}C^{-1}$, which is very close to the value 3.9 mm $day^{-1}{}^{\circ}C^{-1}$, found by using total discharge data from the Dyrdalen precipitation catchment area 1977-79 (Lundquist, 1980). A rather poor model fit is obtained, however (Fig. 4.16, Table 4.15). Table 4.15 also illustrates that the degree-day constants varied strongly during the four years of snowmelt records. The reason for this instability is the variable weather of the area, together with the wind exposure of the site. By computing different degree-day constants during cloudy and fine weather a considerable improvement is obtained. The degree-day factor, k, is very high in cloudy weather, i.e. mild, humid, and windy weather effectively melts the snow. The use of average k-values therefore markedly underestimates the melting during rain-on-snow events during many large snowmelt floods.

Table 4.15. Degree-day factor, k (mm $day^{-1}°C^{-1}$), threshold temperature, T* (°C), and model fit at Dyrdalsvatn for simple degree-day models (3.4.1), and the composite model (3.4.2) using different values of k and T* according to the cloud amount, C .

Classification	Period	Number of days, n	k	T*	Model Efficiency R2	Correlation, coefficient, r
(3.4.1)	1979-82	122	4.0	-0.5	0.41	0.63
(3.4.1) C<0.90	1979-82	84	2.7	-0.7		0.78
(3.4.1) C≥0.90	1979-82	38	9.4	0.5		0.77
(3.4.2)	1979-82	122	—	—	0.67	0.81
(3.4.1)	Apr. 79	30	1.4	-1.9		0.65
(3.4.1)	May 79	21	9.1	-0.1		0.86
(3.4.1)	Feb. 80	8	-1.0	5.5		-0.45
(3.4.1)	Apr. 80	20	2.0	-3.5		0.90
(3.4.1)	May 81	9	4.6	-0.3		0.96
(3.4.1)	Feb. 82	12	5.6	-0.6		0.42
(3.4.1)	Mar. 25-Apr. 8-82	14	2.3	-1.6		0.52
(3.4.1)	Apr. 15-22 -82	8	5.7	0.5		0.82

Table 4.16. Degree-day factor, k (mm $day^{-1}°C^{-1}$), threshold temperature, T_*(°C), and model fit at Frotveit for the simple degree-day method (3.4.1), and the composite model (3.4.2) using different values of k and T_* when the cloud cover, C<0.90 (weather type a), and C≥0.90 (b). Also shown is the energy balance model fit.

site	Model	Coefficients						Model fit: Correl.coeff.			Model effic.
		k	k_a	k_b	T_*	T_{*a}	T_{*b}	r_a	r_b	r	R2
Woodless	Degree Day (3.4.1)	2.6	—	—	-0.6	—	—	—	—	0.83	0.69
	Degree Day (3.4.2)	—	2.3	4.1	—	-0.7	0.5	0.87	0.94	0.90	0.82
	Energy Balance	—	—	—	—	—	—	—	—	0.85	0.71
Wooded	Degree Day (3.4.1)	3.6	—	—	0.2	—	—	—	—	0.93	0.87
	Degree Day (3.4.2)	—	3.8	3.2	—	0.2	0.1	0.96	0.90	0.95	0.90
	Energy Balance	—	—	—	—	—	—	—	—	0.91	0.83

Table 4.17. Degree-day factor, k (mm $day^{-1}°C^{-1}$), threshold temperature, T_*(°C), and model efficiency, R2 , at Austlihylla for the simple degree-day method (3.4.1), and the composite model (3.4.2) using different values of k and T_* when the rain amount, P≤5 mm (category I), and P>5 mm (II).

Classification	Number of days	k	T*	R2
Simple model (3.4.1)	82	2.2	-2.8	0.54
P≤5.0 mm (I)	60	2.3	-2.2	0.73
P>5.0 mm (II)	22	2.1	-4.3	0.17
Composite (3.4.2) model	82	—	—	0.58

The negative response during February 1980 (Table 4.15) is due to the combination of high temperature, very dry air, and net radiation loss prevailing in the days of Feb. 21-22 (Table 4.12).

By correlating daily snowmelt totals recorded at Dyrdalsvatn (1979-82) to air temperature, $\bar{T}$, observed at Bergen-Florida, a correlation coefficient of 0.64 is obtained compared to 0.63 when using $\bar{T}$ records from Dyrdalsvatn. The degree-day factor, k , is 4.0 mm $°C^{-1}day^{-1}$, and the threshold temperature, T_* , is 3.5°C (Dyrdalsvatn: 4.0 mm$°C^{-1}day^{-1}$ and -0.5°C). The systematic deviation between $\bar{T}$ recorded at Bergen and Dyrdalen (mainly due to the height gradient) enters the model through the enhanced threshold temperature. A tuned model is rather insensitive to the random errors in the temperature field introduced by an intersite distance of 10-20 km. The height gradient, however, in general has to be estimated. The average deviation between recorded and estimated (Chapt. 4.2.3) air temperature difference between Bergen and Dyrdalsvatn is 0.8°C. For k = 4.0 mm $°C^{-1}day^{-1}$ this involves an underestimation of 3.2 mm for daily snowmelt totals. This is a significant amount when considering accumulated snowmelt totals, but not for flood situations.

From Table 4.16 (Frotveit) it is seen that the model efficiency, R2 , at the wooded site is remarkably high, and it is notably lower at the woodless site. This can partly be explained by enhanced net radiation at the wooded site during fine weather. The contribution of the longwave radiation from the trees is closely connected to the air temperature. Noteworthy is also the more variable wind speed at the woodless site (Fig. 4.2), and the correlation of the wind speed difference between the two sites to the cloud cover (humidity) (Chapt. 4.1). For these reasons there is a greater model improvement at the open site than in the wood when the simple model (3.4.1) is replaced with the composite model (3.4.2), and better performance of the degree-day method than the energy-balance model at the wooded site. However, the data sample is small, making the results uncertain.

The degree-day factor, k, is highest at the wooded site, mainly due to the enhanced net radiation mentioned. Kuusisto (1980) found lower values of k in coniferous forests than on open land. This illustrates that the constants in general have to be tuned to the actual site to be adequate.

At Austlihylla the performance of the degree-day method is poor (Table 4.17). If only the days with precipitation totals of 5 mm or less are considered, the days of poorest snowmelt record quality are omitted, and the weather variability is reduced. Table 4.17 clearly shows that the model fit is then improved. (The degree-day method performs slightly better than the energy balance model, which, however, showed a rather poor model fit. Due to the poor quality of the snowmelt records this point will not be pursued.)

To conclude, the degree-day model may be favourable in regions where the climate is stable, and at wind-sheltered sites (wood). The optimal degree-day constants, however, show spatial and temporal variations, usually necessitating a tuning of the model.

For wind-exposed sites and areas where the weather during snowmelt frequently changes between dry and moist, the simple degree-day model will not be suitable. It will in particular fail during snowmelt floods when moist and cloudy conditions prevail and in winter foehn situations when warm, but very dry and clear air is advected. However, different constants during rain and fine weather significantly improve the model estimates.

5. Summary and concluding remarks.

Snowmelt is mainly governed by the weather conditions, in particular air temperature, air humidity, wind speed, and net radiation at the surface. Reliable knowledge of the relation between snowmelt, weather and climate are important in planning hydroelectric power production, and for predicting snowmelt floods. Simple models which predict melting as a function of recorded or forecasted weather therefore are of great practical interest.

Snowmelt rate estimation is frequently needed in outlying areas, usually up in the mountains, where regular meteorological observations seldom are carried out. It is therefore important to find methods which can use data extrapolated from stations some distance away.

In this investigation snowmelt is studied in a rough, mountainous area situated in the maximum precipitation zone some 30 km from the sea-coast in Western Norway and some 10 km from Bergen. The climate is maritime, and snowmelt episodes occur throughout the snow accumulation season.

During the years 1979-82 measurements were carried out at three locations. The sites at Dyrdalsvatn (1979-82), a nearly level field (437 m a.s.l.), and Austlihylla (1980-82) at a sloping ground (632 m a.s.l.) were both situated above the timberline, while at the partly wooded area at Frotveit (1981-82, 285 m a.s.l.) one station was located on a woodless site, and a second station in a grove of deciduous trees.

At all the four stations air temperature, air humidity, wind speed, and runoff from the snowpack were recorded. In addition, precipitation, incoming shortwave and all-wave radiation, and albedo were recorded at Dyrdalsvatn.At the Frotveit stations incoming shortwave radiation and net radiation observations were included, as well as albedo and precipitation at the woodless station. Snowmelt (=runoff-rain) was found by lysimetry, measuring runoff from 9 m^2 plots of snow cover.

The highest peaks in the snowmelt records during 1979-82 occurred during heavy rain. The maximum daily snowmelt was 110 mm, when strong wind, high temperature and humidity prevailed, and the sky was overcast except for a few hours at midday, and the albedo was rather low.

The collected data are used to test two models for snowmelt estimation: the energy balance model and the degree-day model.

In the simplified energy balance model the energy consumed by snowmelt, Q_M , is supplied by net radiation, Q_N , sensible heat flux, Q_H , and latent heat flux, Q_E .

The net radiation can be directly measured, or it can be determined by recording/estimating the single terms of eq. (4.2.1):

$$Q_N = Q_S\ (1-\alpha) + Q_{L\downarrow} - \sigma To^4 \quad ,$$

where the snow surface temperature, To = 273°K during snowmelt.

When local topography (shading and surface slope) is taken into account, the incoming shortwave radiation may be extrapolated with satisfactory accuracy from records from stations some distance away (11 km in this study). When such records are not available, eq. (4.2.4d), evolved by using Q_S data from Dyrdalsvatn and the fractional cloud cover, C , from Bergen, may be applied at sites within the maritime region of Western Norway:

$$Q_S = (-0.16(1-C) + 0.81(1-C)^{\frac{1}{2}} + 0.07)Q_{ex} \quad .$$

The albedo, α , during snowmelt is correspondingly modelled by eq. (4.2.6):

$$\alpha = -0.13(1-C) - 0.05\ \ln t + 0.87 \quad .$$

Here, t is the number of days which the snow at the surface has been exposed to the atmosphere (eq. 4.2.5). The multiple correlation coefficient is 0.75. When applied at other climatic regions or at at areas where the dust or pollution deposit on the snow is different

from that of Dyrdalen (e.g. below the timberline) a tuning of the model is required.

Also the incoming longwave radiation, $Q_{L\downarrow}$, may be estimated from records (R) from stations some distance away when first order corrections due to possible systematic differences in the air temperature are made, eq. (4.2.32) (Swinbank, 1963):

$$\Delta Q_{L\downarrow} = 5.31 \cdot 10^{-13} (T_{aR}^6 - T_a^6) \quad (Wm^{-2}) \quad .$$

When reliable records are missing, $Q_{L\downarrow}$ can be modelled by eq. (4.2.11',M4):

$$Q_{L\downarrow} = 1.02\ \sigma T_a^4 + 71C - 92 \quad (Wm^{-2}) \quad ,$$

which is derived using 150 monthly values of $Q_{L\downarrow}$, C and T_a from Bergen. The multiple correlation coefficient is 0.95. The equation yields a cloud cover term of 71 Wm^{-2} for completely overcast weather, which is in good accordance with the value 60 Wm^{-2} given by Paltridge & Platt (1976, pp. 140). The clear sky term, $1.02\sigma T_a^4 - 92$ (Wm^{-2}), yielding 220 Wm^{-2} for $T_a = 273°K$ is well in agreement with the 229 Wm^{-2} predicted by the equation of Swinbank (1963). Eq. (4.2.11',M4) is probably valid within the whole maritime region of Western Norway.

The net radiation flux should be modelled (recorded) in all weather situations except perhaps for snowmelt floods during heavy overcast conditions when the term is known for certain to be small.

The turbulent fluxes of sensible (Q_H), and latent (Q_E) heat are modelled as formulae composed of a wind function factor and a temperature/vapour pressure difference between the air and the snow surface. Three wind functions were tested against the data set from Dyrdalsvatn. The wind functions were optimized by minimizing the residual error, σ_r, between recorded and estimated snowmelt. The energy balance model with a theoretically based wind function including a stability parameter and a critical Richardson number of 0.40 yielded an average surface roughness, Z_o of 0.08 cm, which

is a reasonable value during snowmelt. The model efficiency, R2 , was 0.79. The more simple power law, $f(u) = au^b$, also yielded R2 = 0.79 , and the linear wind function, f(u) = au+b , gave R2 = 0.80 . This indicates that the above-mentioned theoretical sophistication does not improve the method, a result which is probably caused by the deviation from ideal site conditions (surface homogeneity).

The optimal values of a and b in the linear wind function varied somewhat in time and space (from one station to another). However, during snowmelt the equations,

$$Q_H = (3.1\ U + 2.3)(Ta - To) \ , \quad (Wm^{-2})$$

and

$$Q_E = 1.7(3.1U + 2.3)(e_a - e_o) \ , \quad (Wm^{-2})$$

are fairly accurate. The required input data are daily values of the wind speed, u (ms^{-1}), air temperature, Ta (°C), and vapour pressure, e_a (mb), measured 1.3 m above the snow surface. During snowmelt the surface values are set at To = 0°C , and e_o = 6.11 mb. Records made within a horizontal distance of some 30 km are adequate when first order corrections of T and e (height gradients) are made, and u is recorded at a representative wind station. Wind records, U_R , made at a level Z_R differing from 1.3 m (Z_a) should be adjusted according to the formula (4.2.29) (Anderson, 1976),

$$\frac{U_a}{U_R} = \left(\frac{Z_a}{Z_R}\right)^{0.17}$$

to yield the wind speed values, U_a , at the level Z_a .

The values of (a,b) in the linear wind function are in reasonable agreement with results found by other investigators (Table 4.9).

In the degree-day model snowmelt is calculated as a function of the air temperature, T . The simple model, (3.4.1),

$$S_m = \begin{cases} k\,(T - T_*) , & T > T_* \\ 0 , & T \leq T_* \end{cases} \quad (\text{mm day}^{-1}) ,$$

where S_m is the snowmelt rate, is frequently used in snowmelt prediction. A composite model also tested is (3.4.2),

$$S_m = \begin{cases} k_1(T - T_{*1}) , & T > T_{*1} \\ 0 , & T \leq T_{*1} \end{cases} \text{ during dry (less cloudy) weather}$$

$$\begin{cases} k_2(T - T_{*2}) , & T > T_{*2} \\ 0 , & T \leq T_{*2} \end{cases} \text{ during humid (overcast) weather .}$$

In this field study the values of the degree-day constants k (mm day^{-1}°C^{-1}) and T_* (°C^{-1}) at Dyrdalsvatn were 4.0 and 0.5, respectively, while the values of (k_1 , T_{*1}) were (2.7 , -0.7), and (k_2 , T_{*2}) were (9.4 , 0.5). At Frotveit the values of (k , T_*) were (2.6 , -0.6) (woodless site), and (3.6 , 0.2) (wooded site). These variations illustrate that the degree-day coefficients vary considerably with weather conditions and terrain, and that the model has to be optimized to the current conditions. The air temperature recorded within a horizontal radius of 30 km may give satisfactory snowmelt estimates. However, it is important that any height corrections are precise.

At Dyrdalsvatn the energy balance model yielded a significantly better fit than the simple degree-day method (3.4.1), the model efficiency, R2 , being 0.80 and 0.41, respectively. This is due to the fact that the energy balance method models the physics of the snowmelt, and therefore simulates extreme situations better than the degree-day method.

A significant improvement of the degree-day method at Dyrdalsvatn was achieved (R2 = 0.67) by using different degree-day factors during overcast and less cloudy weather.

At Frotveit the degree-day method yields better fit than the energy balance mthod. The variations in the weather conditions (particularly in the wind speed) were less here, especially at the wooded site, and the longwave radiation from the trees is strongly temperature-dependent. The correlation between the air temperature and the energy fluxes to the surface is therefore high.

To conclude, the energy balance model is superior when calculating snowmelt peaks in maritime regions, and at wind-exposed sites. The degree-day method (3.4.1) may give satisfactory estimates in continental climatic regions, while it should be replaced by the composite method (3.4.2) using different degree-day factors during humid (overcast) and dry (less cloudy) weather, in maritime climatic regions.

As an average in this study the net radiation, Q_N , and the turbulent flux of sensible heat flux, Q_H , each provided about 50% of the energy consumed in melting the snowpack, while the contribution from the latent heat flux, Q_E , was minor. However, the contributions of these three principal energy fluxes varied both in space and time. On the average, Q_H constituted 68%, Q_N 36 % and Q_E -5% at Dyrdalsvatn, while at Austlihylla Q_H and Q_N constituted 50% each. At Frotveit the percentages were 43, 43, and 14 (woodless site, FI), and 32, 59, 9 (wooded site, FII). Except for FI and FII, the periods of recorded snowmelt did not coincide. Therefore the contributions at Frotveit-Dyrdalsvatn-Austlihylla are not quite comparable. Moreover, it should be stressed that the low value of Q_E is an average value. On single days fairly large contributions, mainly positive during cloudy weather (condensation) and negative during fine weather (evaporation) occurred. The contribution of condensation/evaporation to the mass budget, however, was negligible.

The distribution of the energy fluxes at Frotveit clearly demonstrates the effect of the deciduous wood on the energy balance at the snow surface. The canopy porousity to downward radiation flux

at the wooded site was estimated to 0.53, corresponding to a sky obscuration factor of 0.47. The net radiation is increased by the presence of trees, mainly due to longwave radiation, $Q_{L\downarrow}$, from the canopy. The increase in $Q_{L\downarrow}$ is greater than the combined effect of the decrease in absorbed solar radiation and the slightly lower sensible and latent heat fluxes caused by the lower wind speed. The difference occurred mainly in fine weather; during cloudy weather the net energy input was slightly higher at the open site. This is consistent with the observed snowmelt rates, which were highest at the wooded site, the difference again occurring in fine weather.

Further research on the topics discussed in this study should include testing/optimizing the wind function constants at other sites in different climatic regions. More work should be done regarding the use of extrapolated/estimated data of air temperature, humidity, wind speed, radiation fluxes and albedo.

When the simplified energy balance model is applied to climatic input data, snowmelt flood events may be simulated, and, by a statistical analysis, the risk for such floods estimated. Attention should, however, be drawn to the fact that the science of snow hydrology includes many topics not discussed here, e.g. snowpack ripening, snowmelt at partly snow-covered ground conditions, water movements in snow, ice damming, all of which should be considered when predicting areal runoff from (partly) snow-covered fields.

References

Abildsnes, H. 1980. Nedbørfordelingen i Dyrdalen. NHK-Rapport 5, Oslo 1980.

Andersen, T., and Ødegaard, H., 1980. Application of satellite data for snow mapping. Estimation of snow cover for hydrologic purposes using a digital interactive system. NHK-Rapport 3, Oslo 1980.

Anderson, E.A., and Crawford, N.H., 1964. The Synthesis of Continuous Snowmelt Runoff Hydrographs on a Digital Computer. Department of Civil Engineering. Technical Report no. 36, Stanford University, Stanford, California, 103 pp.

Anderson, E.A., and Baker, D.R., 1967. Estimating Incident Terrestrial Radiation under all Atmospheric Conditions. Water Resources Research, Vol. 3, No. 4, pp. 975-987.

Anderson, E.A., 1968. Development and Testing of Snow Pack Energy Balance Equations. Water Resources Research, Vol. 4, No. 1, pp. 19-37.

— , 1973. National Weather Service River Forecast System - Snow Accumulation and Ablation Model. NOAA Technical Memorandum NWS HYDRO-17, U.S. Dept. of Commerce, Silver Spring, Md, 217 pp.

— , 1976. A Point Energy and Mass Balance Model of a Snow Cover. NOAA Technical Report NWS 19. U.S. Dept. of Commerce, 150 pp.

Bayne, D.K., 1978. The relation between Shortwave Radiation and Sunshine Hours. Unpublished Internal Rept. No. 24. Division of Hydrology, University of Saskatchewan. 5 pp.

Bergstrøm, S., 1976. Development and application of a conceptual runoff model for Scandinavian catchments. Swedish meteorological Institute, report no. RH07.

Bolz, H.M., 1949. Die Abhängigkeit der infraroten Gegenstrahlung von der Bewölkung. Zeitschr.f. Met. B. 3 1949.

Brutsaert, W., 1972. Radiation, Evaporation, and the Maintenance of Turbulence under Stable Conditions in the Lower Atmosphere. Boundary-Layer Meteorology, Vol. 2, pp. 309-325.

Businger, J.A., 1973. Turbulent Transfer in the Atmospheric Surface Layer. Workshop on Micrometeorology, D.A. Haugen, Editor, American Meteorological Society, pp. 67-100.

Colbeck, S.C., 1972. A Theory of Water Percolation in Snow. Journal of Glaciology, Vol. 11, No. 63, pp. 369-385.

— , 1974. The Capillary Effects of Water Percolation in Homogeneous Snow. Journal of Glaciology 13 (67), pp. 85-97.

Dahlstrøm, B., 1970. A General Classification of Error Sources at Rain-gauging, and some Applications. Nordisk Hydrologisk Konferanse, Stockholm, 1970.

Førland, E.J., 1980. Driftserfaringer med Belfort vektpluviograf 1977-1980. NHK-Rapport 6, Oslo 1980.

— , 1980 a. Nedbørforholdene i Bergensområdet. Sammendrag av noen hovedfagsavhandlinger fra Geofysisk institutt avd. B, UiB. NHK-Rapport 7, Oslo 1980

Furmyr, S., 1975. Resultater og erfaringer av nedbørundersøkelser i Fillefjell representative område 1967-74. Den Norske IHD-komité, Oslo, 1975.

Gjessing, Y., Rasmussen, A., og Fremstad, E., 1980. Dyrdalen felt-forskningsområde. Formål og feltbeskrivelse. NHK-Rapport 4, Oslo 1980.

Granger, K.J., 1977. Energy Exchange During Melt on a Prairie Snow-cover. M. Sc. Thesis. Dept. of Mechanical Engineering. Univ. of Saskatchewan, 122 pp.

Harstveit, K., 1981. Measuring and Modelling Snowmelt in Dyrdalen, Western Norway, 1979 and 1980. Nordic Hydrology, 12, 1981, pp. 235-246.

Hendrie, L.K., and Price, A.G., 1978. Energy balance and snowmelt in a deciduous forest. Proceedings: Modelling of Snow Cover Runoff, Hanover, New Hampshire; pp. 211-221.

Holmgren, B., 1971. Climate and energy exchange on a sub-polar ice cap in summer. Arctic Institute of North America Devon Island Expedition 1961-63. Meddelande från Uppsala Universitets meteorologiska institution. Nr. 112, Uppsala, 1971.

Jordan, P., 1983. Meltwater Movement in a Deep Snowpack. 2. Simulation Model. Water Resources Res. 19 (4) 1983, pp. 979-985.

Kimball, H.H., 1914. Monthly Weather Review, 42: 474.

Killingtveit, Å., 1976. En studie av vannbalansen i Sagelva hydrologiske forskningsfelt. Institutt for vassbygging. N.T.H.-Trondheim.

Kohler, H., 1950. On Evaporation from Snow Surfaces. Arkiv für Geophysik. B. 1, No. 8, Uppsala, Sweden, pp. 159-185.

Kondratjev, K.Y., 1969. Radiation in the Atmosphere. Academic Press. New York - London 1969. 912 pp.

Krauss, H., 1966. Freie und bedeckte Ablation. Khumbu Himal, Ergebn. Forsch. - Unternehmen Nepal Himalaya. Bd 1, 203-235, Springer-Verlag.

Kuusisto, E., 1978. Optimal complexity of a point snowmelt model. Proceedings: Modelling of Snow Cover Runoff, Hanover, New Hampshire, pp. 205-210.

— , 1980. On the Values and Variability of Degree-Day Modelling Factors in Finland. Nordic Hydrology, 11, 1980, pp. 235-242.

Kuzmin, P.P., 1961. Melting ofSnow Cover, Israel Program for Scientific Translations, 290 pp.

Liljequist, G.H., 1956-1957. Energy Exchange of an Antarctic Snowfield. Part 1A-1D. Norwegian-British-Swedish Antarctic Expedition, 1949-52. Scientific Results, Vol. II, Norsk Polarinstitutt, Oslo.

Lundqvist, D., 1981. snømodellstudier i Dyrdalen. Intern Rapport 5 NHK, Oslo 1981.

McCay, D.C., 1970. Energy, Evaporation, and Evapotranspiration. Section III of Handbook on Principles of Hydrology, edited by D.M. Gray, Water Information Centre, Port Washington, N.Y., pp. 3.1 - 3.66.

Meiman, J.R., and Grant, L.O., 1974. Snow-Air Interactions and Management of Mountain Watershed Snowpack. Environmental Resources Center Completion Report Series No. 57, Colorado State University(available as PB-235-825), Ft. Collins, Colo.

Monteith, L.J., 1975. Principle of Environmental Physics. Edward Arnold, London, 1975.

Nyberg, A. och Hårsmar, P.O., 1971. Mätningar av avdunstning-kondensation samt snøsmältning från en snøyta. Sveriges meteorologiska och hydrologiska institutt. Serie meteorologi nr. 25. Stockholm, 1971.

Obled, C., 1973. Mathematical Models of Snowmelt Study of Avalanche Risks.English translation available on loan from Language Services Division F43, National Marine Fisheries Service, NOAA, Washington, D.C. 20235, 73 pp.

Olseth, J.A., 1981. Solstrålingsklimaet i Bergen. Klima 4, Det Norske Meteorologiske Institutt, Oslo. 1981.

Otnæs, J. og Ræstad, E., 1979. Hydrologi i praksis. Ingeniørforlaget, Oslo, 1979.

Paltridge, G.W., and Platt, C.M.R., 1976. Radiative Processes in Meteorology and Climatology. Elsevier Scientific Publishing Company, Amsterdam, 1976.

Paterson, W.S.B., 1969. The physics of glaciers. Pergamon Press, 1969.

Paulsen, H.S., 1967. Some Experiences with the Calibration of Radiation Balance Meters. Archiv für Meteorologie, Gephysic und Bioklimatologie, Band 15 pp. 156-174.

Paulsen, H.S., and Torheim, K.A., 1964. Atmospheric Radiation in Bergen. December 1957 - June 1959. Årbok University, Bergen, Mat.-Nat. Ser. No. 11, Bergen 1964.

Penmann, H.L., 1948. Natural Evporation from open water, bare soil, and grass. Proc. Roy. Soc., London. A 193. pp. 120-145.

Perthu, K.L., 1982. Radiation climate of Northern Forest stands. Sveriges Lantbruksuniversitet, Uppsala, 1982.

Petzold, D.E., and Wilson, R.G., 1974. Solar and Net Radiation over Melting Snow in Sub-Arctic Woodlands. Proc. 31st Eastern Snow Conf., Ottawa, Ontario, pp. 51-59.

Prescott,J.A., 1940. Trans. Royal. Soc. S. Australia, 64, pp. 114.

Radiation yearbook 1-18, 1965-82, Geophysical Institute, University of Bergen. Edited by H.S. Paulsen.

Robinson, N., 1966. Solar Radiation. Elsevier Publishing Company, Amsterdam, 1966.

Simonsen, O. 1976. Strålingsbeskyttere for temperaturmålinger med motstandstermometre. Unpublished thesis. University of Bergen 1976.

Skartveit, A., 1976. Energy exchange at the earth's surface with emphasis on an alpine tundra ecosystem. Rap. Høyfjells-økol. Forskn.St., Finse, Norge 1976 (1), pp. 1-147

Sonntag, D., 1964. Ein Pyranometer mit galvanisch erzeugter Thermosäule. Zeitschrift für Meteorologie. B. 17. H. 12, 1964.

Sverdrup, H.U., 1936. The Eddy Conductivity of the Air over a Smooth Snow Field. Geofysisk Publikasjoner, Vol. XI, No. 7, Oslo, Norway, pp. 5-69.

Swinbank, W.C., 1963. Long-wave Radiation from clear skies. Quart. J. Roy. Meteor. Soc. 89, pp. 339-348.

Tveit, J., 1977. Smeltevassmålaren. Eit hjelpemiddel i studie av snøsmelting og total nedbør. Notat. Institutt for vassbygging, N.T.H. - Trondheim.

— , 1979. Representativitet av målesystem ut frå topografiske parametrar. Institutt for vassbygging, N.T.H. - Trondheim.

U.S.A.C.E , 1955. Lysimeter studies of Snow Melt. Snow investigations research, Note 25, Corps of Engineers, North Pacific Division, Portland, Oreg., 52 pp.

— , 1956. Summary Report of the Snow Investigations, Corps of Engineers, North Pacific Division, Portland, Oreg., 437 pp.

Wallén, C.C., 1948. Glacial-meteorological investigations on the Kårsa glacier in Swedish Lapland, 1942-48. Geogr. Ann, 30 (3-4).

Wankiewicz, A., 1978. A review of water movement in snow. Proceedings: Modelling of Snow Cover Runoff, Hanover, New Hampshire, pp. 222-252.

Østrem, G., 1974. Runoff forecasts for highly glacierized basins. Meddelelse nr. 26 fra Hydrologisk avdeling, NVE. Reprinted from Proceedings of the Banff Symposia, The role of snow and ice in hydrology, 1972.

Ångstrøm, A., 1913. Studies of the Nocturnal Radiation to Space. Astrophysical Journal. Vol. XXXVII 1913.

Acknowledgements

This work is a thesis for the author's doctorate at the University of Bergen. The thesis constitutes a summary of the snowmelt investigations in the Dyrdalen area supported by the Norwegian Commitee for Hydrology (NHK). The author's effort was funded by NHK from 1978 to 1982, and by the Norwegian Research Council for Science and the the Humanities (NAVF) in 1983.

The work was carried out at the Geophysical Institute, Meteorological Division, University of Bergen. The author wishes to thank all who have contributed to this investigation. Special thanks to Mr. Y.T. Gjessing, and Mr. A. Skartveit for valuable help and planning of the data collection, and for valuable discussions during all stages of the investigation. Thanks also to Professor K. Utaaker for his careful criticism and examination of the manuscript. The author would also like to thank: Mr. F. Cleveland for help in preparing the figures, Mr. B. Hackett for improving the English style, and Mrs. E. Thomsen for typing the final report.